Euscorpius

Occasional Publications in Scorpiology

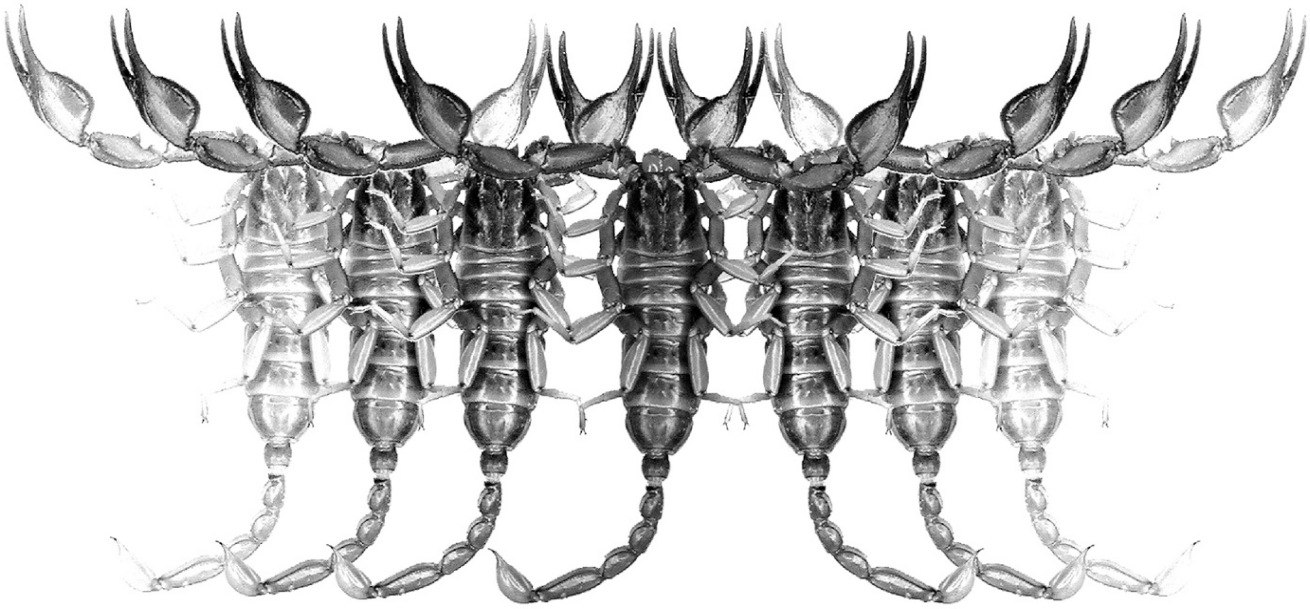

Revision of the genus *Olivierus* in Xinjiang, China, with comments on *Mesobuthus thersites* (Scorpiones: Buthidae)

Victoria Tang, Zhenbang Liu, Matthew R. Graham, Victor Fet, František Kovařík & František Šťáhlavský

February 2024 — No. 383

Euscorpius

Occasional Publications in Scorpiology

EDITOR: **Victor Fet**, Marshall University, **'fet@marshall.edu'**

ASSOCIATE EDITOR: **Michael E. Soleglad, 'msoleglad@gmail.com'**

TECHNICAL EDITOR: **František Kovařík, 'kovarik.scorpio@gmail.com'**

Euscorpius is the first research publication completely devoted to scorpions (Arachnida: Scorpiones). ***Euscorpius*** takes advantage of the rapidly evolving medium of quick online publication, at the same time maintaining high research standards for the burgeoning field of scorpion science (scorpiology). ***Euscorpius*** is an expedient and viable medium for the publication of serious papers in scorpiology, including (but not limited to): systematics, evolution, ecology, biogeography, and general biology of scorpions. Review papers, descriptions of new taxa, faunistic surveys, lists of museum collections, and book reviews are welcome.

Derivatio Nominis

The name ***Euscorpius*** Thorell, 1876 refers to the most common genus of scorpions in the Mediterranean region and southern Europe (family Euscorpiidae).

Euscorpius is located at: https://mds.marshall.edu/euscorpius/
Archive of issues 1-270 see also at: http://www.science.marshall.edu/fet/Euscorpius

(Marshall University, Huntington, West Virginia 25755-2510, USA)

ICZN COMPLIANCE OF ELECTRONIC PUBLICATIONS:

Electronic ("e-only") publications are fully compliant with ICZN (*International Code of Zoological Nomenclature*) (i.e. for the purposes of new names and new nomenclatural acts) when properly archived and registered. All ***Euscorpius*** issues starting from No. 156 (2013) are archived in two electronic archives:

- **Biotaxa,** http://biotaxa.org/Euscorpius (ICZN-approved and ZooBank-enabled)
- **Marshall Digital Scholar**, http://mds.marshall.edu/euscorpius/. (This website also archives all *Euscorpius* issues previously published on CD-ROMs.)

Between 2000 and 2013, ICZN ***did not accept online texts*** as "published work" (Article 9.8). At this time, *Euscorpius* was produced in two ***identical*** versions: online (*ISSN 1536-9307*) and CD-ROM (*ISSN 1536-9293*) (laser disk) in archive-quality, read-only format. Both versions had the identical date of publication, as well as identical page and figure numbers. ***Only copies distributed on a CD-ROM*** from ***Euscorpius*** in 2001-2012 represent published work in compliance with the ICZN, i.e. for the purposes of new names and new nomenclatural acts.

In September 2012, ICZN Article 8. What constitutes published work**,** has been amended and allowed for electronic publications, disallowing publication on optical discs. From January 2013, ***Euscorpius*** discontinued CD-ROM production; only online electronic version (ISSN 1536-9307) is published. For further details on the new ICZN amendment, see http://www.pensoft.net/journals/zookeys/article/3944/.

Publication date: 2 February 2024

http://zoobank.org/urn:lsid:zoobank.org:pub:30439BDB-3775-4ECC-A93F-B3C2328942DD

Euscorpius — Occasional Publications in Scorpiology. 2024, No. 383

Revision of the genus *Olivierus* in Xinjiang, China, with comments on *Mesobuthus thersites* (Scorpiones: Buthidae)

Victoria Tang[1], Zhenbang Liu[2], Matthew R. Graham[3], Victor Fet[4], František Kovařík[5] & František Šťáhlavský[5]

[1]Zhangyang Rd. 200120, Pudong New District, Shanghai, China; email: jibril.flueqel@gmail.com
[2]Youjiang Medical University for Nationalities, Baise, Guangxi, China; email: maziyuu.helgen@gmail.com
[3]Department of Biology, Eastern Connecticut State University, 83 Windham Street, Willimantic, CT06226, USA; email: grahamm@easternct.edu
[4]Department of Biological Sciences, Marshall University, Huntington, West Virginia 25755-2510,USA; email: fet@marshall.edu
[5]Department of Zoology, Charles University, Viničná 7, CZ-128 44 Praha 2, Czech Republic; http://www.scorpio.cz, email: frantisek.stahlavsky@natur.cuni.cz

http://zoobank.org/urn:lsid:zoobank.org:pub:30439BDB-3775-4ECC-A93F-B3C2328942DD

Summary

The genus *Olivierus* Farzanpay, 1987 in Xinjiang Uygur Autonomous Region, China, is revised based on recently collected topotypes and other populations from 12 localities. Brief differential diagnoses are provided, with colored illustrations and photos in vivo habitus, emphasizing the key characters. Chinese appellations, conservation status, and documentation of behavior and post-envenomation symptoms are also included. Only two species are now recognized for this genus in Xinjiang: *O. longichelus* (Sun & Zhu, 2010) and *O. przewalskii* (Birula, 1897), based on both morphological and molecular evidence. The two species exhibit extensive distribution in Xinjiang (China) while also occurring in adjacent countries. Three new synonyms are proposed: *Mesobuthus bolensis* Sun et al., 2010 = *Olivierus longichelus* (Sun & Zhu, 2010), **syn. n.**; *Mesobuthus karshius* Sun & Sun, 2011 = *Olivierus longichelus* (Sun & Zhu, 2010), **syn. n.**; *Olivierus tarabaevi* Fet et al., 2021 = *Olivierus longichelus* (Sun & Zhu, 2010), **syn. n.** Two species, *Olivierus extremus* (Werner, 1936) and *O. hainanensis* (Birula, 1904), are likely synonymous with *O. martensii* (Karsch, 1879). Should future examination confirm this assumption, the total number of species in genus *Olivierus* would be reduced to 16.

Introduction

The Xinjiang Uygur Autonomous Region, constituting the largest province in China, spans an extensive area of 1,664,897 km^2. Currently, it accommodates four scorpion genera belonging to two families (Tang, 2022c): *Mesobuthus* Vachon, 1950, *Olivierus* Farzanpay, 1987, *Razianus* Farzanpay, 1987 (Buthidae) and *Scorpiops* Peters, 1861 (Scorpiopidae). Among them, three are represented by solitary species, two of which are known only from old specimens: *Razianus xinjianganus* Lourenço et al., 2010 was described from a female collected in the vicinity of the border between Kashgar and Tajikistan in 1971, while *Scorpiops taxkorgan* Lourenço, 2018 was based on an adult male and a juvenile female procured from Taxkorgan Natural Reserve in 1986. The genus *Mesobuthus* in Xinjiang is represented by *M. thersites* (C. L. Koch, 1839), a predominant species within the region. This species also occurs in neighboring provinces of China such as Gansu, Inner Mongolia, and Ningxia (Tang, 2022c).

As already summarized in Tang (2022c: 4), Kovařík (2019) revalidated genus *Olivierus* as distinct from *Mesobuthus* based on their morphology (a decision subsequently corroborated by the DNA phylogeny of Štundlová et al. (2022)), elevating all the then valid subspecies of *M. eupeus* (C. L. Koch, 1839) to the species rank. In a subsequent endeavor, Kovařík et al. (2022) conducted a comprehensive revision of this genus and synonymized *M. mongolicus* with *M. thersites* (which were both considered to occur in China and previously regarded as two subspecies of *M. eupeus*) supported by both morphological and molecular evidence. However, in a recently updated version of "*List of terrestrial wildlife with significant ecological, scientific, and social value (2023, No. 17)*" by National Forestry and Grassland Administration of China, the sole protected scorpion species in China was still designated as "*Mesobuthus eupeus*" (p. 55; with the Chinese appellation "条纹正钳蝎). As limited by Kovařík et al. (2022: 41), this species only occurs in Armenia, Azerbaijan, Georgia (type locality in Tbilisi), Iran (West Azerbaijan Province), Russia and Turkey. Personal communication of the first author with a Chinese researcher revealed a highly "primitive" situation in which they were constrained to base their projects on this erroneous list and other outdated Chinese papers that are

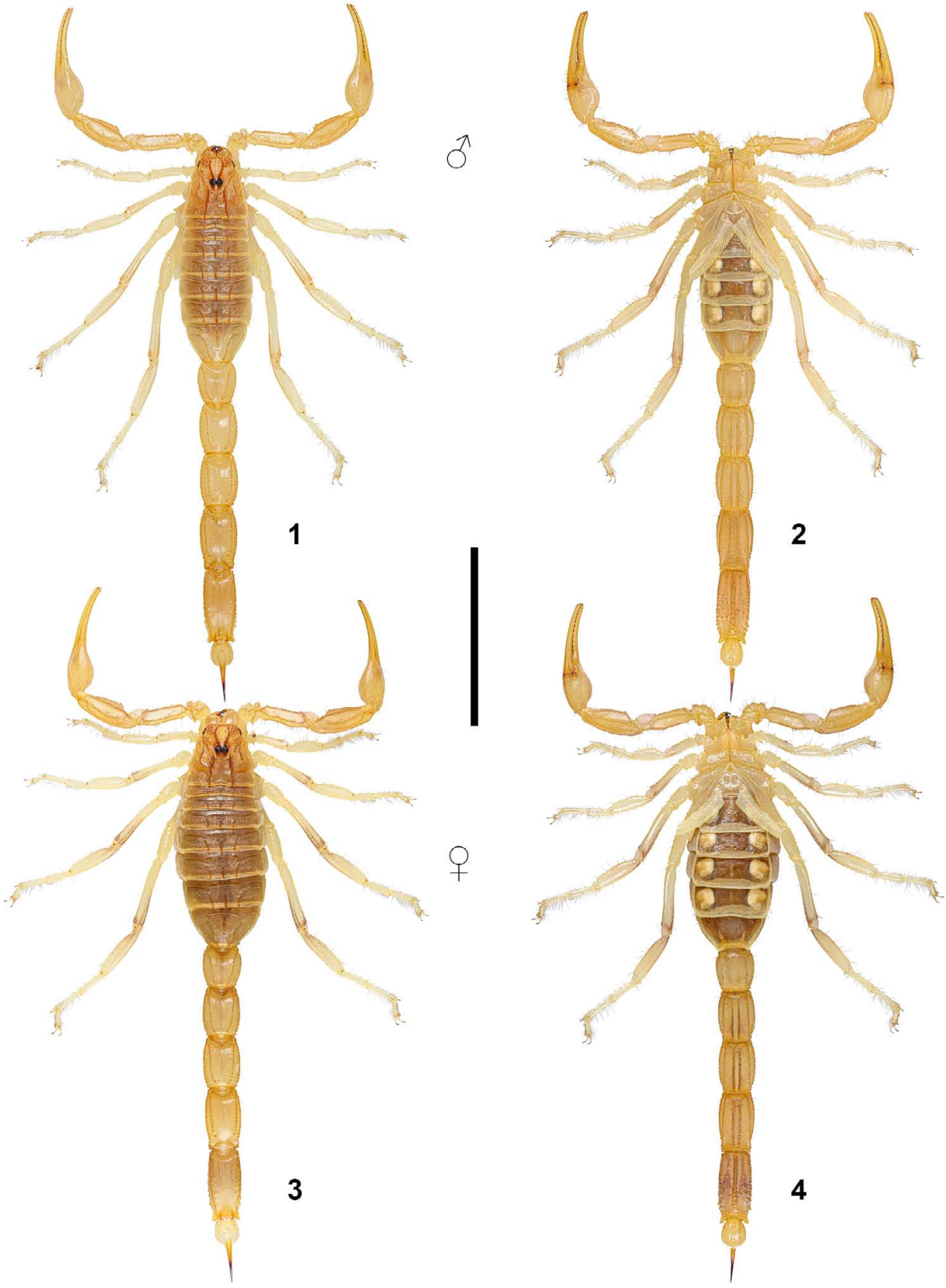

Figures 1–**4**: *Olivierus longichelus* (Sun & Zhu, 2010), habitus under white light. **Figures 1**–**2**. Male from Jinghe County, in dorsal (1) and ventral (2) views. **Figures 3**–**4**. Female from Bole City, in dorsal (3) and ventral (4) views. Scale bar = 20 mm.

annexed to a monetized website known as the China National Knowledge Infrastructure (CNKI). This situation, however, necessitates rectification.

Notably, the genus *Olivierus* stands as the third most diverse scorpion genus within China (5 spp., if one were to ignore *O. hainanensis* (Birula, 1904)), trailing behind *Chaerilus* Simon, 1877 (8 spp.) and *Scorpiops* Peters, 1861 (32 spp., including, *S. rufus* Lv & Di, 2023, in addition to the list in Tang, 2023). *Olivierus* also includes the most common scorpion species in China, *O. martensii* (Karsch, 1879). Within China, all the remaining species are restricted to Xinjiang and proximate provinces, with the exception of the dubious species *O. hainanensis*, plausibly a synonym of *O. martensii* (Tang, 2022c: 13). Previous studies acknowledged four species in Xinjiang, viz. *O. bolensis* (Sun et al., 2010), *O. karshius* (Sun & Sun, 2011), *O. longichelus* (Sun & Zhu, 2010) and *O. przewalskii* (Birula, 1897), all of which were then classified under *Mesobuthus* (except for *O. przewalskii* which was originally described as a subspecies of *Buthus caucasicus* Nordmann, 1840 (now *O. caucasicus*)). However, all of those species were poorly described.

In the present investigation, a collection of 104 topotypes from the type localities of the aforementioned four species of *Olivierus* as well as 23 additional specimens from other localities was obtained through an expedition by a local collector in Xinjiang. The outcomes of this study unveil the presence of only two *Olivierus* species within the province. Succinct diagnostic criteria are provided, accentuating characteristics of potential utility in the interspecific differentiation within this genus.

Methods, Material & Abbreviations

Morphology. Nomenclature and measurements mostly follow Stahnke (1971), except for trichobothriotaxy (Vachon, 1974), chelicera (Soleglad & Fet, 2003b), sternum (Soleglad & Fet, 2003a), pedipalp patellar and femur carinae (Prendini et al., 2021), chela width measurement (Tang, 2023), and pedipalp finger sensilla (Lowe & Fet, 2024). Hemispermatophore terminology follows Monod et al. (2017). The present investigation encompasses an array of morphological attributes: (1) coloration; (2) total length; (3) relative length of tarsal setation; (4) carinae and granulation of carapace and tergites; (5) serration of ventrolateral carinae of metasoma segment V; (6) pectinal tooth count; (7) denticle subrow count of pedipalp movable finger; (8) length/width ratio of pedipalp chela (measured two pedipalps for each individual; averaged values used in diagnoses, raw values used in comparison and analysis); (9) length/depth ratio of metasoma segment IV; (10) length/depth ratio of metasoma V. The measurement of total length was approximative due to the dependence on the extent to which tergites were unveiled since some preserved specimens were resistant to extension. It was therefore roughly measured from carapace anterior margin to aculeus tip, rather than separately measured for each segment, resulting in provided data of relative accuracy. If certain pectinal teeth were concealed/lost, the pectinal tooth count (PTC) was inferred by the number of fulcra (N_f) (PTC = N_f + 1). If only one complete pectine was available, then the mean PTC for that individual was represented by the value obtained from the available pectine; "/" indicates left and right PTC in ventral view, "–" indicates PTC variation range. All statistical calculations involving variance were based on the formulas for sample. However, our data do not reliably constitute an estimation for the wild population, given that not all localities had a sufficient ($n \geq 30$) sample size, especially those for *O. longichelus*. Statistical tests were performed online by a robust non-parametric approach, two sample Mann-Whitney U test (two-tailed), which also deals with cases where $n < 30$. Null hypothesis H_0 set as no difference in the median between two groups, significance level $\alpha = 0.05$, automatic method. When the Z approximation with continuity correction is used, the critical Z-value has an absolute value of 1.96 corresponding to the significant level, see: www.statskingdom.com/test_mann_whitney.html.

Materials. All topotypes were collected during a trip across Xinjiang by a local collector from July to August in 2023 and examined by the first author. Some specimens were preserved in ethanol following their demise from elevated temperatures during collection, while others were sent to the author in live condition. Partial photographs were taken under UV light to serve diagnostic purposes and were matted by the second author (ex. Leonhard Liu). Sexes were determined by the morphology of pedipalp chela, pectines and relative mesosoma width (see Tang et al. (2023: 12, 14–15) for elaboration). Sexual dimorphism of studied species is further discussed below. The maturity was primarily determined by size and visually perceived ratio. In particular, the maturity of the male specimens was additionally determined by the presence of the pronounced lobe present basally on the dentate margin of pedipalp movable finger. If the male was relatively small and slender while still had a pronounced lobe, its maturity was further substantiated by the presence of hemispermatophores. Maturity evaluations for female specimens took into account coloration and the robustness of the pedipalp chela. In cases of immaturity, the analysis was confined to finger denticle subrow and pectinal tooth counts.

Most live specimens were not euthanized; they were immersed in water and intermittently agitated with tweezer (to accelerate oxygen consumption) for approximately 20 to 30 minutes to cause temporary hypoxia prior to the inspection. Intriguingly, those arid scorpions could stay alive under water for up to at least 1 hour if left undisturbed. Since not all the localities included sexually paired specimens, the bivariate scatterplots were not depicted as males against females. Both pectinal tooth count and denticle subrow count (age-independent variables) were represented by discrete integers of limited range. If they were plotted in the same figure, localities with fewer specimens could be overshadowed by others due to the overlapped variation range. To cover the data from all localities, the two variables were respectively plotted against continuous variables (total length and ratiometrics). However,

those variables are age-dependent, leading to the exclusion of age-independent values (pectinal tooth count and denticle subrow count) obtained from the immatures, which might had included the only specimens of a particular sex. Photos of carapace and tergites, dentate margin of pedipalp movable finger, pectines and metasoma V of all studied specimens can be downloaded from Research Gate (in two ZIP. Files): www.researchgate.net/profile/Victoria-Tang-8/publications. The first ZIP. File also includes several Chinese references cited herein that might prove elusive for non-Chinese readers to locate.

DNA sequencing and phylogenetic tree reconstruction. This part was performed by the third and fourth authors. The genomic DNA was extracted using the Genomic DNA Mini Kit (Tissue) (Geneaid Biotech Ltd.). A fragment of the cytochrome oxidase I (COI) gene (~600 bp) was amplified by PCR using the standard primers LCO 5'-GGTCCACAAATCATAAAGATATTGG-3' and HCO 5'-TAAACTTCAGGATGACCAAAAAATCA-3'. A fragment of the gene for 16S rRNA (16S) (~350 bp) was amplified using the primers 16SF 5'-CGATTTGAACTCAGATCA-3' and 16SR 5'-GTGCAAAGGTAGCATAATCA-3'. Following PCR conditions were used for both fragments: initial denaturation 94°C for 5 min, followed by 45 cycles of 94°C for 35s, 45°C for 35s, and 72°C for 45s. The final extension was at 72°C for 5 min (see Štundlová et al., 2022). PCR products were purified by Gel/PCR DNA Fragments Extraction Kit (Geneaid Biotech Ltd.) and were sent for sequencing to Macrogen Europe Inc. The obtained DNA sequences were edited and aligned using SeqMan 5.05 program. All new DNA sequences were deposited in GenBank (www.ncbi.nlm.nih.gov/), with the following accession numbers: **(1)** *Olivierus longichelus* (Sun & Zhu, 2010): PP229931 (1 adult ♀ from Bole, Xinjiang, China), PP229932 (1 adult ♂ from Ghulja, Xinjiang, China), PP229933 (1 adult ♂ from Yarkant, Xinjiang, China), PP229934 (1 juv. ♀ from Makit, Xinjiang, China), PP229935 (1 adult ♂ from Jinghe, Xinjiang, China), PP229936 (1 adult ♂ from Khorgos, Xinjiang, China), PP229937 (1 adult ♀ from Wujiaqu, Xinjiang, China), and PP229938 (1 adult ♂ from Shawan, Xinjiang, China); **(2)** *Olivierus przewalskii* (Birula, 1897): PP229927 (1 adult ♂ from Bole, Xinjiang, China), PP229928 (1 adult ♂ from Ghulja, Xinjiang, China), PP229929 (1 adult ♀ from Yarkant, Xinjiang, China), and PP229930 (1 adult ♂ from Makit, Xinjiang, China).

Our phylogenetic analysis of *Olivierus* followed an approach similar to the previous study of *Mesobuthus* by Kovařík et al. (2022). Mitochondrial COI sequences were aligned using MUSCLE with default parameters in AliView 1.7.1 (Larsson, 2014). Following manual visual inspection and end trimming in AliView, the trimmed alignment served as the basis for phylogenetic inference and divergence time estimation for *Olivierus* spp. with BEAST 1.8.0 (Drummond et al., 2012). Molecular Evolutionary Genetics Analysis (MEGA X; Kumar et al., 2018) identified GTR+G as the best-fit nucleotide substitution model. Using this model, two independent Markov Chain Monte Carlo (MCMC) runs were conducted with 100 million iterations each, sampling every 10,000 iterations. Initial runs employed a Yule tree prior and uncorrelated lognormal clock model, but ucld.stdev values were low (<1.0), suggesting clock-like evolution. Accordingly, a strict clock model was used for final runs, as suggested by the BEAST manual. Following established practices for buthid scorpions, the molecular clock was calibrated using a normal mean rate prior (ucld.mean) of 0.007 substitutions per site per million years (Gantenbein et al., 2005; Graham et al., 2019). Standard deviation was set to 0.00146 to capture 95% of the normal distribution of COI substitution rates reported for scorpions (Bryson et al., 2014; Graham et al., 2017). Convergence among runs was verified with Tracer 1.7 (Rambaut et al., 2018), ensuring all parameters well-exceeded an ESS value of 200. Individual tree files were combined using TreeAnnotater (part of the BEAST package), and the resulting maximum clade credibility tree was visualized in Figtree 1.4.0 (tree.bio.ed.ac.uk/software/).

To delineate the boundaries among *Olivierus* species, we employed the ASAP (Assemble Species by Automatic Partitioning) program (Puillandre et al., 2021) to analyze the COI sequence data. This method operates by first calculating pairwise genetic distances between individual sequences. It then utilizes hierarchical clustering techniques to construct a list of potential species partitions based on the genetic distances. Each partition is assigned a score that reflects both the magnitude of the barcode gap and the likelihood of panmixia within a species. Notably, ASAP does not necessitate any prior knowledge about the study system, such as the anticipated number of species, a phylogenetic tree, or predefined genetic distances. We submitted our COI alignment to the ASAP web server (bioinfo.mnhn.fr/abi/public/asap/) and selected the Jukes-Cantor (JC69) substitution model for the calculation of genetic distances. The ASAP model that yielded the lowest score was deemed to represent the optimal partitioning of species within our dataset.

Abbreviations. D, depth; L, length; W, width; TL, total length; CL/W, length to width ratio of pedipalp chela; PTC, pectinal tooth count; DSC, denticle subrow (complex; definition see below) count; CL, central lateral carina(e); CM, central median carina(e); PM, posterior median carina(e); ML, median lateral carina(e); VL, ventrolateral carina(e); VM, ventromedian carina(e); EAD, external accessory denticle(s); MD, median denticle(s); IAD, internal accessory denticle(s); SPS, subrow proximal sensilla; UV, ultraviolet; 16S, 16S ribosomal RNA; COI, mitochondrial cytochrome c oxidase I; MaL, Maximum Likelihood; BI, Bayesian Inference; mya, millions of years ago; UTN, unpublished translated name; ET-G/S/SS, erroneous translation for generic/specific/subspecific epithet; TM-S, translation missing for specific epithet; VN, vernacular name; $\bar{x}$, sample mean; S, sample standard deviation; D, sample index of dispersion; G_1, adjusted Fisher-Pearson standardized moment coefficient (skewness).

Specimen Depositories. FKCP, personal collection of František Kovařík, Prague, Czech Republic (will in future be merged with the collections of the NMPC); IOZ-CAS

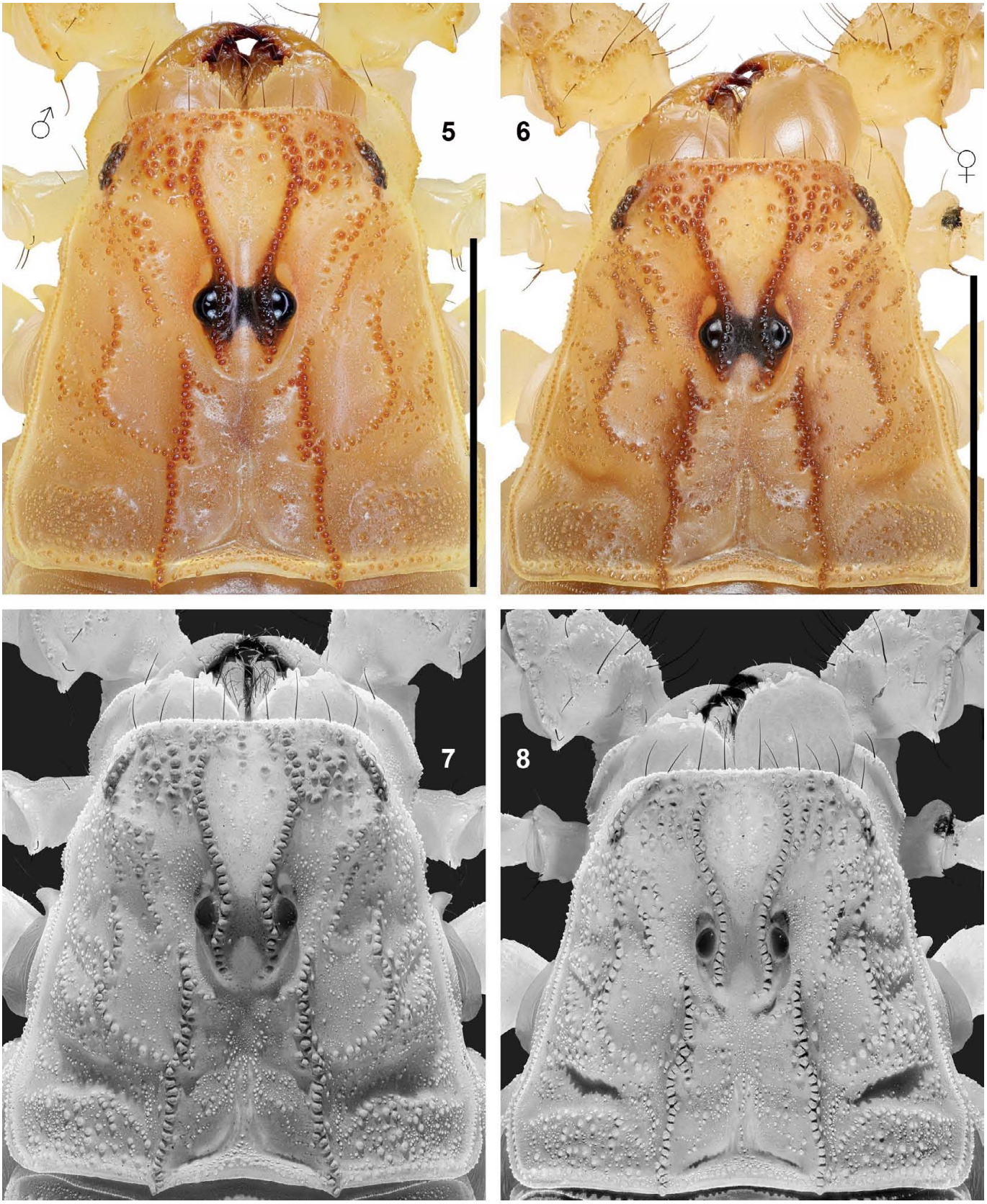

Figures 5–**8**: *Olivierus longichelus* (Sun & Zhu, 2010), carapace of male from Jinghe County (5, 7) and female from Bole City (6, 8). **Figures 5**–**6**. Under white light. **Figures 7**–**8**. Under UV light. Scale bars = 5 mm.

(Institute of Zoology, Chinese Academy of Sciences, Beijing, China); MHBU (Museum of Hebei University, Baoding, China); NMPC (National Museum of Natural History, Prague, Czech Republic); VT (Personal collection of Victoria Tang, Shanghai, China); ZISP (Zoological Institute, Russian Academy of Sciences, St. Petersburg, Russia).

Comparative material (VT & FKCP). *Olivierus* sp., **China**, *Xinjiang Uygur Autonomous Region*, Changji Prefecture, Wujiaqu City, 44°21'11.6"N 87°39'28.5"E (44.353222°N 87.657917°E), 441 m a. s. l., 25 September 2021, 2♂2♀10 juvs [preserved as dry specimens and used for general comparison; photos available in Tang (2022c)], leg. Qiu Du; Changji Prefecture, Wujiaqu City, 44°32'01.4"N 87°32'02.9"E (44.533722°N 87.534139°E), 427 m a. s. l., 25 June 2022, 12♂1♀ [preserved as dry specimens and used for crude comparison; partially used for DNA analysis as fresh specimens when sent to Charles University, Prague, Czech Republic], leg. Qiu Du; Changji Prefecture, Wujiaqu City, 44°33'42.0"N 87°36'55.0"E (44.561669°N 87.615275°E), 351 m a. s. l., 3 September 2023, 1♂9♀ [all live specimens, recorded for PTC only; partially used for DNA analysis], leg. Qiu Du; Tacheng Prefecture, Shawan City, near Huluyu Village, 44°39'31.0"N 85°54'43.8"E (44.658608°N 85.912159°E), 356 m a. s. l., 2 September 2023, 6♂4♀1 juv. [all live specimens, recorded for PTC only; partially used for DNA analysis], leg. Qiu Du.

Additional material for DNA analysis (FKCP). *Olivierus* sp., **China**, *Xinjiang Uygur Autonomous Region*, Ili Kazakh Autonomous Prefecture, Korgas (or Huocheng) County, Sandaohe Township, Taerji Village Sizu, 44°01'01.0"N 80°48'24.4"E (44.016948°N 80.806775°E), 599.8 m a. s. l., 5 August 2023, 1 juv., leg. Yizun Wang; Ili Kazakh Autonomous Prefecture, Khorgos (or Korgas) City, near Hongkazi, 44°17'25.8"N 80°25'28.0"E (44.290490°N 80.424436°E), 3088 m a. s. l., 7 August 2023, 1♂, leg. Yizun Wang. Those specimens were recorded for PTC only and leg tissues were used for molecular analysis.

Review of published literature on Xinjiang *Olivierus*

1. Character conflicting with the generic diagnosis

In his reanalysis, Kovařík (2019: 26) defined genus *Olivierus* as having 12–14 subrows (we referred to "row" as to "subrow", see below) on the dentate margin of pedipalp movable finger, whereas *Mesobuthus* exhibited a lesser count of 11–12 subrows. This led to the reassignment of all previously categorized Chinese species, formerly classified under *Mesobuthus*, into *Olivierus*, except for *M. mongolicus* and *M. thersites* (the former is now a junior synonym of the latter). Additionally, the author raised the status of *M. caucasicus przewalskii* to that of an independent species, designated as *O. przewalskii*. Subsequently, a comprehensive investigation into the distributional range of this species was undertaken by Zhang et al. (2020). However, they upheld the classification of this species within *Mesobuthus*, referring to it as *M. przewalskii*. This placement was extended to include other Chinese members previously transferred to *Olivierus*. In their revised diagnosis, only 11 subrows of denticles were recognized on the movable finger (Zhang et al., 2020: 85). Supporting their taxonomic assertions, their figure 6 (Zhang et al., 2020: 86) displayed the movable finger (mistakenly written as "fixed finger") of a male *O. przewalskii* with a discernible count of, indeed, 11 subrows. This numerical incongruence likely resulted in their decision of not reclassifying this species under *Olivierus*. In spite of this, Štundlová et al. (2022) and Kovařík et al. (2022) both distinguished *Mesobuthus* from *Olivierus* on the basis of molecular evidence, a taxonomic treatment to which the present study adheres.

2. The enigmatic Xinjiang "*M. c. intermedius*"

In the preceding Chinese papers, *O. intermedius* (as *M. caucasicus intermedius*) and *O. przewalskii* (as *M. caucasicus przewalskii*) were considered as subspecies of *O. caucasicus* (as *M. caucasicus*) and to occur in China, following Fet & Lowe (2000: 191–192, as *Olivierus caucasicus intermedius* and *O. c. przewalskii*). However, subsequent research has unequivocally confirmed their status of being independent, with *O. intermedius* confined to Tajikistan and *O. przewalskii* to China and Mongolia (Fet et al., 2018; Kovařík, 2019). This renders the identification of Chinese "*O. intermedius*" (from Bole and Yining, Xinjiang) erroneous, a misclassification that Zhang et al. (2020: 90) continued to perpetuate through their reference to those outdated sources. Considering these, we referred to those false "*O. intermedius*" as to "*M. c. intermedius*".

As pointed out in Tang (2022c), a plethora of confusions and inconsistencies stemmed from several earlier Chinese papers (Sun & Zhu, 2010; Sun, 2010; Sun & Sun, 2011). In Sun & Zhu (2010: 3), they examined 11 specimens of "*M. c. intermedius*" from Shardara (or Chardara) and Balkhash (as "Kurty", but this location deviated from their coordinates which lied in Taukum) districts of Kazakhstan (*erratum*: this paper was published before Sun's dissertation in 2010). This yielded a PTC range of 26–30 for males and 20–25 for females. Later, in Sun's dissertation (Sun, 2010: 74) where he described a new subspecies as "*M. caucasicus karshius*" (or "*kaxgaricus*"; there were two different subspecific epithets used), data regarding the "*M. c. intermedius*" he examined included two specimens from Yining (Xinjiang, China), one specimen from Bole (Xinjiang, China), and 14 specimens from the same two districts in Kazakhstan. However, in his dichotomous key (Sun, 2010: 64), the recorded PTC range shifted to 26–30 for males and 21–25 for females. That is, the material series of a larger sample size in Sun (2010) yielded a reduced range compared to the earlier series of a smaller size in Sun & Zhu (2010) which is logically paradoxical. Oddly enough, there was a secondary shift in the diagnosis (Sun, 2010: 74): 21–24 for males and 17–20 for females. Despite the inclusion of more specimens in Sun's dissertation, the provided PTC range failed to encompass the earlier range obtained from a smaller sample size.

The three specimens of "*M. c. intermedius*" from China examined by Sun (2010) were the same as those in a published

version of "*M. karshius*" (Sun & Sun, 2011). Sun & Sun (2011: 61) also claimed to have examined specimens from Kazakhstan, for which they wrote "*see Sun* ***et al****. (2010)*". From their reference list, it must refer back to "Sun & Zhu (2010)" rather than "Sun, Zhu & Lourenço (2010)" since the latter publication, the original description of *O. bolensis*, did not mention any "*M. c. intermedius*" materials. This indicates a lower sample size (minus three specimens from Kazakhstan) than Sun (2010); nevertheless, the PTC range they gave (Sun & Sun, 2011: 62) was the same as that of Sun & Zhu (2010: 3), with the latter of which not including any Chinese specimens. Several plausible explanations can be posited for the data confusion and incoherence, given the premise that the data in Sun & Zhu (2010) was accurate: (i) the PTC range of the three new Chinese specimens examined in Sun & Sun (2011) was omitted from their given PTC range; (ii) the PTC range of the three new Chinese specimens fell within the PTC range of the 11 Kazakhstan specimens examined in Sun & Zhu (2010); (iii) either of the PTC ranges given in Sun (2010: 64, 74) exclusively pertained to the three new Kazakhstan specimens that were not examined in Sun & Zhu (2010); (iv) either of the PTC ranges given in Sun (2010: 64, 74) exclusively pertained to the three Chinese specimens and was not encompassed within the PTC range given in Sun & Sun (2011); (v) enumeration errors. Scenarios (i) and (ii) account for the congruence in PTC range between Sun & Zhu (2010) and Sun & Sun (2011). On the other hand, scenarios (iii) and (iv) rationalize the deviations in data presented by Sun (2010) compared to the other two papers, isolating the six new specimens (3 from China and 3 from Kazakhstan) that were not accounted for in Sun & Zhu (2010). Finally, scenario (v) accommodates for the possibility of errors across all the provided data.

Fet et al. (2018: 28) inferred that the type locality of the authentic *O. intermedius* resides within Tajikistan, where they also listed Kazakhstan, Kyrgyzstan, and Uzbekistan to be the origins of a reconstructed syntype series. However, these designations were subject to doubt, particularly in the case of Kazakhstan. Similarly, Kovařík (2019: 26) excluded Kazakhstan while casting skepticism on Kyrgyzstan and Uzbekistan. The PTC range they provided for this species was 21–23 for males and 17–19 for females (Fet et al., 2018: 26), closely resembling the range disclosed in Sun's dissertation (2010: 74). Fet et al. (2021) described three new cryptic species of *Olivierus* from Kazakhstan and Uzbekistan, two of which (*O. mikhailovi* and *O. tarabaevi*) were geographically close to the "*M. c. intermedius*" studied by those Chinese authors. *O. tarabaevi* from Khantau Village and Qonayev (or Konaev, previously known as Kapchagai, Kapchagay or Kapshagay) City is geographically close to "*M. c. intermedius*" from Balkhash District, both located in the Almaty Region, while *O. mikhailovi* and "*M. c. intermedius*" were sympatric in Shardara District ([41.2705°N, 67.8839°E] for *O. mikhailovi* and [41°16.106'N, 67°53.228'E] for "*M. c. intermedius*"). Fet et al. (2021: 61) listed the "*M. c. intermedius*" identified by Sun & Zhu (2010) and Sun & Sun (2011) under *O. tarabaevi*. The provided PTC range for *O. mikhailovi* was 26–28 for males and 21–23 for females, while that for *O. tarabaevi* was 24–27 for males and 19–22 for females (Fet et al., 2021: 60, 65). Solely considering the PTC range, the materials examined by Sun & Zhu (2010) exhibit a closer affinity to *O. mikhailovi*. However, taking the geographic provenance into account, it is plausible that these authors had studied both species.

3. Currently accepted *Olivierus* species in Xinjiang

Setting aside those foreign specimens, it is still intriguing regarding the three specimens of "*M. c. intermedius*" from Xinjiang, China. Notably, both Sun (2010) and Sun & Sun (2011) were published after the descriptions of two species from that region, namely *O. bolensis* (as "*M. bolensis*") and *O. longichelus* (as "*M. longichelus*"). The Chinese "*M. c. intermedius*" originated from the same two localities in the initial description for *O. bolensis*, but neither Sun (2010) nor Sun & Sun (2011) provided a well-justified differentiation of those specimens from that species. Their diagnoses for "*M. c. intermedius*" (which were employed for comparative purposes with other Xinjiang *Olivierus*) might have pooled both the Chinese and Kazakhstan specimens, and will not be rediscussed here (see Tang, 2022c: 4–12). Below, taxonomic problems of the three *Olivierus* species endemic to Xinjiang, China, are reiterated. The true identities for the two unpublished species described by Zhang (2009) in his thesis under the guidance of Mingsheng Zhu (the second author of *O. bolensis* and *O. longichelus*), "*M. beijiangensis*" and "*M. nanjiangensis*", as deduced by Tang (2022c: 12–13), are *nomina nuda* conspecific with *M. thersites* and *O. przewalskii* respectively and will not be further expounded upon.

The original descriptions of those species were often hindered by limited specimen availability and, at times, inadequately substantiated comparisons. The illustrations for those species were all hand-drawn and their precision relies on the technical setup for visual inspection (e.g., optically preferred with UV illumination) and the degree of personal bias. Description of new species within a genus comprising highly resemblant congeners necessitates a meticulous approach, particularly when involving scant adult specimens. In such instances, the justification of a new species hinges on the presence of unique qualitative characters or non-overlapping (or nearly so) quantitative characters. The challenge of a deficient sample size lies in its potential to obscure intraspecific variations, thereby introducing biases during morphological evaluations. When describing a new species, prioritizing the determination of sex and maturity is paramount. Regrettably, this facet was often neglected in the aforementioned papers. For most buthids, the only useful characters in juveniles are the denticle subrows of chela movable finger and the pectine morphology (i.e., PTC and presence/absence of enlarged basal tooth/lamella). Contrarily, other age-independent attributes typically lack discriminatory value within the same genus (e.g., lateral ocelli number and cheliceral dentition). Total length, development of carinae and granules, and ratiometrics of telson (including shape, presence/absence of subaculear tubercle, and relative aculeus length) and pedipalp chela are all age-dependent and often used as

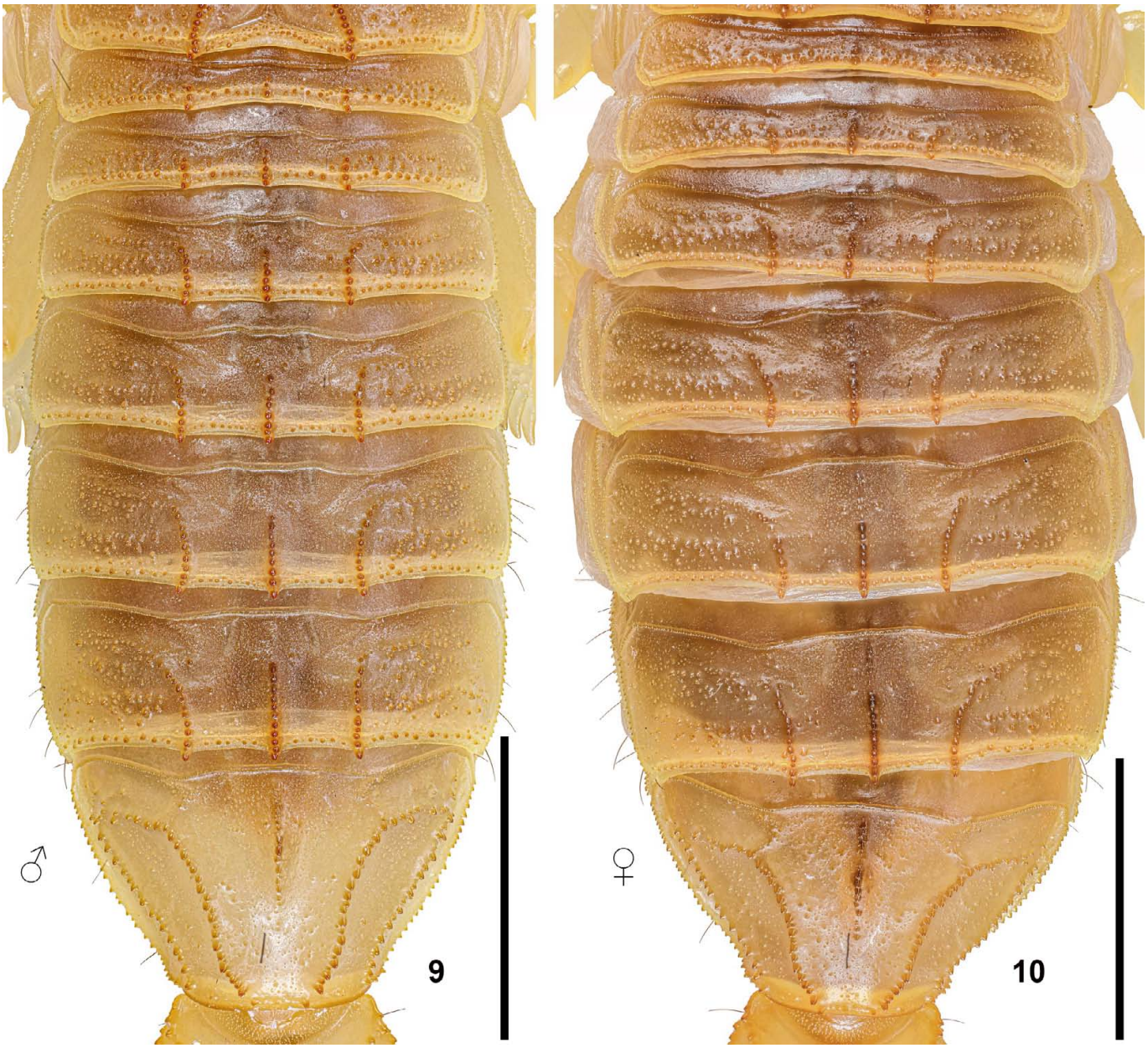

Figures 9–10. *Olivierus longichelus* (Sun & Zhu, 2010), tergites of male from Jinghe County (9) and female from Bole City (10) under white light. Scale bars = 5 mm.

diagnostic characters. It is crucial to note that characteristics like the infuscation of metasoma V (laterally and ventrally), as depicted in Tang (2022c: fig. 6), may be susceptible to intraspecific variability.

To begin with, *O. longichelus* was based on a female and a pair of juveniles (Sun & Zhu, 2010: 5) from Jinghe. The authors compared their new species with "*M. c. intermedius*" from Kazakhstan and *O. przewalskii* by the following characters: (1) CL/W ("shape of chela"); (2) ML of metasoma II and III; (3) VL of metasoma V. All three characters are age-dependent, with characters 2 and 3 displaying discernable intraspecific variability; however, only a single "adult" female was available. Later the same year, *O. bolensis* was described with a holotype male from Bole and a paratype female from Yining (Sun et al., 2010: 36). The authors juxtaposed their new species against the holotype of *O. longichelus*, underscoring the following differential characters: (1) TL: larger in *O. bolensis* (male 57 mm, female 71 mm), vs. *O. longichelus* (female 52 mm); (2) metasoma V coloration: non-infuscate in *O. bolensis* vs. infuscate in *O. longichelus*; (3) carapace granulation: denser in *O. bolensis*; (4) carapace and patella carinae: dispersive granular in *O. bolensis*, but formed by single, explicit rows of granules in *O. longichelus*; (5) VL of metasoma V: posterior denticles larger in *O. longichelus*; (6) CL/W: more robust in *O. bolensis* (male 4.08, female 4.77), vs. *O. longichelus* (female 5.42) (erroneously cited as length/width ratio of telson in Tang (2022c: 5)). Upon scrutinizing the original data and figures alone, based on a prior knowledge: (i) characters 1 and 2 are intraspecifically variable and can be biased by low sample size (character 1 is also age-

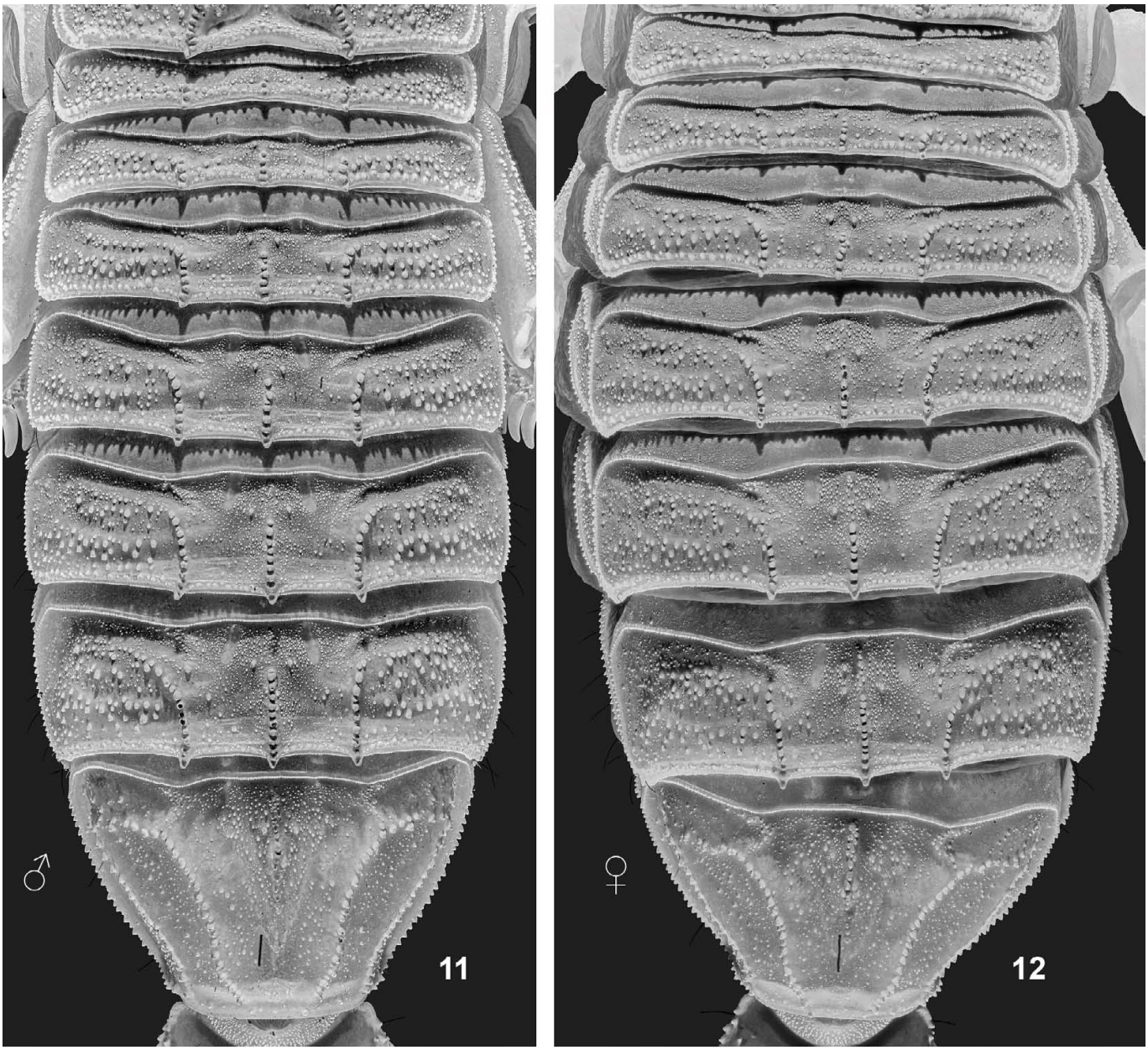

Figures 11–**12**. *Olivierus longichelus* (Sun & Zhu, 2010), tergites of male from Jinghe County (11) and female from Bole City (12) under UV light.

dependent); (ii) character 3 can be age-dependent, or biased either subjectively (owing to the absence of photos) or by low sample size; (iii) characters 4 and 5 can be age-dependent; (iv) character 6 is highly age-dependent. Tang (2022c) studied 14 specimens of *O*. sp. from Wujiaqu, Xinjiang (unpublished data). Following those results: (i) character 2 was rejected for its utility; (ii) character 3 was found age-dependent, denser in adults; (iii) carapace carinae of character 4 was somewhat age-dependent but also intraspecifically variable, while patella carinae of character 4 was more similar to the illustration for *O. longichelus*, notwithstanding those illustrations for *O. bolensis* could have potentially been exaggerated for enhanced differentiation; (iv) character 5 was not significantly age-dependent, yet the intraspecific variability remained. Most importantly, characters 1 and 6 in combination suggested a a strong likelihood for the holotype of *O. longichelus* to be immature. Moreover, pedipalp femur of both species was also depicted differently in Sun et al. (2010: figs. 7, 12). The *O*. sp. from Wujiaqu resembled more with *O. longichelus* in terms of the carinal granulation, while a likeness towards *O. bolensis* was observed concerning intercarinal granulation (which was somewhat age-dependent). Again, those carinae could have been dramatized for distinct differentiation. Since the two species also shared an overlapped PTC range (Tang, 2022c: table 1; collectively: male 27–28, female 22–23), Tang (2022c: 6) speculated that *O. bolensis* is most likely a junior synonym of *O. longichelus*.

On the contrary, the description of *O. karshius* was founded upon a more substantial sample size, encompassing 45 specimens from Yarkant (“Shache”), alongside 15 additional

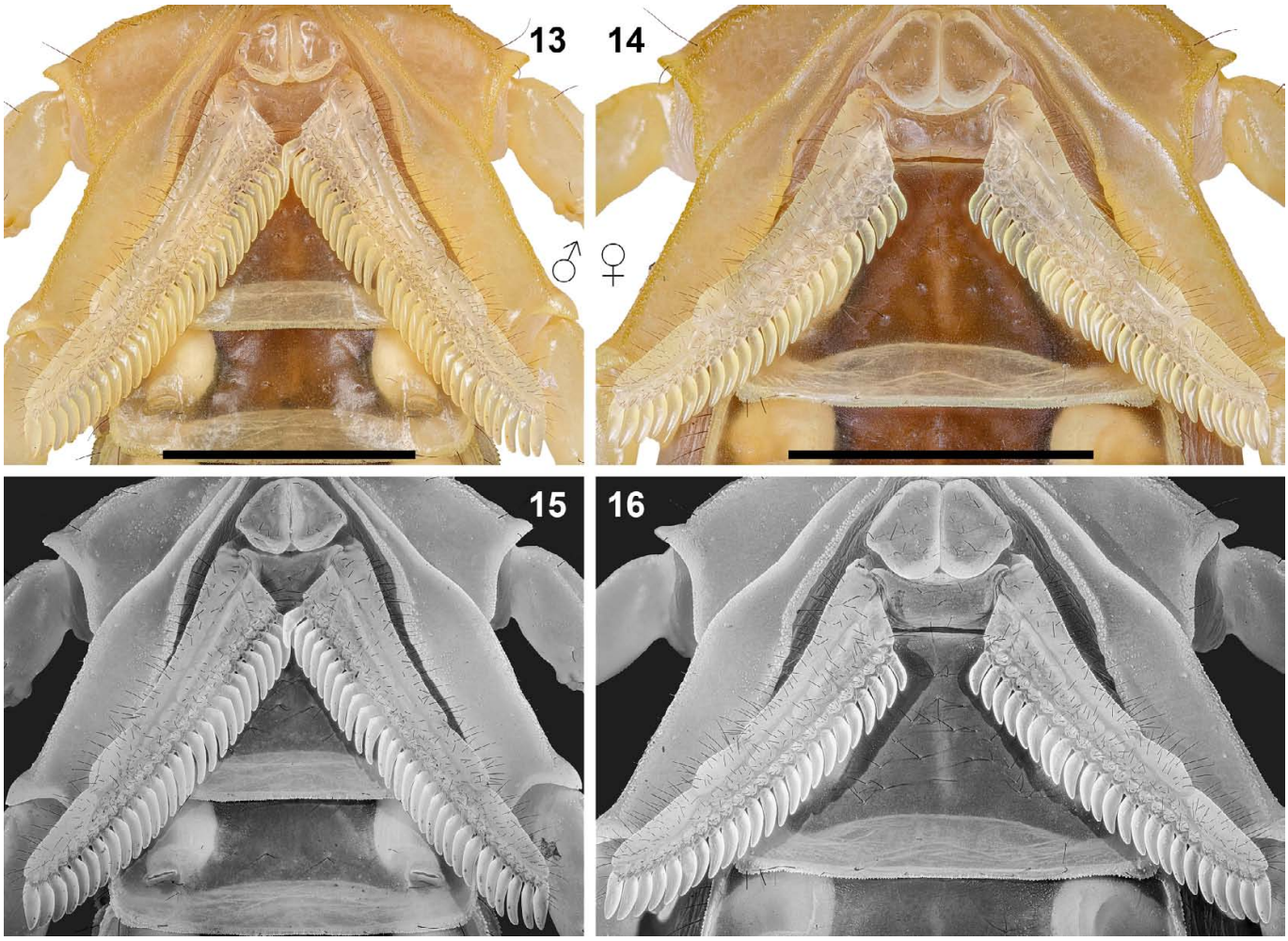

Figures 13–**16**: *Olivierus longichelus* (Sun & Zhu, 2010), pectines of male from Jinghe County (13, 15) and female from Bole City (14, 16). **Figures 13**–**14**. Under white light. **Figures 15**–**16**. Under UV light. Scale bars = 5 mm.

specimens collectively obtained from Artux and Kashgar cities (Sun & Sun, 2011: 63). Although this may seem like a sufficient number for study, as documented by Tang (2022c), certain confusions persisted (e.g., metasoma V infuscation). A serious problem is concerned with the "*M. c. intermedius*" specimens they studied (and used to compare with their new species), which included both Xinjiang and Kazakhstan materials. The three specimens from Xinjiang, as aforementioned, were all sourced from the vicinity of the type locality of *O. bolensis*. However, in the original description of *O. bolensis*, there was no direct comparison with "*M. c. intermedius*", and Sun & Sun (2011) did not investigate whether those materials belonged to the same species with Kazakhstan "*M. c. intermedius*" or the sympatric *O. bolensis*. They opted instead to directly compare *O. karshius* with those "*M. c. intermedius*" and listed four differences: (1) PTC: male 23–28 and female 19–23 in *O. karshius* vs. but male 26–30 and female 20–25 in "*M. c. intermedius*"; (2) metasoma V infuscation (those on other body parts are hereby neglected): absent in *O. karshius* vs. present in "*M. c. intermedius*" (however, as what they stated for their new species "*...Several individuals with light brown to brownish-yellow pigmentation on the ventral surfaces of metasoma segment V, and most individuals without...*"); (3) EAD on pedipalp fingers: uniform in size from base to tip and nearly as large as IAD in *O. karshius* vs. reducing in size from base to tip and smaller than IAD in "*M. c. intermedius*" (this was not clearly illustrated; cf. Sun & Sun, 2011: figs. 4j and 6h); (4) longitudinal setation row on tarsus of legs: short in *O. karshius* vs. long in "*M. c. intermedius*" (not illustrated). Even if all those differences were justifiable, assuming they did study both Xinjiang and Kazakhstan materials, uncertainty remains as to whether those characters described for "*M. c. intermedius*" can be applied to both populations or if they simply merged characters of two species. Two new features for comparison were proposed, EAD and tarsal setation row. For the first character, *O. longichelus* and *O. przewalskii* were both described as having the same condition with that of "*M. c. intermedius*" (Sun & Zhu, 2010: 5, 9) while this character was ignored for *O. bolensis*. For the second character, *O. bolensis*, *O. longichelus* and *O. przewalskii* ("moderate to long") all matched the state of "*M. c. intermedius*" (Sun & Zhu, 2010: 5, 10; Sun et al., 2010: 36). Those qualitative characters can be, however, biased if they were not objectively measured. Furthermore, *O. karshius* was also compared with

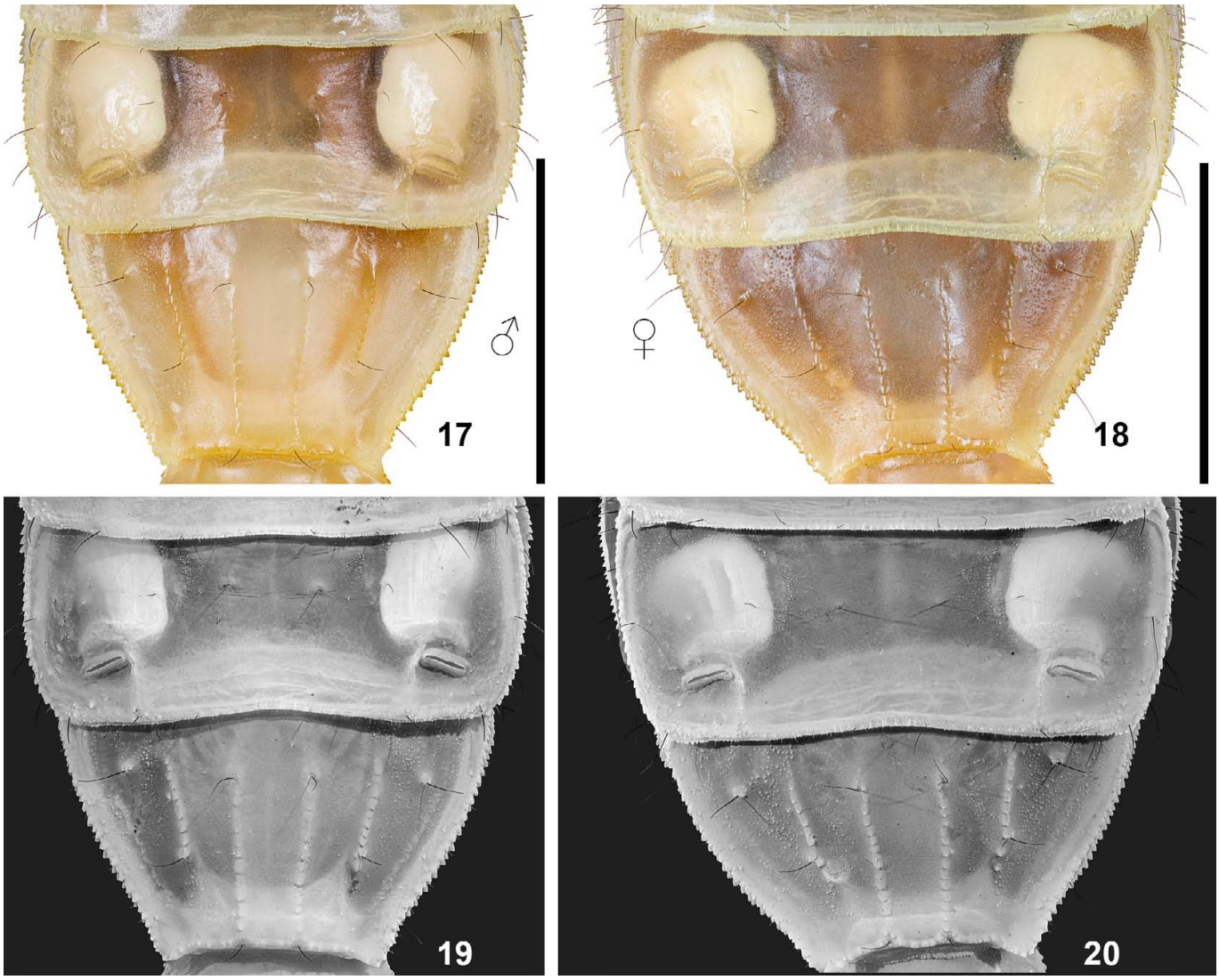

Figures 17–**20**: *Olivierus longichelus* (Sun & Zhu, 2010), sternites VI–VII of male from Jinghe County (17, 19) and female from Bole City (18, 20). **Figures 17**–**18**. Under white light. **Figures 19**–**20**. Under UV light. Scale bars = 5 mm.

its geographic neighbor, *O. przewalskii*, incorporating a few qualitative (carapacial carinae and granules development, infuscation, and length of tarsal setae) and quantitative characters (DSC and PTC).

The key feature shared by *O. bolensis*, *O. longichelus* and *O. karshius*, as outlined in their respective original descriptions, is the presence of 12 denticle subrows on movable finger. Conversely, *O. przewalskii* has consistently been described as having only 11 subrows (Sun & Zhu, 2010: 5; Sun & Sun, 2011: 65; Zhang et al., 2020: 85). For PTC, as above discussed, *O. bolensis* and *O. longichelus* share an overlapping range (male 27–28, female 22–23). *O. przewalskii* was recorded with the lowest range (male 19–23, female 15–19; Sun & Zhu, 2010: 5), with these data seemingly merely reutilized across different subsequent publications (e.g., Sun & Sun, 2011; Zhang et al., 2020). In terms of the number of specimens upon which the description of *O. przewalskii* was based, Sun & Zhu (2010: 4) examined 182 specimens, while Zhang et al. (2020: 85) studied 78 specimens. *O. karshius* was featured with an intermediate PTC range (male 23–28, female 19–23). The holotype female of *O. karshius* was illustrated with 12 denticle subrows and a PTC of 22/21, while the male paratype was illustrated with a PTC of 25/25 (Sun & Sun, 2011: figs. 6d–e, 6h).

Denticle subrow of pedipalp movable finger

The row of denticles/granules on the pedipalp movable finger often serve important diagnostic purposes. Three main denticle types are recognized as internal accessory denticle (IAD), median denticle (MD) and external accessory denticle (EAD) (Tang et al., 2023: 9) in Buthidae. Most buthids possess all three types, with the exception of certain taxa that lack EAD (Tang et al., 2023: 10) and several taxa that have additional accessory denticles (in Centruroidinae; e.g., Lowe & Fet, 2024: figs. 106, 115, 118, 121). MD constitutes the primary axial denticle series, flanked internally by IAD along the MD series, and externally by EAD next to the most proximal MD

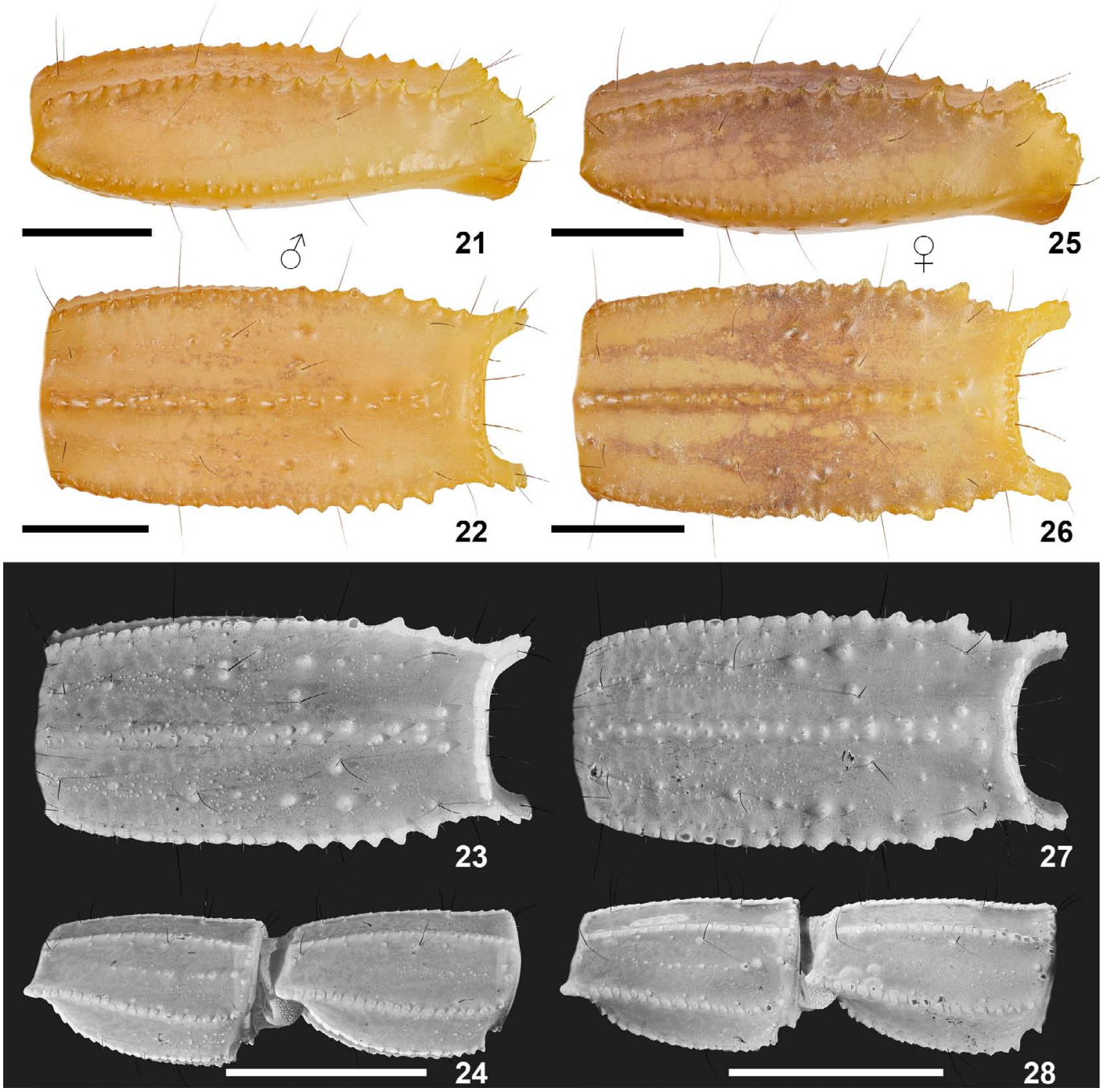

Figures 21–**28**: *Olivierus longichelus* (Sun & Zhu, 2010), metasoma V in lateral (21, 25) and ventral (22, 26) views under white light, metasoma V in ventral view (23, 27) and metasoma II–III in lateral view under UV light (24, 28). **Figures 21**–**24**. Male from Jinghe County. **Figures 25**–**28**. Female from Bole City. Scale bars = 2 mm (21–22, 25–26) and 5 mm (24, 28).

that is usually enlarged. This spatial arrangement often renders an exteriorly oblique configuration, with IAD being the most distal and EAD being the most proximal. The entire denticle series comprising all three denticle types along the dorsal edge of movable finger can be termed a "row", while each MD section within each group of "IAD-MD-EAD" is considered a "subrow" (but see below for further discussion). Since not all scorpion species have a well partitioned denticle row (e.g., Lowe & Fet, 2024: figs. 265, 271, 289, 292, 295, 301, 310, 334), the term "row" is therefore recommended to equivocally denote the entire series regardless of the potential intricacy, as above defined. Notably, the distal series composed of several subterminal denticles is typically too short to be referred to as a row (as "apical row" when it consists sufficient denticles), although it is apparently homologous with the subsequent subrows and the terminal denticle could be considered a special case of an enlarged MD (Lowe & Fet, 2024: 77). The arrangement of each pair of adjacent subrows gives rise to the two categories for the entire denticle row, imbricated and non-imbricated, defined by the degree of overlapping therebetween

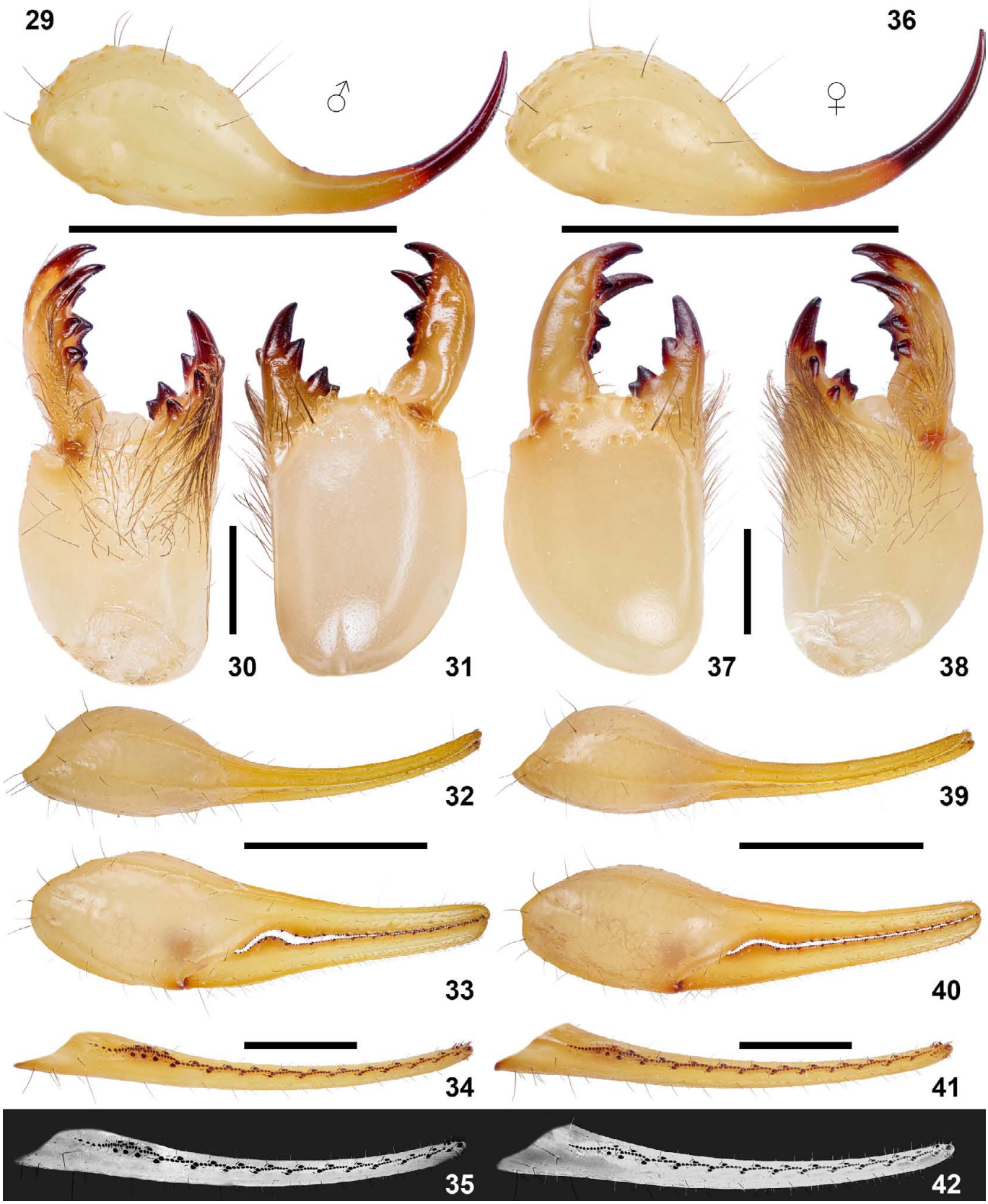

Figures 29–**42**: *Olivierus longichelus* (Sun & Zhu, 2010), telson in lateral view (29, 36), chelicera in dorsal (31, 37) and ventral (30, 38), right pedipalp chela in dorsal (32, 39) and external (33, 40) views under white light, and dentate margin of right movable finger under white (34, 41) and UV (35, 42) light. **Figures 29**–**35**. Male from Jinghe County. **Figures 36**–**42**. Female from Bole City. Scale bars = 5 mm (29, 33, 36, 40), 2 mm (34, 41) and 1 mm (31, 37).

(Tang et al., 2023: 10). The genus *Olivierus* is considered as having non-imbricated denticle rows. Despite this, its subrows still exhibit a somewhat slanted arrangement.

However, as mentioned earlier, having only 11 subrows excluded *O. przewalskii* from its concordance with the generic diagnosis proposed by Kovařík (2019: 26), in which *Olivierus* was defined as having 12–14 subrows. After comparing photos of movable fingers in the past literature (Fet et al., 2018: figs. 304–313; Fet et al., 2021: figs. 32, 43, 73, 84, 107; Zhang et al., 2020: fig. 6), in combination with the inspection upon materials examined in this study, it became apparent that this discordance resulted from the ambiguity of adjacent subrows at the proximity. The separation between the two most proximal subrows can be inexplicit and appear linear in one row, owing to the negligible obliqueness of the penultimate subrow (e.g., Fet et al., 2018: 307, 312–313), which depends on whether a denticle is present immediately anterior to the final EAD (i.e., small interdental distance) to ensure continuity, thereby including the EAD in the penultimate subrow. The identification of the most proximal subrow hence hinges on whether it is unambiguously departed from the penultimate subrow. Since the degree of obliqueness is variable, the enumeration could be susceptible to subjective bias. This prompted a reconsideration of the subrow discrimination method for genus *Olivierus*.

Using the distal denticle row groups which are often unequivocally separated as the example, typically, the MD subrow must be accompanied by an IAD and an EAD as above defined, rendering it a slightly slanted configuration. Therefore, the EAD or the conspicuously enlarged MD can be used as the indicator for the presence of subrow. It must also be noted that the MD might reduce in size when approaching proximity, rendering its adjacent EAD appear larger than the most proximal MD. However, the EAD appears only at the end of the subrow, it thus leaves the most proximal subrow devoid of an EAD (as well as an IAD). In that case, the number of subrows would equal the number of EAD plus 1. Such enumeration method promotes *O. przewalskii* to be regarded as having 12 subrows, aligning it with the generic diagnosis, should one only consider the exemplary illustration provided by Zhang et al. (2020). However, this would also render *O. fuscus* (Birula, 1897) and *O. mischi* (Fet et al., 2018) having 15 subrows given their presence of 14 EAD (Fet et al., 2018: figs. 308, 311). To reduce ambiguity and subjective bias, we recorded DSC for our studied materials based solely on the number of EAD instead. Surprisingly, results derived from this enumeration method evidently did not deviate from the past documentations (see below), which may suggest a similar method may had been used by the previous authors. Nevertheless, this still warrants a revised generic diagnosis.

One way to ensure a consistent and unbiased enumeration method is to define two types of subrows – one accompanied by both IAD and EAD ("complex subrow") and the other lacking any accessory denticles ("simple subrow", always being the most proximal subrow), thus the total DSC is defined as the number of complex subrows plus one (being the simple subrow). Following the previous definition for subrow, the complex subrow includes neither IAD or EAD, only that it is topologically flanked by those two accessory denticles. This method is thus restricted to taxa possessing IAD and EAD (or one consistently enlarged MD within each complex subrow). Therefore, the DSC recorded for the Xinjiang *Olivierus* species in this paper accounts for the "complex subrow" only. As an exemplary illustration, readers are free to refer to Figs. 169–187 pertaining to the issues hereby discussed, which visualized our considerations for the denticle row count.

Results

Morphological analysis

Primary inspections upon those specimens discerned only two unidentified species (or morphological groups) with overlapping origins: **(1)** Group A: species with larger size, more slender chela and metasoma, and more serrated metasoma V (26 specimens); **(2)** Group B: species with smaller size, more robust chela and metasoma, and less serrated metasoma V (78 specimens). Consequently, two separate groups were established for analysis, one for each type within each locality (where applicable). To encapsulate, the following specimens were scrutinized: 8 specimens from Jinghe County (all alive when received; all belonged to Group A), 12 specimens from Bole City (all alive when received; four belonged to Group A), 5 specimens from Ghulja (or Gulja, Yining) County (all alive when received; one belonged to Group A), 23 specimens from Yarkant (or Shache) County (14 dead when received; two belonged to Group A including a dead adult female highly desiccated and unrecorded for PTC), 24 specimens from Makit County (17 dead when received; four belonged to Group A), 19 specimens from Qiemo County (all dead when received; six belonged to Group A), and 13 specimens from Ruoqiang County (all dead when received; one belonged to Group A). Two and seven *M. thersites* were also found in the specimen series from Yarkant and Qiemo counties respectively, judged by their relatively bulbous telson, robust chela and dentate metasoma; these specimens were excluded from above tally and not subjected to detailed examination (overall photographs available in aforementioned ZIP. files).

In agreement with the crude visual inspection, the morphometric analyses conducted upon several quantitative characters delimited only two morphological groups, irrespective of the geographical origin (Figs. 120–127). Within Group A, topotypes of *O. longichelus* from Jinghe and those of *O. bolensis* from Bole showed no difference from those of Wujiaqu (cf. Tang, 2022c: figs. 4, 6–7) studied in Tang (2022c) which were used to suggest *O. bolensis* being synonymous with *O. longichelus*. These two specimen series also exhibited no distinct differences from the one from Ghulja (paratype locality of *O. bolensis*), as well as from the remaining localities. Despite the sympatric distribution of two morphological groups in Bole, distinct characters rejected the likelihood that the type series of *O. bolensis* completely or partially falls under Group B,

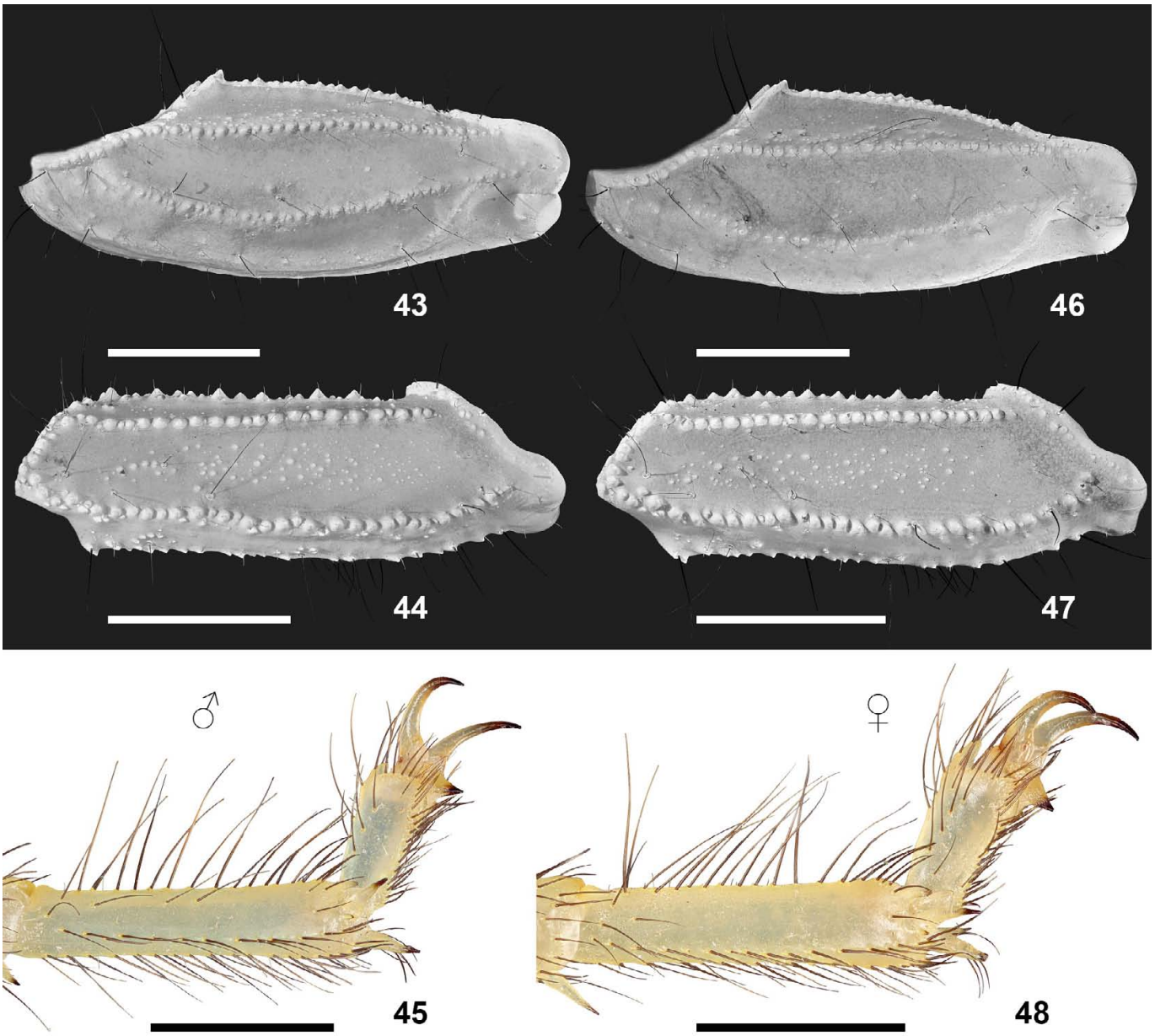

Figures 43–**48**: *Olivierus longichelus* (Sun & Zhu, 2010), right pedipalp patella (43, 46) and femur (44, 47) in dorsal view under UV light, and telo- and basitarsi of right 3rd leg in retrolateral view under white light (45, 48). **Figures 43**–**45**. Male from Jinghe County. **Figures 46**–**48**. Female from Bole City. Scale bars = 2 mm.

particularly when referring to the PTC data. Hence, based on the current finding and the original description of *O. bolensis*, a new synonym is proposed: *Mesobuthus bolensis* Sun et al., 2010 = *Olivierus longichelus* (Sun & Zhu, 2010), **syn**. **n**.. All members in Group A were therefore identified as *O. longichelus*. Both morphological groups were identified in the specimen series from Yarkant (type locality of *O. karshius*), as well as an adjacent county, Makit. However, the original description of *O. karshius* only documented the presence of a single species among the 44 paratypes from Yarkant. Given that the type materials were not accessible for external examination (either as photos or virtual specimens), a valid assumption could be made that the type series of *O. karshius* possibly encompassed more than one unique species.

Problems with this species are complicated. Since neither the material nor photo of the holotype was accessible, comparisons were confined to the original description and materials obtained from Yarkant, Makit, Qiemo and Ruoqiang in this study. A few perplexing characters associated with the holotype female *O. karshius* impeded identification. Many qualitative characters portrayed in the original paper appeared to bear greater resemblance to *O. przewalskii* than to *O. longichelus* (or *O. bolensis*): **(1)** chela manus lateral dilation degree (cf. Sun et al. (2010: fig. 15) and Sun & Sun (2011: figs. 2g, 6f)); **(2)** chela lateral profile (cf. Sun et al. (2010: fig. 16) and Sun & Sun (2011: figs. 2f, 6g)); **(3)** metasoma V lateral profile (cf. Sun et al. (2010: fig. 22) and Sun & Sun (2011: figs. 2m, 6m)); **(4)** VM of metasoma V (cf.

Sun et al. (2010: figs. 21, 23) and Sun & Sun (2011: figs. 2i, 6i)); **(5)** relative length of aculeus (cf. Sun et al. (2010: fig. 22, 24) and Sun & Sun (2011: figs. 2m, 6m)); **(6)** intercarinal distance on mesosoma somewhat wide relative to the tergite width and approximated that of the *O. przewalskii* specimens examined herein (cf. Sun & Sun, 2011: fig. 5). Particularly focusing on character 4, the VM in *O. przewalskii* and *O. karshius* were both depicted as a disordered row of dispersive granules, while *O. bolensis* and *O. longichelus* showcased a single row of continuous granules. In tandem with the examination upon materials inspected in this study, most individuals in Group A displayed a single row (or subtly dispersive at some sections), while individuals with highly dispersive VM only appeared in Group B (see ZIP. files on ResearchGate). In addition, the VL of metasoma V illustrated for the holotype female *O. karshius* seemed to lie between those of *O. bolensis* or *O. longichelus* and *O. przewalskii*. The latter was illustrated as discrete granules (Sun & Sun, 2011: fig. 2i), while the former exhibited enlarged denticles posteriorly (Sun et al., 2010: figs. 21, 23). The size of those denticles illustrated for the holotype female *O. karshius* more closely aligned with the specimens in Group B, lacking the drastic size surge posteriorly as observed in Group A. On the contrary, carapace carination and granulation seemed to show more similarity with Group A (cf. Sun et al. (2010: figs. 2–4) and Sun & Sun (2011: figs. 2a, 6a)). This apparent "chimera" of intermediate characters reminded us of *Heterometrus liangi* described by Zhu & Yang in 2007, which was featured by a combination of partial *H. silenus* (Simon, 1884) (as *H. petersii* (Thorell, 1876)) and *H. laoticus* Couzijn, 1981 characters, subsequently suggested as a junior synonym (again, based on immature specimens) of the former species (Prendini & Loria, 2020: 287). In any case, it must be acknowledged that qualitative traits can be susceptible to biases introduced through hand-drawn illustrations (e.g., Graeme & Kovařík, 2022: 59).

The two quantitative characters used by Sun & Sun (2011) to distinguish their new species from *O. przewalskii* were DSC and PTC. In the present study, *O. przewalskii* has indeed been recorded with 12 subrows; however, the DSC of most individuals coalesced at the value of 11 (Table 3, Fig. 122). In terms of the PTC, the maximal value for male and female *O. przewalskii* were given as 23 and 19 respectively (Sun & Zhu, 2010: 5), both lower than the holotype female (22/21) and paratype male *O. karshius* (25/25). According to the authors, *O. karshius* was abundant in the type locality (Sun & Sun, 2011: 67), which may suggest a relatively high likelihood of a successful collection targeting this species. However, as above discussed, the current expedition failed to uncover any specimens fully conforming to the original description of the holotype female *O. karshius*. Given the susceptibility of qualitative characters presented in hand-drawn illustrations to inaccuracies, *O. karshius* is hereby tentatively deemed synonymous with *O. longichelus* based on two quantitative characters (DSC and PTC), therefore: *Mesobuthus karshius* Sun & Sun, 2011 = *Olivierus longichelus* (Sun & Zhu, 2010), **syn**. **n**. Nevertheless, we acknowledge the possibility of an alternative, less common species representing the abstruse *O. karshius* holotype occurring sympatrically, in the event that future scrutiny of the type specimen reveals distinct morphological features.

Molecular analysis

To rule out the possibility of the presence of cryptic species as observed previously in *O. gorelovi* (Fet et al., 2018) (Graham et al., 2019; Fet et al., 2021), we attempted to sequence all the populations studied. Unfortunately, both 16S and COI sequences were not retrieved for both species from Qiemo and Ruoqiang, since all the specimens were already dead and not preserved in pure ethanol by the collector. In terms of *O. przewalskii*, the aforementioned morphological analysis detected four new putative localities which were successfully sequenced. The absence of molecular data from Qiemo and Ruoqiang where *O. przewalskii* was previously reported prevented us from determining the identity of the four new populations. To address this, we incorporated the previous data of *O. przewalskii* from those two counties as well as those of the other reported localities of this species retrieved by Zhang et al. (2020) which only included COI sequences. Additionally, we also appended the COI sequences of *O. martensii* retrieved by Shi et al. (2013) in our tree.

Our tree was based only on the COI sequences in order to maximize the information included (Fig. 131). Aside from the two dubious species (see below), another two species were also omitted, *O. brutus* (Fet et al., 2018) (no DNA available; Fet et al., 2018: 9) and *O. mischi* (Fet et al., 2018) (phylogenetic position uncertain: Fet et al., 2018: 66). The topological deviation observed in comparison to previous trees (Fet et al., 2018: fig. 329; Zhang et al., 2020: fig. 9; Fet et al., 2021: fig. 109) can be ascribed to the absence of whole-genome data in any of the trees, thereby rendering its higher sensitivity to the alteration of included sequences. However, the lineages examined in this study were consistently recovered as two distinct clades. The examined new populations of *O. przewalskii* grouped well within the formerly investigated lineages. In addition, the coalescence of various lineages of *O. longichelus* rejects the assumption for cryptic species. As there was no preceding sequence for *O. longichelus* from Qiemo and Ruoqiang, we were unable to incorporate the two lineages or molecularly confirm their identities. However, morphological analysis did not detect any conspicuous differences between the two lineages and others. Furthermore, referring to the currently observed geographic pattern, we believe that they also represent *O. longichelus*. Our study discovered that *O. longichelus* and *O. przewalskii* are sympatric in many regions of Xinjiang, including the Makit and Yarkant counties in the west, and Bole and Ghulja counties in the north. It would be unsurprising if *O. longichelus* has also extended to the southeast region (Qiemo and Ruoqiang counties) as *O. przewalskii*.

The type locality of *O. tarabaevi* is located in the Shieli District of Kazakhstan, somewhere northwest of Baygekum (as "Baigakum"; Fet et al., 2021: 65). Additional populations were found in Talas (mislabeled as "Balkhash") District, Khantau Village, and Qonayev (as "Kapchagay") City (Graham et al., 2019: table 1). The genetic sequences for those populations were labeled as VF3002 (Baigakum), VF3005 ("Balkhash"), VF3007 (Khantau) and VF3009 (Kapchagay or Kapchagai), respectively (Graham et al., 2019: table 1; Fet et al., 2021: fig. 109). Notably, in Graham et al. (2019), only 16S gene was used for all populations, while VF3009 lacked COI sequence, leaving it with a grey mark in their figure 4 where species delimitation methods based solely on COI were employed. Its COI was used once in Gantenbein et al. (2003: table 1, coded as "AJ550692"). During our preliminary phylogenetic analysis based on COI, we found this population to be grouped with *O. mikhailovi* from Chardara (labeled VF3006), rendering *O. tarabaevi* lineage paraphyletic. We suspect the original locality label "Kapchagai" was incorrect (which may, in fact, be somewhere in the southwest region, closer to *O. mikhailovi*), and therefore excluded this sequence from our study. Likewise, earlier studies placed a lineage from Talas ("Balkhash") closely with "Kapchagai" (Graham et al., 2019: fig. 4; Fet et al., 2021: fig. 109), a sequence which also rendered an anomalous position in our current analysis based on both MaL and BI, and was thus excluded. As shown in Fig. 131, our current molecular analysis does not support *O. tarabaevi* as a distinct species from *O. longichelus*, hence the synonym: *Olivierus tarabaevi* Fet et al., 2021 = *Olivierus longichelus* (Sun & Zhu, 2010), **syn**. **n**.. An additional analysis based on ASAP method has also consistently recovered those lineages (two lineages of *O. tarabaevi* from Kazakhstan and eight lineages of *O. longichelus* from China) as one species (unpublished data). However, we have retained this species in Figs. 130, 181–182 and Table 5 so as to provide additional information for its distribution and morphological characters in comparison with *O. longichelus*. An alternative explanation is the mitochondrial introgression that led to the apparent amalgamation of the two species within the tree. However, if the holotype of *O. longichelus* was already a hybrid, then logically, for the introgression to account for the observed results, the authentic Chinese species that is distinct and isolated from *O. tarabaevi* must be first determined, which is out of our scope. Given the inaccessibility to the type materials, we cannot confirm if it would be placed outside the clade recovered herein, representing the putative "pure breed" of *O. longichelus*. The synonymization of *O. tarabaevi* with *O. longichelus* suggests that the "*M. c. intermedius*" from Taukum in Almaty Region studied by previous Chinese authors (Sun & Zhu, 2010; Sun & Sun, 2011) also represents the latter species. Additional report of "*M. c. intermedius*" in China falls within the distribution range of *O. longichelus* implied by the current study (Bole and Yining; Sun & Sun, 2011: 61).

Specimens from two localities located in the Gurbantünggüt Desert of the Junggar Basin, viz. Shawan and Wujiaqu, as well as two localities near the border between Kazakhstan and China, viz. Korgas and Khorgos, were also genetically confirmed to be conspecific with *O. longichelus* in this study. The COI sequence of *O.* sp. from Korgas was not retrieved, but we confirmed its position within the tree by additionally performing the analysis based on its 16S sequence (unpublished data). All these results suggest a substantial distribution area for both species. Conclusively, the widespread *O. longichelus* represents a sister species to *O. mikhailovi*, *O. gorelovi* and *O. voldemari* Fet et al., 2021. It is noteworthy that the observed within-clade positions of different lineages of *O. longichelus* do not align with their relative geographic proximity, which is a consequence of the recency of this clade that diverged at approximately 0.5 mya.

Interspecific comparison

Despite their seemingly morphological resemblance based on the prior knowledge from the past papers, it here turned out that *O. longichelus* can be confidently distinguished from *O. przewalskii* by at least a total of 15 aspects (expressed in $\bar{x} \pm S$ for quantitative characters; full data range in diagnoses):

(1) General coloration darker in *O. przewalskii*, which often has a more infuscate anterolateral region on carapace internal to the lateral ocellus, more infuscate carapacial carinae and more infuscate lateral and ventral surfaces of metasoma V.

(2) Size larger in *O. longichelus* (♂ (*n* = 17) 58.01±2.2 mm, ♀ (*n* = 5) 60.64±2.74 mm) than *O. przewalskii* (♂ (*n* = 55) 47.48±2.58 mm, ♀ (*n* = 9) 53.7±4.71 mm), but more sexually dimorphic in the latter. Differences were statistically significant despite the low sample size: male-male, $p < 0.05$ (5.934e-10), $Z = 6.1922$; female-female, $p < 0.05$ (6.993e-3), $Z = 2.6972$. Although the result with females should be treated with caution, adult female *O. longichelus* from other localities (see below) were never smaller than the examined 5 specimens here. Therefore, we believe the size discrepancy to be stable.

(3) CM and PM of carapace extend towards the posterior margin of carapace in the same direction with the lateral margin thereof in *O. longichelus* (forming a greater included angle if they were extended anteriorly to the infinity), while PM become nearly parallel with each other in *O. przewalskii*.

(4) Carapace adorned by finer granules with finely granulated intercarinal surfaces and appear matte in *O. longichelus*, but adorned by coarser granules with smoother intercarinal surfaces and appear lustrous in *O. przewalskii*.

(5) Intercarinal distance of the three tergal carinae smaller in *O. longichelus* with respect to the lateral margins, but greater in *O. przewalskii*.

(6) PTC higher and more sexually dimorphic (Fig. 128; see Table 4 for relative PTC frequencies) in *O. longichelus* (♂ (*n* = 51) 27.63±0.98, ♀ (*n* = 40) 22.95±0.93) than *O. przewalskii* (♂ (*n* = 114) 20.66±1.22, ♀ (*n* = 34) 17.79±0.91), with index of dispersion lower in *O. longichelus* (♂: *D* =

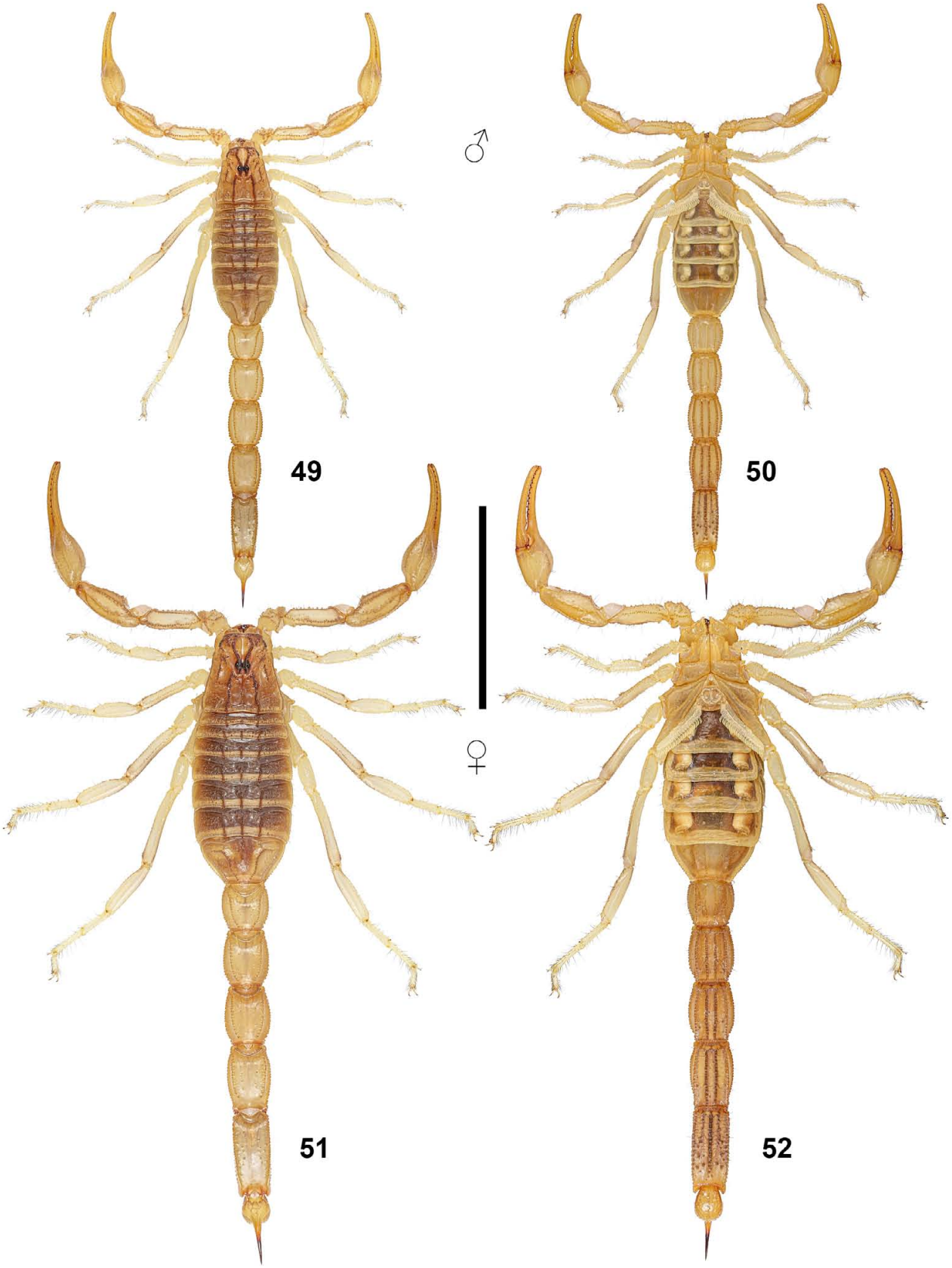

Figures 49–**52**: *Olivierus przewalskii* (Birula, 1897), habitus under white light. **Figures 49**–**50**. Male from Ghulja (Yining) County, in dorsal (49) and ventral (50) views. **Figures 51**–**52**. Female from Yarkant (Shache) County, in dorsal (51) and ventral (52) views. Scale bar = 20 mm.

0.035; ♀: D = 0.04) than *O. przewalskii* (♂: D = 0.059; ♀: D = 0.05). Differences in PTC were statistically significant: male-male, $p < 0.05$ (≈ 0), $Z = 10.377$; female-female, $p < 0.05$ (8.26e-14), $Z = 7.648$.

(7) Pedipalp movable finger with higher DSC (males and females pooled together) in *O. longichelus* (12.49±0.4, $n = 51$) than *O. przewalskii* (10.92±0.5, n = 155). Differences were statistically significant: $p < 0.05$ (≈ 0), $Z = 12.3604$.

(8) Pedipalp chela more slender and sexually dimorphic in *O. longichelus* (CL/W: ♂ (n = 34) 4.59±0.11, ♀ (n = 10) 4.8±0.16) than *O. przewalskii* (CL/W: ♂ (n = 108) 4.1±0.15, ♀ (n = 18) 4.25±0.12; one male with abnormally slender chela (CL/W = 4.81) was excluded), also with proportionally longer fingers in the former (more prominent when comparing juveniles). Differences in CL/W were statistically significant: male-male, $p < 0.05$ (8.882e-16), $Z = 8.7603$; female-female, $p < 0.05$ (1.524e-7), $Z = 5.2496$.

(9) Dorsal intercarinal area of pedipalp femur granulate in *O. longichelus* but nearly smooth in *O. przewalskii*.

(10) Setae of basi- and telotarsi relatively denser, thinner, and longer in *O. longichelus*.

(11) Metasomal segments more slender in *O. longichelus* (L/D: of IV, ♂ (n = 17) 1.97±0.05, ♀ (n = 15) 2±0.07; of V, ♂ (n = 17) 2.9±0.06, ♀ (n = 5) 2.9±0.04) than *O. przewalskii* (L/D: of IV, ♂ (n = 55) 1.71±0.09, ♀ (n = 9) 1.75±0.09; of V, ♂ (n = 58) 2.48±0.13, ♀ (n = 9) 2.43±0.12). Differences were statistically significant: male-male-IV, $p < 0.05$ (1.157e-9), $Z = 6.0861$; male-male-V, $p < 0.05$ (5.936e-10), $Z = 6.1921$; female-female-IV (same as for female-female-V), $p < 0.05$ (9.99e-4), $Z = 3.2908$. Again, the result for female comparison should be treated with caution; slenderness is not visually obvious as opposed to the size above.

(12) Dorsal surface of metasoma V more granular in *O. przewalskii*.

(13) VL of metasoma segment V armed with denticles of contrasting size in *O. longichelus* but of even size in *O. przewalskii*.

(14) Lateral lobes of anal arch extroversive in *O. longichelus* but weakly introversive or parallel in *O. przewalskii*.

(15) Hemispermatophore more slender in *O. longichelus* with proportionally shorter capsule than in *O. przewalskii*.

Most sample distributions were found approximately symmetrical (i.e., median ≈ mean; skewness around zero, p-value for asymmetry > 0.05), except for the DSC of *O. przewalskii* (G_1 = -1.386; left-skewed). In fact, the two species can be easily discriminated by character 6 alone. It must be stated, however, those ratiometrics do not inherently serve diagnostic purposes. As elaborated in Tang (2023), manual measurement barely derives accurate or consistently reproducible values. The quantified characters, as exemplified by those ratiometrics, were only meant to evaluate the morphological disparities between the two species. A sufficiently large sample size can aid in alleviating bias stemming from individual measurements and facilitate differentiation, despite that the hereby provided ranges of these ratiometrics would imaginably contract when a more precise methodology is employed.

Subordinate taxa of genus *Olivierus*

The current investigation recognized merely two species of *Olivierus* in Xinjiang (and three for China) as well as synonymizing one species from Kazakhstan, thereby diminishing the total species number within the genus to 18, with two of them warranting scrutiny. As per Qi et al. (2004: 137), the original description of *O. martensii* by Karsch (1879: 112–113) was based solely on a single male specimen, ostensibly collected from Singapore – a type locality subsequently disputed by Kishida (1939). Birula (1904: 27) proposed a subspecies (as "*Buthus martensii hainanensis*") based on the specimen series devoid of information on sex and quantity, collected by O. Herz in 1895, purportedly from Hainan Island. The author only mentioned two morphological variations compared to the mainland population: (1) coloration darker; (2) dorsal granulation significantly stronger. The first character may have been markedly influenced by the undesirable preservation of specimen (in fact, chromatic variation in tonality in *O. martensii* has been observed by Qi et al. (2004: 142)), while the latter can only be verified under UV illumination. Kovařík (2019: 24, figs. 177–180) presented the first photographic evidence for the syntypes of this subspecies and elevated it to the species rank, reclassifying it under *Olivierus*. Although no redescription was provided, it is highly likely that the type locality of this species was erroneous (presumably "Henan" rather than "Hainan" if it was a mislabeling; Tang, 2022c: 13) since the natural conditions there do not align with the typical habitat of this genus, particularly that of *O. martensii*.

Similarly, Werner (1936: 173) briefly described *O. extremus* (as "*Buthus extremus*") based on a holotype female collected by K. Kucschinski on 23 August 1924. His description, provided only with several general characters, was solely made in comparison to "*Mesobuthus eupeus*" (as "*Buthus eupeus*"). The type locality was given as "Hinderindien, Straits Settlements, Pulo Pinang". Since "Straits Settlements" included the British-controlled port cities of Malaysia (including Malacca, Penang and Dindings) and Singapore, it is highly probable that "Pulo Pinang" specifically referred to "Pulau Pinang" (Penang State in Malaysia). This species was then only tangentially mentioned by Takashima (1945: 77), Weidner (1959: 99), Vachon (1950: 325) and Pérez (1974: 26), evading re-examination, according to Fet & Lowe (2000: 176). While Fet et al. (2018: 3) and Kovařík (2019: 26) considered its type locality to be Singapore, earlier studies suggested Malaysia (Vachon, 1950: 325; Fet & Lowe, 2000: 176), as deduced above. *O. martensii* has been widely applied as the raw material of Chinese medicine (Tang, 2022a: 4). This species can even be found in lollipops and artificial ambers sold in the United States and several other countries. It is hence highly probable that the holotype of *O. extremus* was in fact a female *O. martensii* which had been exported to Malaysia. Inferring from the available original information, its sole distinction from *O. martensii* was the presence of 14 denticle subrows (Table 1), provided that the count was correct.

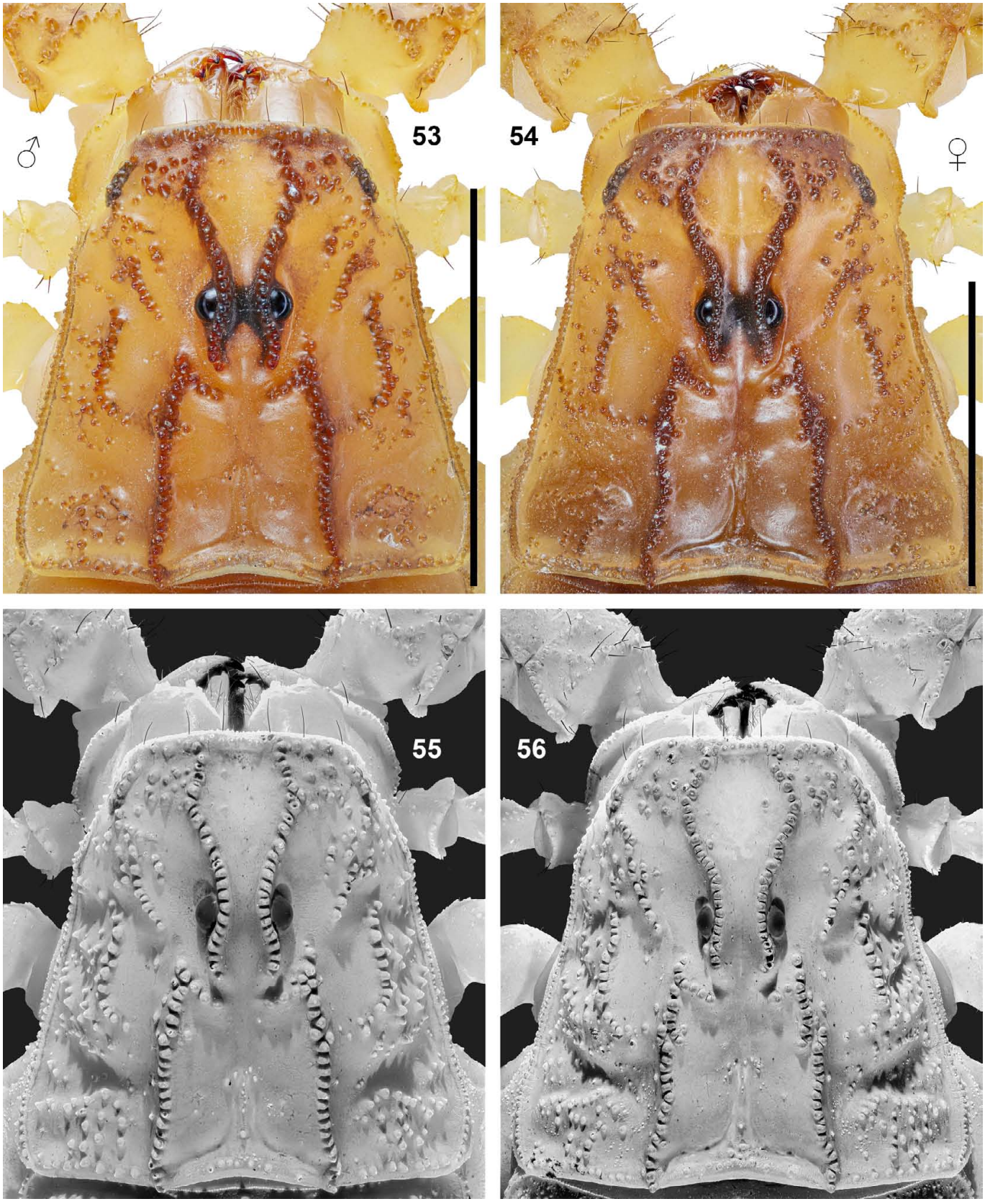

Figures 53–**56**: *Olivierus przewalskii* (Birula, 1897), carapace of male (53, 55) from Ghulja (Yining) County and female (54, 56) from Yarkant (Shache) County. **Figures 53**–**54**. Under white light. **Figures 55**–**56**. Under UV light. Scale bars = 5 mm.

In Table 5, morphological characters of potential diagnostic utility for all *Olivierus* species were retrieved from previous papers, as well as incorporating the current findings. It is noteworthy that several qualitative characters (e.g., manus profile, movable finger lobe, metasoma V ventrolateral carina serration) were hereby subjectively categorized after juxtaposing the available photos of those species.

Systematics

Family Buthidae C. L. Koch, 1837
Olivierus Farzanpay, 1987
Olivierus longichelus (Sun & Zhu, 2010)
(Figures 1–48, 97–98, 101–105, 115–116, 119, 132–139, 150–156; Tables 1–5)

http://zoobank.org/?lsid=urn:lsid:zoobank.org:act:701C6466-5B03-46D5-ADD2-42A4EFDACA21

Protonym. *Mesobuthus longichelus* Sun & Zhu, 2010: 5–10, figs. 1, 4–10, 17–21.

Synonyms.

Mesobuthus bolensis Sun, Zhu & Lourenço, 2010: 35–40, 42, figs. 2–3, 5–11, 14–18, 21–22, table 1. **Syn**. **n**.
https://zoobank.org/urn:lsid:zoobank.org:act:47CCA805-DA8F-4302-9D84-937FA02216E3
Type locality and type depository. China, *Xinjiang Uygur Autonomous Region*, Bortala Mongol Autonomous Prefecture, 15 km SW of Bole City, 44°44'N 81°59'E; MHBU.
Other localities and specimen depository. China, *Xinjiang Uygur Autonomous Region*, Ili Kazakh Autonomous Prefecture, area close to Ghulja (or Gulja, Yining) County, 44°00'N 81°32'E (Sun et al., 2010: 36); MHBU.

Mesobuthus karshius Sun & Sun, 2011: 59, 62–67, 73, figs. 5, 6, 10, table 1. **Syn**. **n**.
https://zoobank.org/urn:lsid:zoobank.org:act:8F5C3E69-CBDC-49F7-97BD-3251FE390BEE
Type locality and type depository. China, *Xinjiang Uygur Autonomous Region*, Kashgar (or Kaxgar) Prefecture, Yarkant (or Shache) County, 38°24'N 77°05'E; MHBU.
Other localities and specimen depository (MHBU). China, *Xinjiang Uygur Autonomous Region*, Kashgar (or Kaxgar) Prefecture, area near to Kashgar (or Karshi) City, 39°28'N 75°58'E (Sun & Sun, 2011: 63) [population not examined in this study]; Kizilsu Kyrgyz Autonomous Prefecture, Artux (or Artush) City, area near to Arhu Town, 39°42'N 76°09'E (Sun & Sun, 2011: 63) [population not examined in this study]; Kizilsu Kyrgyz Autonomous Prefecture, 2 km S of Artux (or Artush) City, near to Songtake Village, 39°41'N 76°11'E (Sun & Sun, 2011: 63).

Olivierus tarabaevi Fet, Kovařík, Gantenbein & Graham, 2021: 54, 61–65, 69–70, figs. 45–85, table 2. **Syn**. **n**.
https://zoobank.org/urn:lsid:zoobank.org:act:BF1FB341-4A45-4B1D-BACF-F063BA20B18B
Type locality and type depository. Kazakhstan, *Qyzylorda Region*, Shieli District, ca 2.5 km NW of Baygekum (Baigakum), 44.65°N 66.02°E; FKCP.
Other localities and specimen depository (FKCP). Kazakhstan, *Jambyl Region*, Moiynkum District, Khantau, 44.180°N 73.815°E (Graham et al., 2019: table 1); *Talas Region*, Talas District, 44.173°N 71.120°E (Graham et al., 2019: table 1, mislabeled as "Balkhash").

References (selected):

Mesobuthus longichelus: Zhang, 2009: 34, 49–50, 60, 135, fig. 55, table 7; Sun et al., 2010: 35–36, 38–40, figs. 4, 12–13, 19–20, 23–24, table 1; Sun, 2010: 63–64, 78–80, 183–187, 247–249, figs. 39–41; Sun & Sun, 2011: 72–73, fig. 10; Yang et al., 2013: 1, 5–7, figs. 3M&N, table 1; Di et al., 2014: 5, 7, 14; Di et al., 2015: 111; Fet et al., 2018: 3; Zhang et al., 2020: 82.
Mesobuthus bolensis: Sun, 2010: 63–64, 80–82, 186–189, 250–252, figs. 42–44; Sun & Sun, 2011: 59, 73, fig. 10; Yang et al., 2013: 2, 5–7, figs. 3K&L, table 1; Di et al., 2014: 7, 14; Di et al., 2015: 111; Fet et al., 2018: 3; Zhang et al., 2020: 82.
Olivierus bolensis: Kovařík, 2019: 26; Tang, 2022a: 44; Tang, 2022c: 1, 3–6, 14.
Olivierus longichelus: Kovařík, 2019: 26; Tang, 2022a: 44; Tang, 2022c: 1, 3–11, 14.
Mesobuthus caucasicus kaxgaricus (part): Sun, 2010: 63–64.
Mesobuthus caucasicus karshius (part): Sun, 2010: 75–78, 189–192, 245, figs. 37–38.
Mesobuthus karshius (part): Yang et al., 2013: 1, 5–7, figs. 3O&P, table 1; Di et al., 2014: 5, 7, 14, 17; Di et al., 2015: 111; Fet et al., 2018: 3 (misspelled as "*M. karschius*"); Zhang et al., 2020: 82.
Olivierus karshius (part): Kovařík, 2019: 26; Tang, 2022a: 44; Tang, 2022c: 3–5, 9–12, 14.
Mesobuthus caucasicus (part): Gantenbein et al., 2003: 413.
Mesobuthus caucasicus parthorum (part): Fet, 1989: 104; Fet, 1994: 528.
Olivierus caucasicus parthorum (part): Fet & Lowe, 2000: 192.
Mesobuthus caucasicus intermedius (part): Fet, 1989: 107; Gromov & Kopdykbaev, 1994: 20; Sun & Zhu, 2010: 2–4, 6–8, 10, figs. 2, 11–13; Sun & Sun: 61–65, 73, figs. 3–4, 11, table 1; Di et al., 2014: 4, 7, 14; Zhang et al., 2019: 90; Tang, 2022c: 5, 6, 9, 11, fig. 3, table 1.
Olivierus caucasicus intermedius (part): Fet & Lowe, 2000: 191.
Mesobuthus gorelovi (part): Fet et al., 2018: 1–2, 21–26, 52, 54, 58, 61, 63, 74, fig. A5, table 6.
Olivierus gorelovi (part): Graham et al., 2019: 1–9; Kovařík, 2019: 26.
Olivierus tarabaevi: Sulakhe et al., 2022: 9; Tang, 2022a: 44; Tang, 2022c: 1, 5, 6, 9, fig. 3, table 1.

Type locality and type depository. China, *Xinjiang Uygur Autonomous Region*, Bortala Mongol Autonomous Prefecture, 10 km south of Jinghe County, 44°31'N 82°54'E; MHBU.

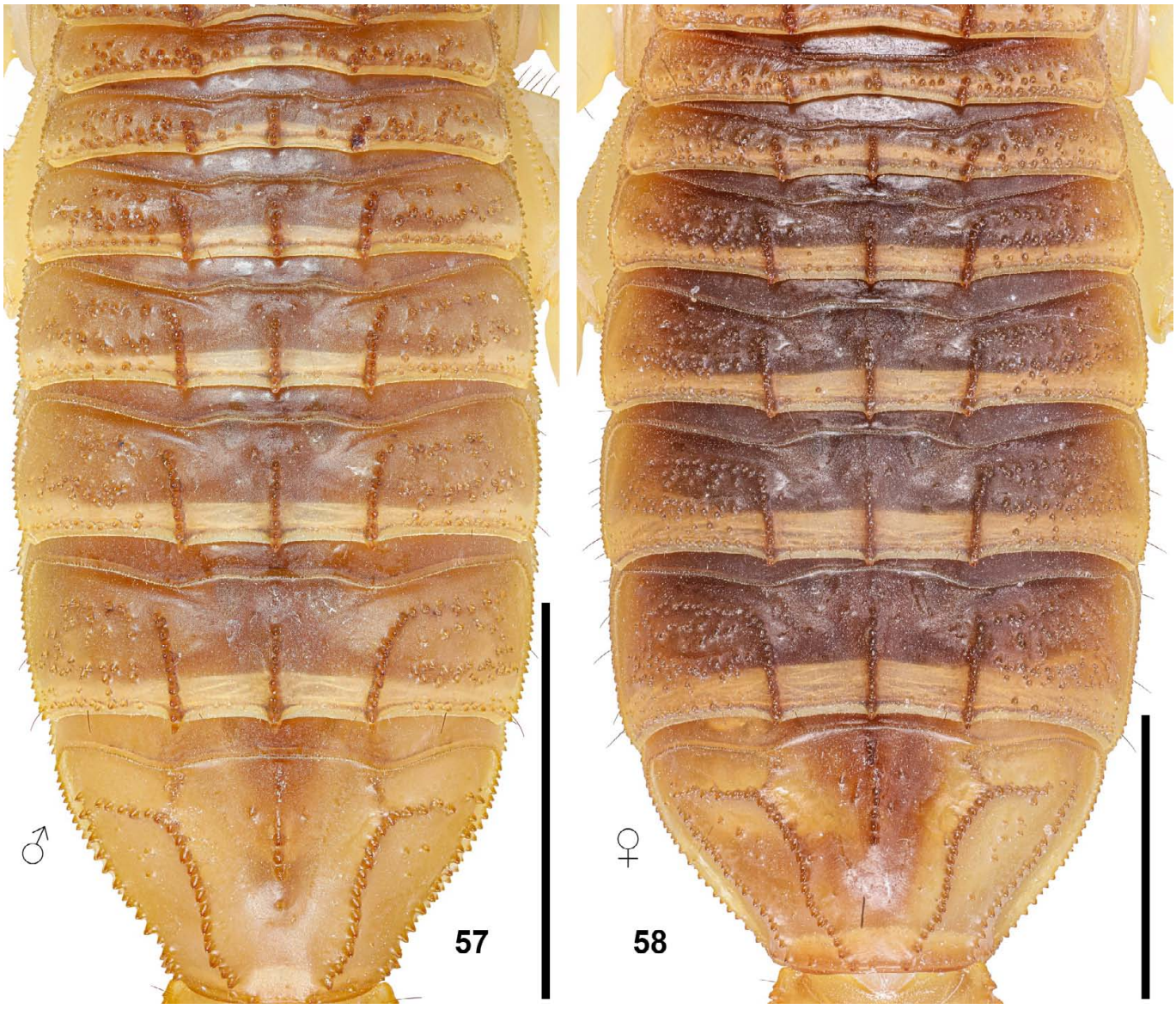

Figures 57–58. *Olivierus przewalskii* (Birula, 1897), tergites of male from Ghulja (Yining) County (57) and female from Yarkant (Shache) County (58) under white light. Scale bars = 5 mm.

Material examined (VT). **China**, *Xinjiang Uygur Autonomous Region*, Bayingolin Mongol Autonomous Prefecture, Qiemo County, near Bage'airike Township, 38°12'15.9"N 85°31'57.7"E (38.204414°N 85.532694°E), 1171 m a. s. l., 22 July 2023, 3♂2♀1 juv., leg. Qiu Du; Bayingolin Mongol Autonomous Prefecture, Ruoqiang County, 39°08'03.3"N 88°10'09.4"E (39.13425692°N 88.16928659°E), 824 m a. s. l., 21 July 2023, 1♂, leg. Qiu Du; Bortala Mongol Autonomous Prefecture, Bole City, near Dalete Town, 44°48'06.3"N 82°04'14.1"E (44.801749°N 82.070584°E), 496 m a. s. l., 5 August 2023, 1♂2♀1juv., leg. Qiu Du; Bortala Mongol Autonomous Prefecture, Jinghe County, 44°29'03.7"N 82°53'12.3"E (44.484348°N 82.886744°E), 485 m a. s. l., 6 August 2023, 8♂, leg. Qiu Du; Ili Kazakh Autonomous Prefecture, Ghulja (or Gulja, Yining) County, near Yingyeer Town, 43°59'47.9"N 81°09'02.7"E (43.996643°N 81.150745°E), 685 m a. s. l., 3 August 2023, 1♂, leg. Qiu Du; Kashgar (or Kaxgar) Prefecture, Yarkant (or Shache) County, near Kalasu Township, 38°18'15.2"N 77°31'51.5"E (38.304231°N 77.530962°E), 1186 m a. s. l., 29 July 2023, 2♂, leg. Qiu Du; Kashgar (or Kaxgar) Prefecture, Makit County, near Kumuku Sa'er Village, 38°50'37.8"N 77°43'27.1"E (38.843819°N 77.724182°E), 1129 m a. s. l., 1 August 2023, 2♂2 juvs., leg. Qiu Du.

Diagnosis (based on material examined in this study). Adult TL ca. 55–62 mm in ♂ and 58–67 mm in ♀. Base coloration light yellow, carinae darkened (orangish to brownish), moderately on carapace; anterolateral region of carapace weakly infuscate; lateral and ventral surfaces of metasoma V barely to moderately infuscate. Carapace with CL, CM and PM forming lyre configuration; PM pair slants in the same

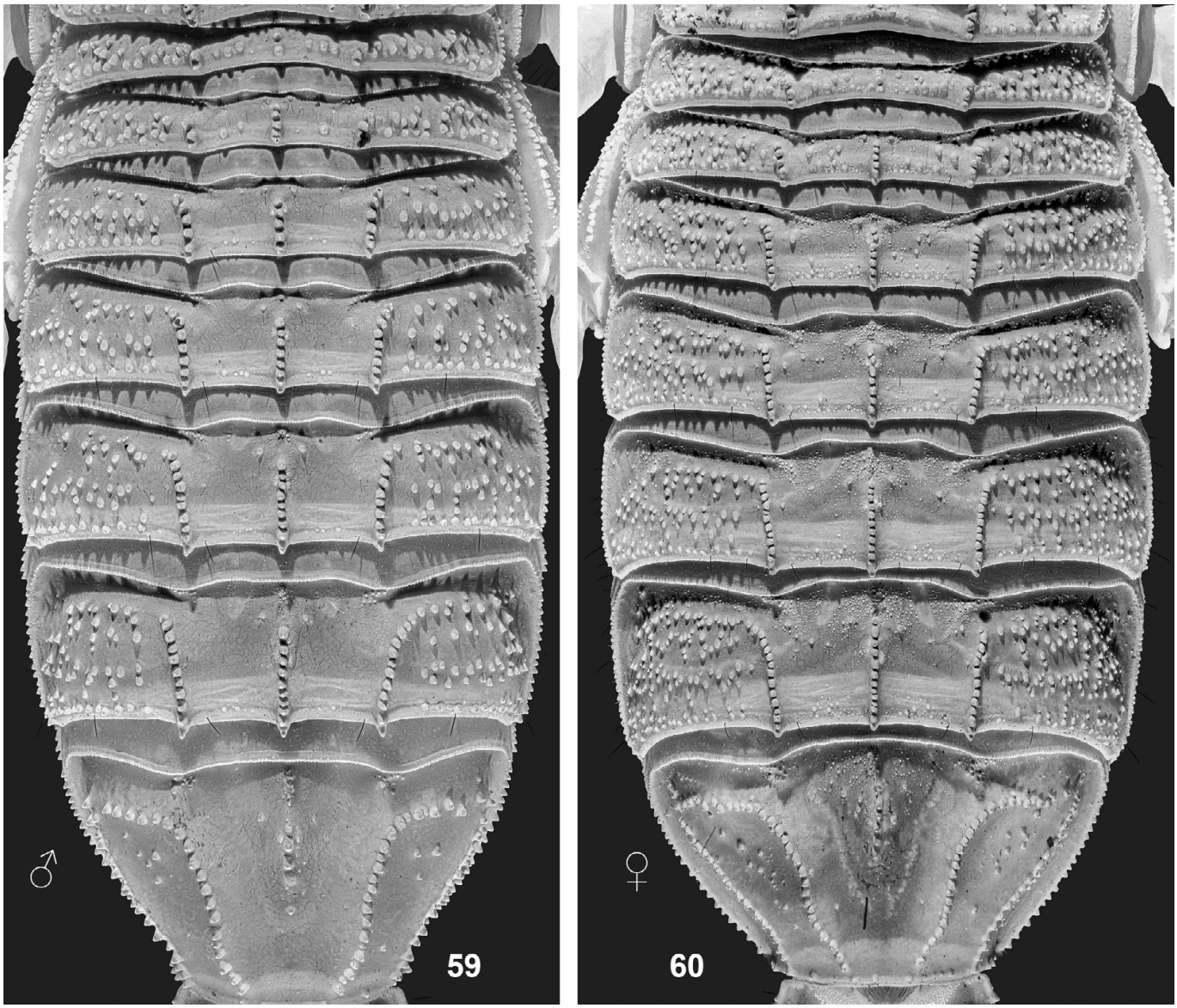

Figures 59–60. *Olivierus przewalskii* (Birula, 1897), tergites of male from Ghulja (Yining) County (59) and female from Yarkant (Shache) County (60) under UV light.

direction with carapace margins; granules finer and denser. Tergites I–VI tricarinate (carinae extend beyond posterior margin) with narrow intercarinal distance; VII pentacarinate. Sternite with finely serrated margins and slit-like spiracles; sternite III with setae arranged in V-shaped configuration; sternite VII bears 4 well marked granulate carinae, external ones often more granulate. Pedipalp femur with 4 complete, finely granulated carinae and 1 dispersive granulated carina, dorsal intercarinal area granulate; patella with 4 granulated and 4 smooth carinae; chela with smooth carinae indicated. Pedipalp chela relatively slender; adult CL/W 4.42–4.81 in ♂ and 4.6–4.97 in ♀. Dentate margin of pedipalp movable finger with 12–13 subrows of denticles and 3–5 terminal denticles, SPS non-fluorescent; proximity of movable finger with a lobe present in both sexes, stronger in males. Pectines highly sexually dimorphic, with well-developed fulcra; PTC 25–30 in ♂ and 21–25 in ♀. Metasomal segment relatively slender; adult L/D of metasoma IV 1.88–2.07 in ♂ and 1.9–2.1 in ♀, of metasoma V 2.79–3 in ♂ and 2.85–2.96 in ♀. Metasoma I–V with 10-8-8-8-5 complete carinae; ML of metasoma II obsolete, indicated by discrete granules covering variable length; VM of metasoma V often displayed in a single row; VL of metasoma V armed with discrete denticles of contrasting size (outward extension degree distinct); ventral surface of metasoma V embellished with enlarged granules posteriorly. Legs with femur bearing two serrated ventral carinae; basi- and telotarsus III ventrally equipped with two longitudinal rows of long setae; bristle comb composed of dense, fine setae; external pedal spur hirsute.

Variation and sexual dimorphism. No prominent size class was observed in adults examined; size discrepancy negligible

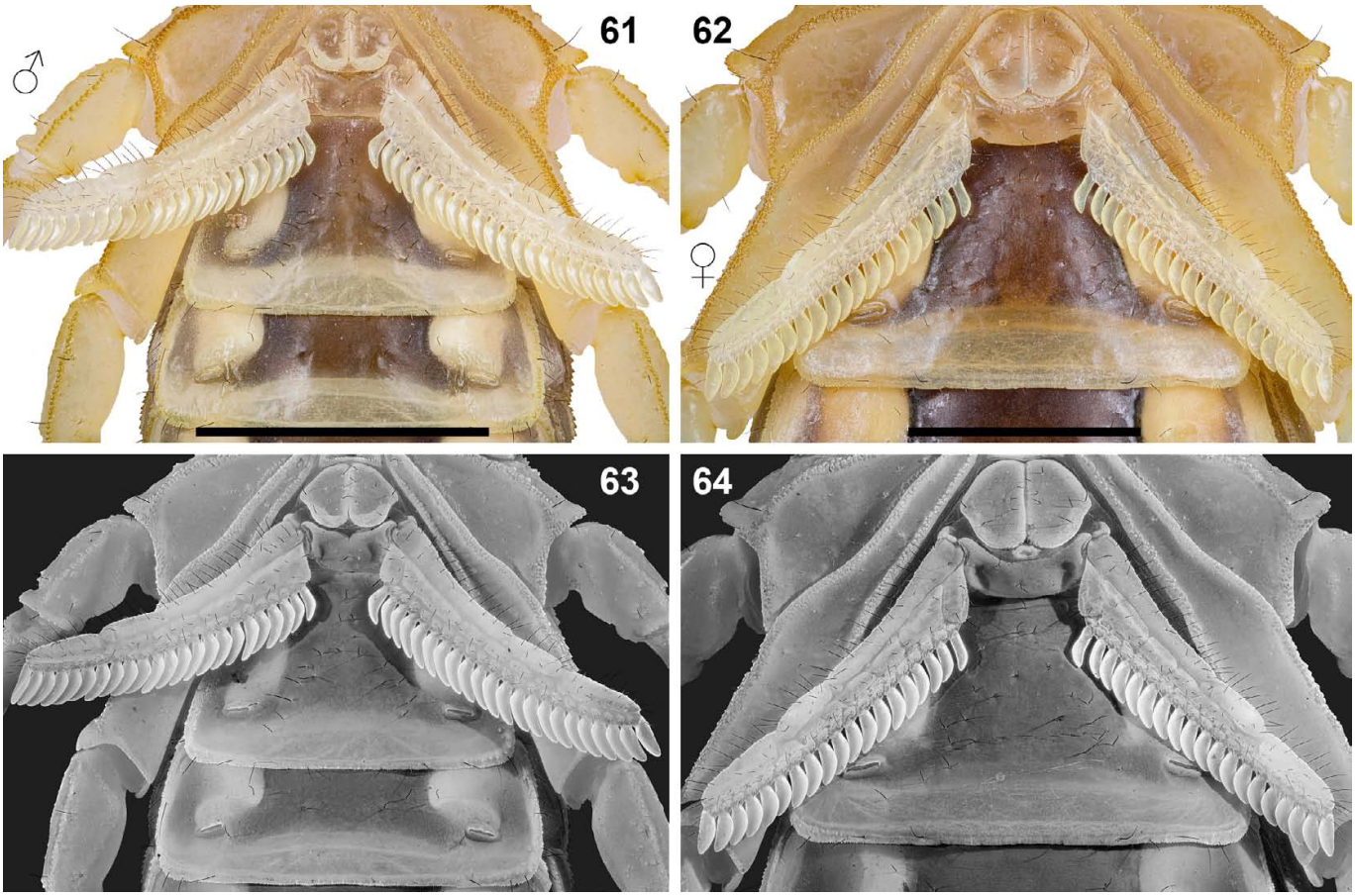

Figures 61–**64**: *Olivierus przewalskii* (Birula, 1897), pectines of male (61, 63) from Ghulja (Yining) County and female (62, 64) from Yarkant (Shache) County. **Figures 61**–**62**. Under white light. **Figures 63**–**64**. Under UV light. Scale bars = 5 mm.

in adult females but relatively higher in adult males. Major qualitative intraspecific variation presented in two features: coloration and serrated VL of metasoma V. Color pattern showcased two main phenotypes (age-independent), both characterized by a yellow base coloration: the orange morph and the brown morph. In the orange morph, the carinae and granules of the carapace, tergites and pedipalps exhibited an orangish hue, and the region near the joint of the femur and patella of the walking legs was tinged with an orange shade. While in the second morph, these color tones shifted towards brown. The infuscation of metasoma V varied intraspecifically and could be nearly the same color (pale yellow) as the anterior segments in some individuals. The enlarged extroversive denticles of VL of metasoma V varied in size and number bilaterally within the same individual (thus intraspecifically) but were age-independent. Quantitative intraspecific variations for PTC and DSC recorded in Tables 2–4. Incorporating the data of its junior synonym, *O. tarabaevi*, it would yield a total range of 24–30 in ♂ and 19–25 in ♀. Notably, populations from Shawan and Wujiaqu were recorded with a higher average PTC for both sexes, while populations from Yarkant, Makit, Qiemo and Ruoqiang showed lower PTC (Fig. 129; Table 4). In addition, the former populations (11 females and 7 males in total) were also somewhat larger than the latter populations (females typically above 62 mm), and the largest female was measured to give the upper limit (67 mm) observed. Conversely, the female (56 mm) studied in Tang (2022c: table 1) also from Wujiaqu was not larger than the latter populations. However, our molecular results did not reveal distinct genetic divergence between those populations. Their averagely higher PTC and total length might be attributed to their successful dispersal into the inner region of China.

O. longichelus exhibits the following key ontogenetic variation: **(1)** coloration of pedipalps and body often generally orangish or brownish, with paler legs and consistently infuscate metasoma V in juveniles, in contrast with the yellow adults having only partial structures orangish or brownish (see above); **(2)** basal lobe on dentate margin of pedipalp movable finger weakly developed in juveniles (see files on ResearchGate comparing juveniles, presumed subadults and adults of specimens from Wujiaqu); **(3)** carapacial carinae finer in juveniles. *O. longichelus* exhibits the following sexual dimorphism: **(1)** carapacial carinae coarser in males; **(2)** tergites proportionally wider in females; **(3)** basal lobe on dentate margin of pedipalp movable finger stronger in males; **(4)** pectines prominently longer with more and longer teeth in males, leaving smaller interpectinal space basally; **(5)** genital operculum dome-shaped (single-peaked) in males, but the anterior margin is bilobate in females, appearing as two peaks flanking the middle longitudinal suture.

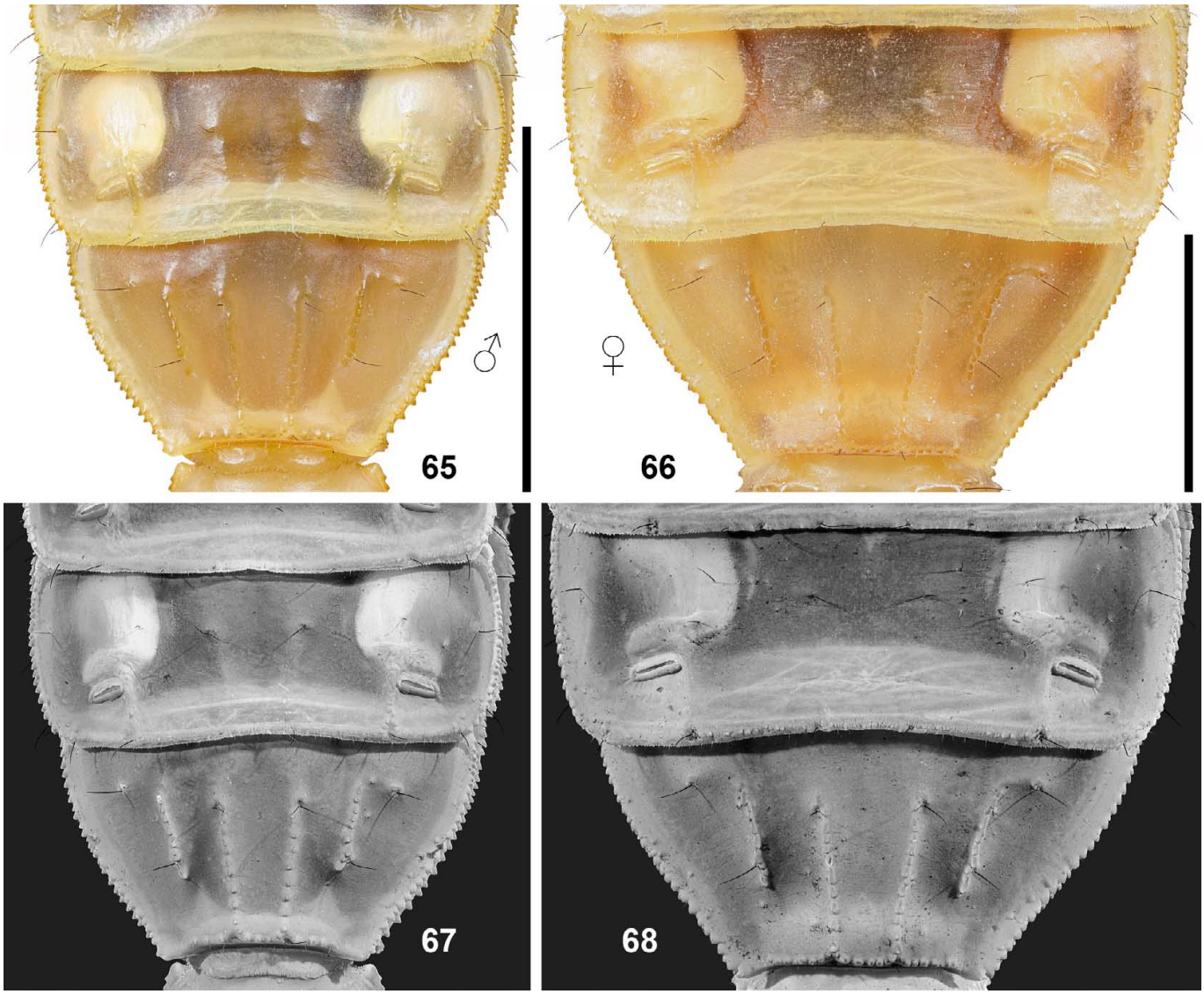

Figures 65–68: *Olivierus przewalskii* (Birula, 1897), sternites VI–VII of male from Ghulja (Yining) County (65, 67) and female from Yarkant (Shache) County (66, 68). **Figures 65–66**. Under white light. **Figures 67–68**. Under UV light. Scale bars = 5 mm.

Distribution. In China, this species is predominant in the northern region of Xinjiang (including Bole, Ghulja and Jinghe, Korgas, Khorgos, Shawan and Wujiaqu), but may also be found in the western (Yarkant and Makit) and southern (Qiemo and Ruoqiang) regions. Other reports by local residents corroborated its occurrence in Shihezi City, located between Shawan and Wujiaqu. Current study confirmed its distribution in Kazakhstan (Jambyl, Qyzylorda and Talas regions). Report of "*M. c. intermedius*" from Taukum, Balkhash District in Almaty Region by Sun & Zhu (2010: 3, as "Kurty"; 44°53.002'N 75°17.138'E) likely referred to this species as well.

Chinese equivalent. 长螯奥氏蝎 (Tang, 2022a). Other Chinese names applied to this taxon include: (1) *Mesobuthus longichelus*: 长螯中杀牛蝎 (Tang; UTN), 细螯正钳蝎 (Sun, 2010; ET-G&S), 长螯正钳蝎 (Di et al., 2015; ET-G); (2) *Olivierus bolensis*:博乐奥氏蝎(Tang, 2022a); (3) *Mesobuthus bolensis*:博乐中杀牛蝎 (Tang; UTN), 博乐正钳蝎 (Di et al., 2015; ET-G); (4) *Olivierus karshius*: 喀什奥氏蝎 (Tang, 2022a); (5) *Mesobuthus caucasicus karshius* (or *kaxgaricus*): 喀高正钳蝎 (Sun, 2010; ET-G); (6) *Mesobuthus karshius*: 喀什中杀牛蝎 (Tang; UTN), 喀什正钳蝎 (Di et al., 2015; ET-G); (7) *Olivierus tarabaevi*: 塔氏奥氏蝎 (Tang, 2022a); (8) *Buthus caucasicus intermedius* [part, when applied to Balkhash and Xinjiang populations]: 高加索钳蝎间型亚种 (Li et al., 2016; ET-G); (9) *Mesobuthus caucasicus intermedius* [part]:媒介高加索钳蝎 (Yang, 2008; ET-G&SS),媒高正钳蝎 (Zhang, 2009; ET-G&SS), 高加索正钳蝎间型亚种 (Di et al., 2015; ET-G); (10) *Olivierus caucasicus intermedius* [part]: 媒介橄蝎 (Zhu et al., 2004; ET-G&SS, TM-S).

Olivierus przewalskii (Birula, 1897)
(Figures 49–96, 99–100, 111–114, 117–118, 140–149, 155–156; Tables 1–3, 5)

https://zoobank.org/urn:lsid:zoobank.org:act:62CA85DB-80B2-40D4-9019-9AB9AEE73B6F

Protonym. *Buthus caucasicus przewalskii* Birula, 1897: 387–388.

Nomen nudum. *Mesobuthus nanjiangensis* Zhang, 2009: 1, 34–36, 60, 114, 116–118, 139–141, figs. 1, 59–61, table 7.

References (selected):

Buthus caucasicus przewalskii: Kraepelin, 1899: 25; Birula, 1917: 71; Birula, 1927: 201–209; Sun, 2010: 208, table 5; Fet et al., 2018: 1–2.

Buthus caucasius przewalskii: Birula, 1904: 24.

Buthus przewalskii: Kishida, 1939: 44.

Mesobuthus caucasicus przewalskii: Vachon, 1958: 150, fig. 31; Fet, 1989: 111; Shi & Zhang, 2005: 475; Sun & Zhu, 2010: 4–5, figs. 3, 14–16; Sun, 2010: 8, 64, 70–73, 181–183, 186, 190, 208, 233, 239–241, figs. 24-1, 31–33, table 5; Sun & Sun, 2011: 60–61, figs. 1–2, 10; Yang et al., 2013: 1, 5–7, figs. 3 G&H, table 1; Di et al., 2014: 4, 7, 14; Di et al., 2015: 111; Heddergott et al., 2016: 147, 157–158; Fet et al., 2018: 2.

Mesobuthus "caucasicus" przewalskii: Fet et al., 2018: 3, 12, 53.

Olivierus caucasicus przewalskii: Farzanpay, 1987: 156; Fet & Lowe, 2000: 192; Zhu et al., 2004: 113.

Mesobuthus przewalskii: Zhang et al., 2020: 81–83, 85–91, 96, figs. 1–11, tables 1–2.

Olivierus przewalskii: Kovařík, 2019: 25–26, figs. 181–182; Tang, 2022a: 44; Tang, 2022c: 1, 4–5, 9–10, 12, 14.

Mesobuthus caucasicus kaxgaricus (part): Sun, 2010: 63–64.

Mesobuthus caucasicus karshius (part): Sun, 2010: 75–78, 189–192, 245, figs. 37–38.

Mesobuthus karshius (part): Yang et al., 2013: 1, 5–7, figs. 3O&P, table 1; Di et al., 2014: 5, 7, 14, 17; Di et al., 2015: 111; Fet et al., 2018: 3 (misspelled as "*M. karschius*"); Zhang et al., 2020: 82.

Olivierus karshius (part): Kovařík, 2019: 26; Tang, 2022a: 44; Tang, 2022c: 3–5, 9–12, 14.

Type locality and type depository. China, *Xinjiang Uygur Autonomous Region*, Bayingolin Mongol Autonomous Prefecture, near Lop Nur (or Lobnor) Lake (Ruoqiang County) and Cherchen (or Charchan, Qarqan) Oasis (Qiemo County), in the east edge of the Tarim Basin; ZISP.

Other localities and specimen depository. **China**, *Xinjiang Uygur Autonomous Region*, Aksu Prefecture, Aksu City, 41°07'N 80°11'E, MHBU (Sun & Sun, 2011: 60); Aksu Prefecture, Kuqa (or Kuche, Kuchar) City, 41°44'N 82°55'E, IOZ-CAS (Zhang et al., 2020: 85); Bayingolin Mongol Autonomous Prefecture, Qiemo County, 38°15'N 85°32'E, IOZ-CAS (Zhang et al., 2020: 85); Bayingolin Mongol Autonomous Prefecture, Ruoqiang County, 39°01'N 88°10'E, IOZ-CAS (Zhang et al., 2020: 85); Bayingolin Mongol Autonomous Prefecture, Yuli (or Lopnur) County, 40°38'N 84°18'E, IOZ-CAS (Zhang et al., 2020: 85); Kizilsu Kyrgyz Autonomous Prefecture, Artux (or Artush) City, 39°42'N 76°09'E, MHBU (Sun & Sun, 2011: 60); Kizilsu Kyrgyz Autonomous Prefecture, Wuqia County, 39°44'N 75°14'E, MHBU (Sun & Sun, 2011: 60); Turpan City, Gaochang District, 42°57'N 89°06'E, IOZ-CAS (Zhang et al., 2020: 85); Turpan City, Shanshan County, 42°51'N 90°13'E, IOZ-CAS (Zhang et al., 2020: 85) ; Turpan City, Toksun (or Tuokexun) County, 42°47'N 88°40'E, IOZ-CAS (Zhang et al., 2020: 85); Tiemenguan City, 41°47'N 86°11'E, IOZ-CAS (Zhang et al., 2020: 85); Tumxuk (or Tumushuke) City, 39°53'N 78°55'E, IOZ-CAS (Zhang et al., 2020: 85); Yizhou District, Hami City, 42°41'N 93°27'E, IOZ-CAS (Zhang et al., 2020: 85); Yizhou District, Hami City, 42°52'N 93°26'E, IOZ-CAS (Zhang et al., 2020: 85). Records from Bügür (or Luntai) County and Korla City (Bayingolin Mongol Autonomous Prefecture) without coordinates (Sun et al., 2010: 4).

Material examined (VT). **China**, *Xinjiang Uygur Autonomous Region*, Bayingolin Mongol Autonomous Prefecture, Qiemo County, near Bage'airike Township, 38°12'15.9"N 85°31'57.7"E (38.204414°N 85.532694°E), 1172 m a. s. l., 22 July 2023, 7♂2♀4juvs., leg. Qiu Du; Bayingolin Mongol Autonomous Prefecture, Ruoqiang County, 39°08'03.3"N 88°10'09.4"E (39.13425692°N 88.16928659°E), 824 m a. s. l., 21 July 2023, 10♂2juvs., leg. Qiu Du; Bortala Mongol Autonomous Prefecture, Bole City, near Dalete Town, 44°48'06.3"N 82°04'14.1"E (44.801749°N 82.070584°E), 496 m a. s. l., 5 August 2023, 5♂2♀1juv., leg. Qiu Du; Ili Kazakh Autonomous Prefecture, Ghulja (or Gulja, Yining) County, near Yingyeer Town, 43°59'47.9"N 81°09'02.7"E (43.996643°N 81.150745°E), 685 m a. s. l., 3 August 2023, 3♂1♀, leg. Qiu Du; Kashgar (or Kaxgar) Prefecture, Yarkant (or Shache) County, near Kalasu Township, 38°18'15.2"N 77°31'51.5"E (38.304231°N 77.530962°E), 1186 m a. s. l., 29 July 2023, 12♂3♀5juvs., leg. Qiu Du; Kashgar (or Kaxgar) Prefecture, Makit County, near Kumuku Sa'er Village, 38°50'37.8"N 77°43'27.1"E (38.843819°N 77.724182°E), 1128 m a. s. l., 1 August 2023, 18♂1♀1juv., leg. Qiu Du.

Diagnosis (based on material examined in this study). Adult TL ca. 44–53 mm in ♂ and 49–63 mm in ♀. Base coloration light yellow, carinae darkened (brownish), strongly on carapace; anterolateral region of carapace moderately infuscate; lateral and ventral surfaces of metasoma V moderately infuscate (may fade after fixation in ethanol). Carapace with CL, CM and PM forming lyre configuration; PM pair relatively parallel; granules coarser and scarcer. Tergites I–VI tricarinate (carinae extend beyond posterior margin) with wide intercarinal distance; VII pentacarinate. Sternite with finely serrated margins and slit-like spiracles; sternite III with setae arranged in V-shaped configuration;

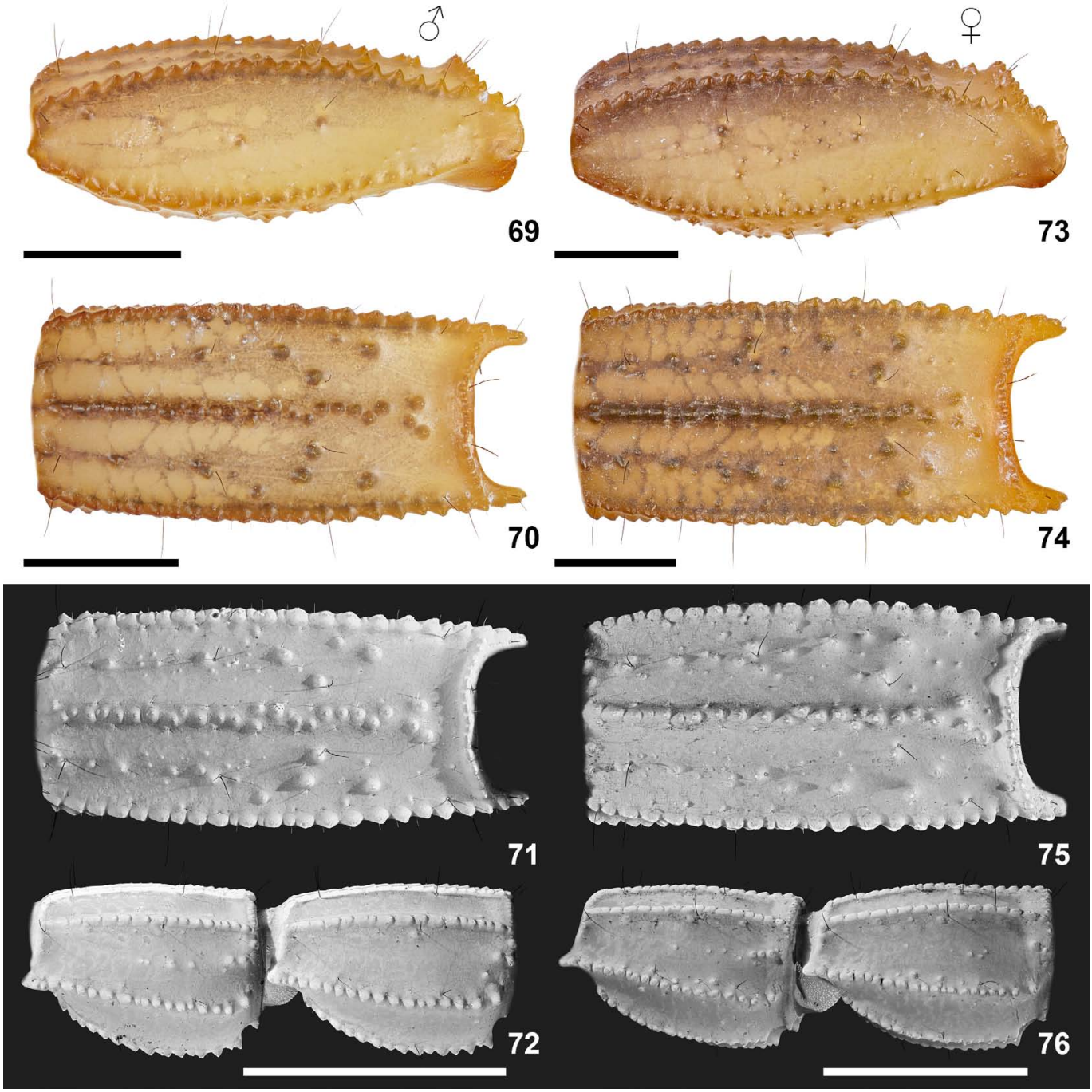

Figures 69–76: *Olivierus przewalskii* (Birula, 1897), metasoma V in lateral (69, 73) and ventral (70, 74) views under white light, metasoma V in ventral view (71, 75) and metasoma II–III in lateral view under UV light (72, 76). **Figures 69–72**. Male from Ghulja (Yining) County. **Figures 73–76**. Female from Yarkant (Shache) County. Scale bars = 2 mm (69–70, 73–74) and 5 mm (72, 76).

sternite VII bears 4 well marked granulate carinae, external ones often more granulate, internal ones may be smooth. Pedipalp femur with 4 complete, finely granulated carinae and 1 dispersive granulated carina, dorsal intercarinal area nearly smooth; patella with 3 (or 4) granulated and 5 (or 4) smooth carinae; chela with smooth carinae indicated. Pedipalp chela relatively slender; adult CL/W 3.79–4.39 in ♂ and 4.01–4.46 in ♀. Dentate margin of pedipalp movable finger with 9–11 subrows of denticles and 3–5 terminal denticles, SPS non-fluorescent; proximity of movable finger with a lobe present in both sexes, stronger in males. Pectines relatively sexually dimorphic, with well-developed fulcra; PTC 18–24 in ♂ and 16–20 in ♀. Metasomal segment relatively robust; adult L/D of metasoma IV 1.51–1.94 in ♂ and 1.62–1.88 in ♀, of metasoma V 2.23–2.77 in ♂ and 2.27–2.68 in ♀. Metasoma I–V with 10-8-8-8-5 complete carinae; ML of metasoma II obsolete, indicated by discrete granules covering variable length; VM of metasoma V often displayed in two rows; VL

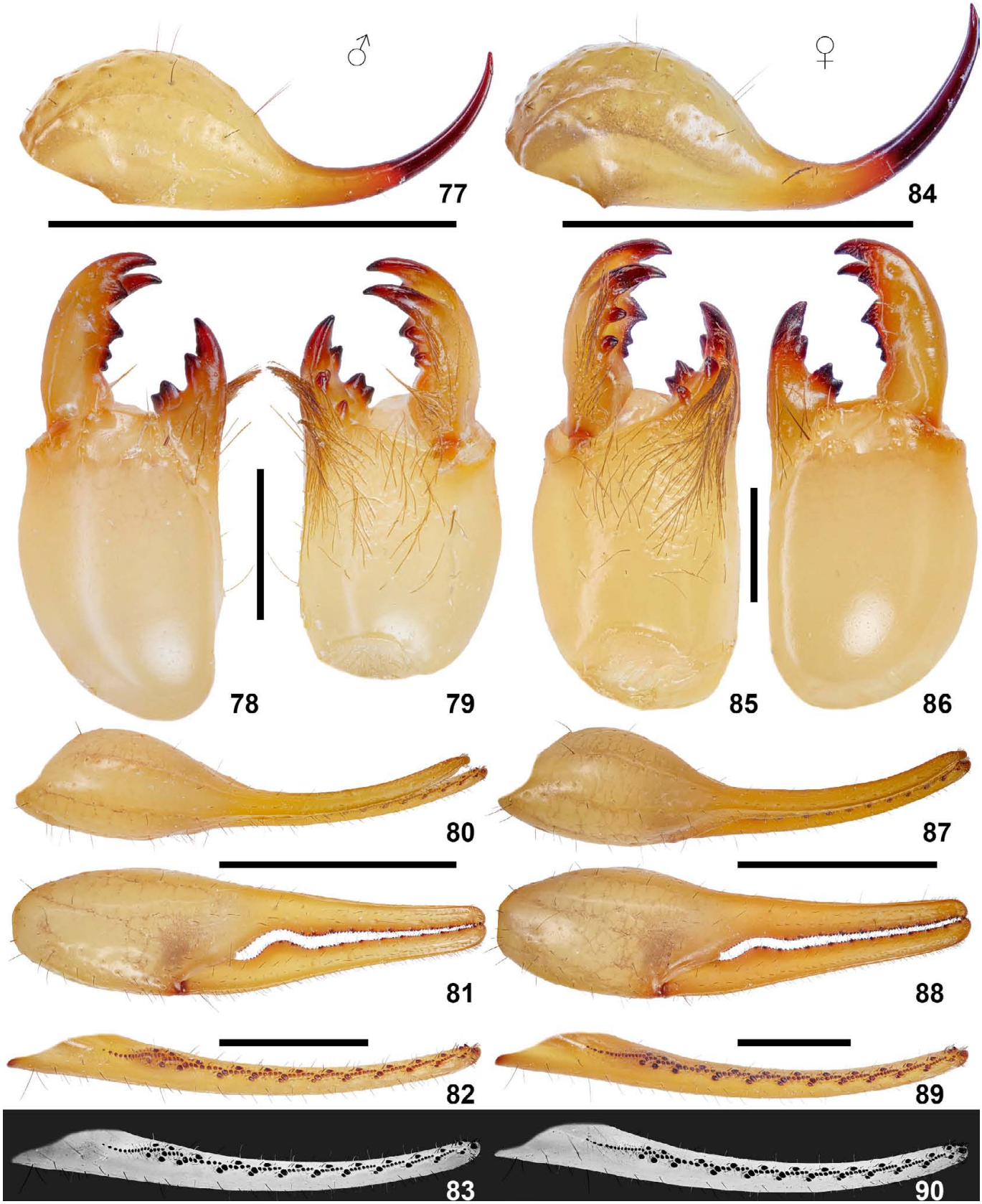

Figures 77–**90**: *Olivierus przewalskii* (Birula, 1897), telson in lateral view (77, 84), chelicera in dorsal (78, 86) and ventral (79, 85) views, right pedipalp chela in dorsal (80, 87) and external (81, 88) views under white light, and dentate margin of movable finger under white (82, 89) and UV (83, 90) light. **Figures 77**–**83**. Male from Ghulja (Yining) County. **Figures 84**–**90**. Female from Yarkant (Shache) County. Scale bars = 5 mm (77, 81, 84, 88), 2 mm (82, 89) and 1 mm (78, 86).

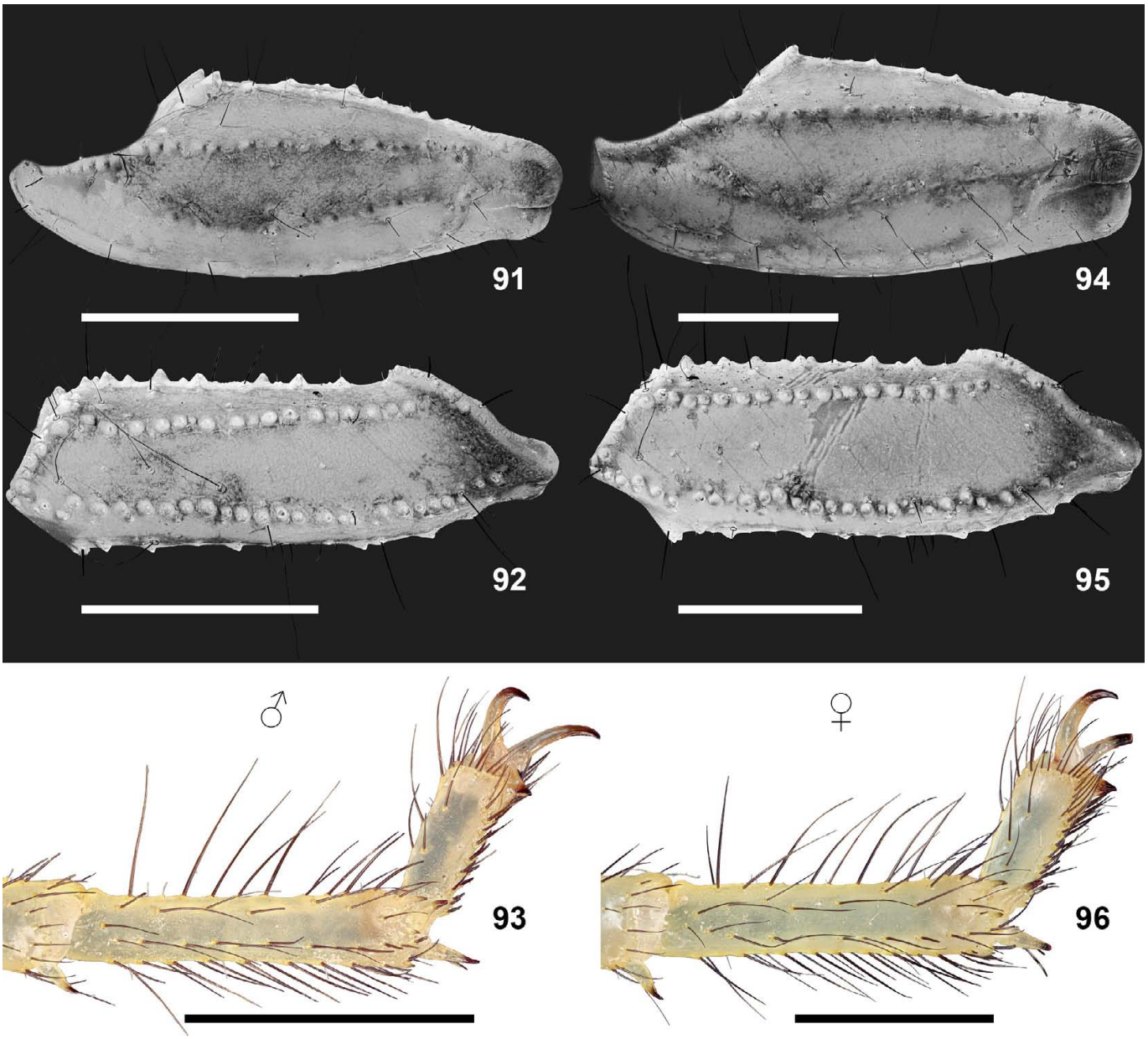

Figures 91–**96**: *Olivierus przewalskii* (Birula, 1897), right pedipalp patella (91, 94) and femur (92, 95) in dorsal view under UV light, and telo- and basitarsi of right 3rd leg in retrolateral view under white light (93, 96). **Figures 91**–**93**. Male from Ghulja (Yining) County. **Figures 94**–**96**. Female from Yarkant (Shache) County. Scale bars = 2 mm.

of metasoma V armed with continuous denticles of even size (outward extension degree nearly equal); ventral surface of metasoma V embellished with enlarged granules posteriorly. Legs with femur bearing two serrated ventral carinae; basi- and telotarsus III ventrally equipped with two longitudinal rows of moderate setae; bristle comb composed of several thick setae; external pedal spur hirsute.

Variation and sexual dimorphism. In the dead specimen series from Yarkant, thirteen *O. przewalskii* were identified. Among these, six were confidently identified as adult males based on the morphology of their pedipalp chela, while four were determined to be juveniles. Notably, there were three remaining specimens that exhibited a proximal lobe on their movable finger, which was ratiometrically almost identical with the adult males. However, those specimens were visibly smaller. Uncertainty arose regarding whether the presence of a well-developed proximal lobe definitively indicates an adult male. To address this, the specimens were dissected to extract their hemispermatophores. Two of them were successfully retrieved with a hemispermatophore respectively (due to their extended immersion in ethanol, internal organs were clumped), confirming their status as adult males. The remaining one had no hemispermatophores. Intriguingly, this individual exhibited traits that were somewhat contradictory: the relative length of its pectines and the relative width of its mesosoma were more reminiscent of a female specimen. This potentially suggests a rare occurrence of gynandromorphism, a phenomenon where

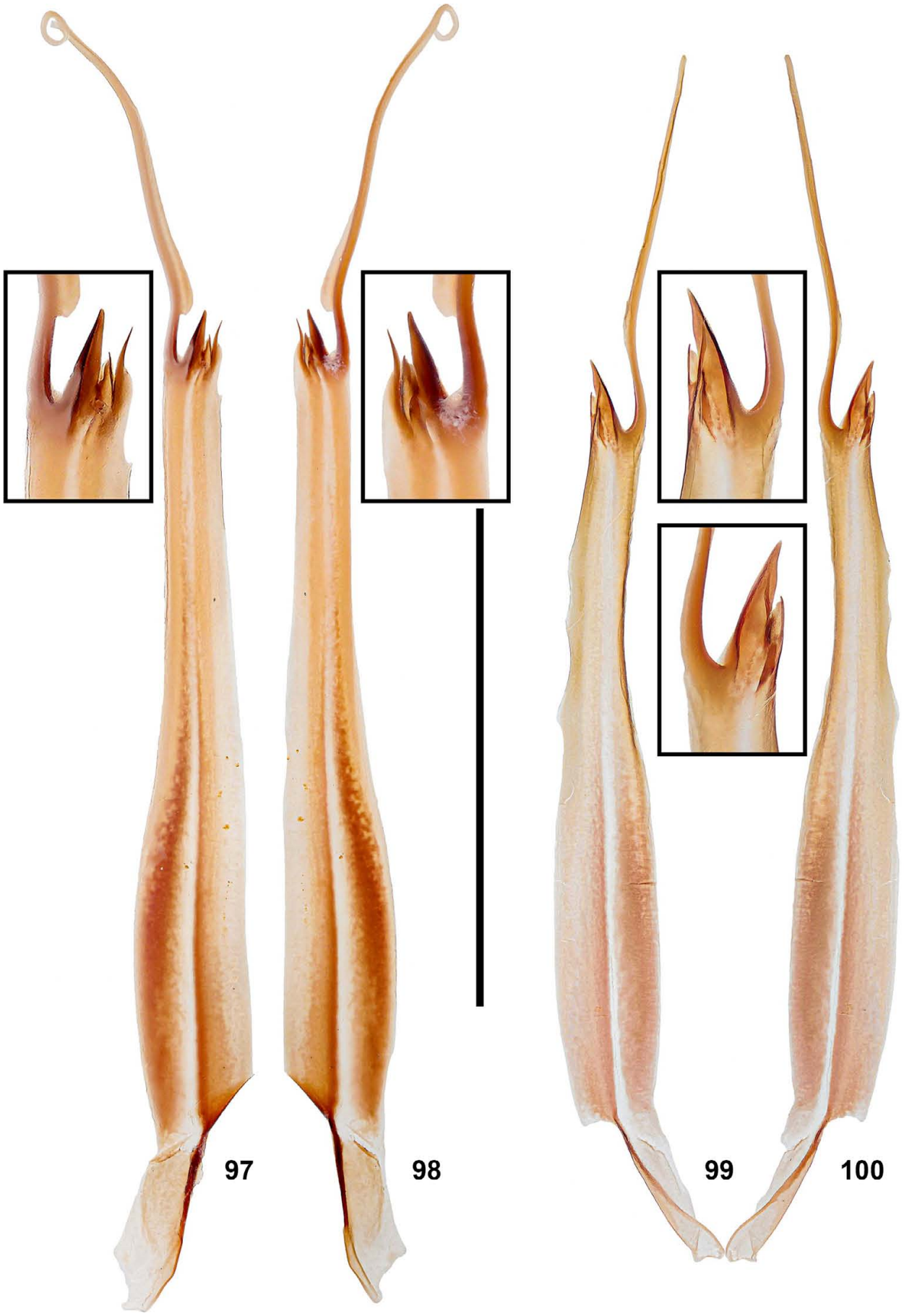

Figures 97–**100**: Comparison of hemispermatophores between *Olivierus longichelus* (Sun & Zhu, 2010) and *Olivierus przewalskii* (Birula, 1897) in convex (97, 99) and concave (98, 100) aspects under white light. **Figures 97**–**98**. Male *O. longichelus* from Jinghe County. **Figures 99**–**100**. Male *O. przewalskii* from Ghulja (Yining) County. Scale bar = 5 mm.

an organism displays a combination of male and female characteristics. However, the individual also might had failed to regenerate the hemispermatophores prior to its death as a male. Consequently, due to the ambiguity surrounding this specimen, its data were excluded from all analyses. Similar male size discrepancy was also observed in the series from Makit (Figs. 111–112). The observed findings led to the identification of two primary size categories for males of *O. przewalskii*: those around 50 mm and those around 45 mm in length. Likewise, the size discrepancy was also confirmed for the conspecific females (Figs. 113–114). Quantitative intraspecific variations for PTC and DSC recorded in Tables 2–3. Female *O. przewalskii* has been recorded with 15 teeth in Sun & Zhu (2010), but it could be a rare value.

O. przewalskii exhibits the following key ontogenetic variation: (1) coloration darker in juveniles, often brownish, with dark, carina-fitted streaks appearing on pedipalps, sometimes forming reticulate patterns (no prominent dark streaks on chela appear in adults); (2) basal lobe on dentate margin of pedipalp movable finger weakly developed in juveniles; (3) carapacial and tergal carination and granulation less developed in juveniles. *O. przewalskii* exhibits the following sexual dimorphism: (1) tergites proportionally wider in females; (2) basal lobe on dentate margin of pedipalp movable finger stronger in males; (3) pectines relatively longer with more teeth in males, leaving smaller interpectinal space basally; (4) genital operculum dome-shaped (single-peaked) in males, but the anterior margin is bilobate in females, appearing as two peaks flanking the middle longitudinal suture.

Distribution. In Xinjiang, this species mainly distributes in the western, southern and eastern regions, but may also be found from Bole and Ghulja in the north. In China, this species is also found in provinces of Gansu (Dunhuang, 40°18'N 94°44'E; Guazhou, 40°29'N 96°02'E) and Inner Mongolia (Ejina, 42°04'N 101°12'E) (Zhang et al., 2020: 85). Beyond China, it is recorded from Mongolia. Records from Uzbekistan and Tajikistan remain dubious and likely erroneous (Fet et al., 2018: 53).

Chinese equivalent. 普氏奥氏蝎 (Tang, 2022a). Other Chinese names applied to this taxon include: (1) *Mesobuthus przewalskii*: 普氏中杀牛蝎 (Tang; UTN); (2) *Buthus caucasicus przewalskii*:高加索钳蝎普氏亚种 (Li et al., 2016; ET-G); (3) *Mesobuthus caucasicus przewalskii*: 普氏高加索钳蝎 (Yang, 2008; ET-G), 普高正钳蝎 (Zhang, 2009: ET-G), 高加索正钳蝎普氏亚种 (Di et al., 2015: ET-G); (4) *Olivierus caucasicus przewalskii*:普氏橄蝎 (Zhu et al., 2004; ET-G, TM-S); (5) *Mesobuthus nanjiangensis*; 南疆正钳蝎 (Zhang, 2009: ET-G).

Mesobuthus Vachon, 1950
Mesobuthus thersites (C. L. Koch, 1839)
(Figures 153–154)
http://zoobank.org/urn:lsid:zoobank.org:act:FFA27933-C18B-4928-80A3-E4269B4272BA

Protonym. *Androctonus thersites* C. L. Koch, 1839: 51–52, pl. CXCIII, fig. 466.

Nomen nudum. *Mesobuthus beijiangensis* Zhang, 2009: 1, 33–36, 60, 113–116, 121–123, figs. 41–43, table 7.

Type locality and type depository. Koch's type is lost and type locality is unclear. Neotype (designated by Kovařík et al., 2022): **Kazakhstan**, *Kyzylorda Province*, south of Kyzylorda, 44°39'25"N 66°01'36"E (44.66°N 66.02°E), 127–135 m a. s. l.; NMPC.

Synonym. *Buthus eupeus mongolicus* Birula, 1911: 195–199. Syn. by Kovařík et al. (2022)
http://zoobank.org/urn:lsid:zoobank.org:act:EDCBCD86-7D10-4FD6-AAEF-90CBD121B1A1
Type locality and type depository. **China**, *Inner Mongolia Autonomous Region*, Alxa League (Alashan Prefecture), Ting-yuan-ying (Bayanhot) (38.83°N 105.66°E); ZISP.

Diagnosis. See Kovařík et al. (2022: 139). Phenotypic variation in coloration exemplified in Tang (2022c: figs. 8–10). Additional photographs of phenotypic variation available on iNaturalist (www.inaturalist.org/observations/; observation IDs = 108739616, 108740310).

Remarks. When this taxon was considered as a subspecies of *M. eupeus*, its distribution in China was initially suggested by Fet (1989, 1994) and Fet & Lowe (2000). The first formal report of its presence in Xinjiang was documented in Sun & Sun (2011) from Ghulja (or Yining) County (44°00'N 81°31'E) based on 22 specimens. After examining a total number of 93 specimens (64 of which were adults) from Ürümqi County, Tang (2022c; in fact, the examination was conducted in October 2021) found no consistent differences between any putative morphological groups (see the above iNaturalist link for photographic evidences); that it is, the three features proposed by Sun & Sun (2011: 71) are ineffectual in explicitly distinguishing *M. e. thersites* from *M. e. mongolicus*. Recent molecular study based on materials from Kazakhstan, Kyrgyzstan, Mongolia, and China by Kovařík et al. (2022: 140) confirmed their synonymy.

Distribution. China (Gansu, Inner Mongolia, Ningxia, and Xinjiang), Kazakhstan, Kyrgyzstan, and Mongolia.

Chinese equivalent. 斗士中杀牛蝎 (Tang, 2022a). Other Chinese names applied to this taxon include: (1) Mesobuthus eupeus [misidentification]: 条纹正钳蝎 (Zhang, 2009; ET-G&S, translation for the specific epithet was derived from its English common name, "mottled scorpion"), 条斑钳蝎 (VN), 条斑金蝎 (VN); (2) Mesobuthus eupeus thersites: 粗正钳蝎 (Zhu et al., 2004; ET-G&SS, TM-S), 粗条正钳蝎 (Sun, 2010; ET-G&S&SS), 条纹正钳蝎特氏亚种 (Di et al., 2015; ET-G&S&SS); (3) Mesobuthus mongolicus: 蒙古中杀牛蝎 (Tang; UTN); (4) Buthus eupeus mongolicus: 条纹钳蝎蒙

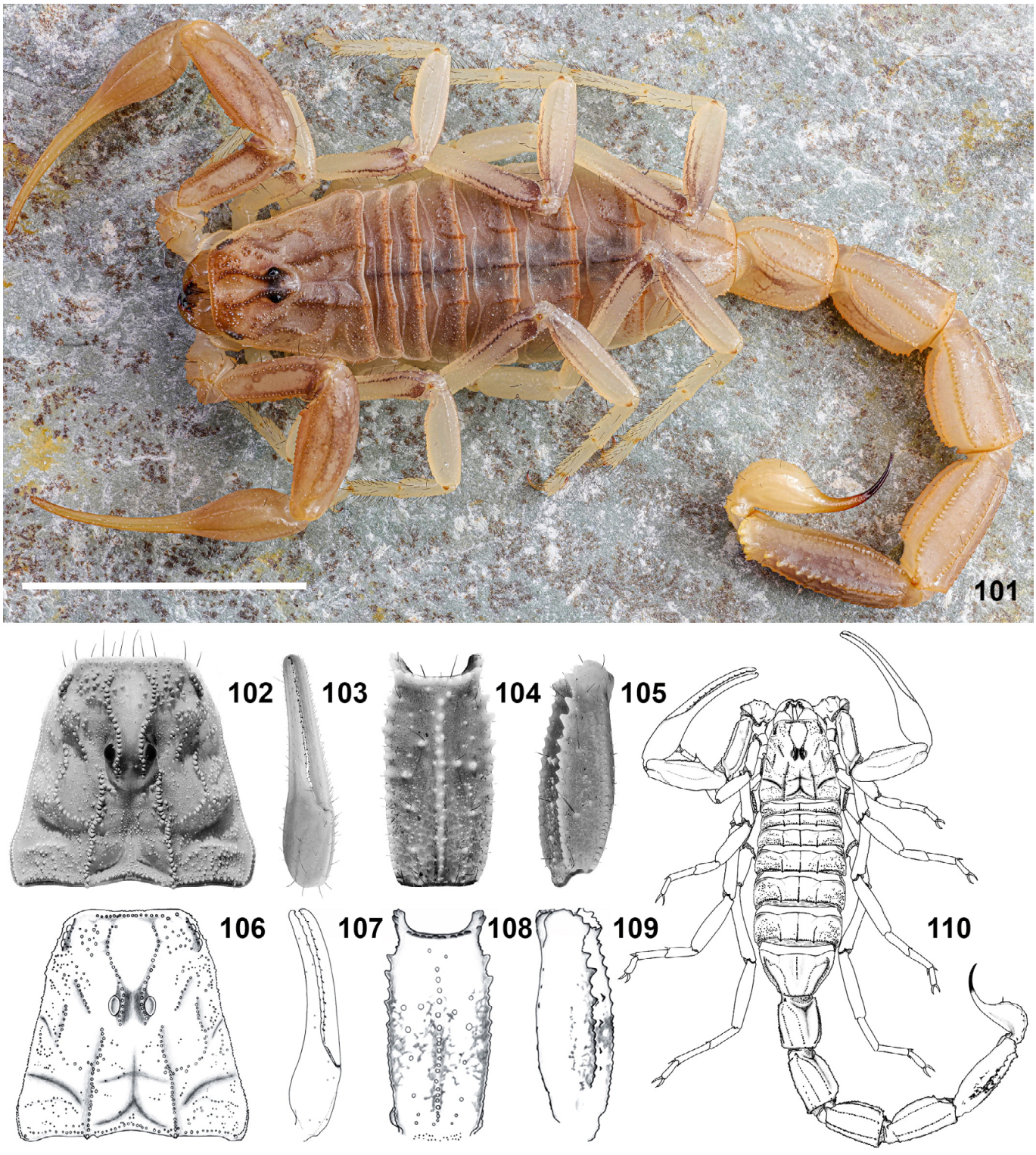

Figures 101–**110**: A juvenile female *Olivierus longichelus* from Bole City, presumably 6th instar (crude total length ca. 51 mm, pretergites concealed), comparing with illustrations of the holotype female *O. longichelus* from Jinghe County from the original description (modified from Sun & Zhu (2010)). **Figures 101**–**105**. Habitus under white light (101), carapace (102), pedipalp chela in external view (103), metasoma V in ventral (104) and external (105) views under UV light. **Figures 106**–**110**. Original illustration of holotype female *O. longichelus*: carapace (106), pedipalp chela in external view (107), metasoma V in ventral (108) and external (109) views, and habitus (110). Scale bar = 10 mm.

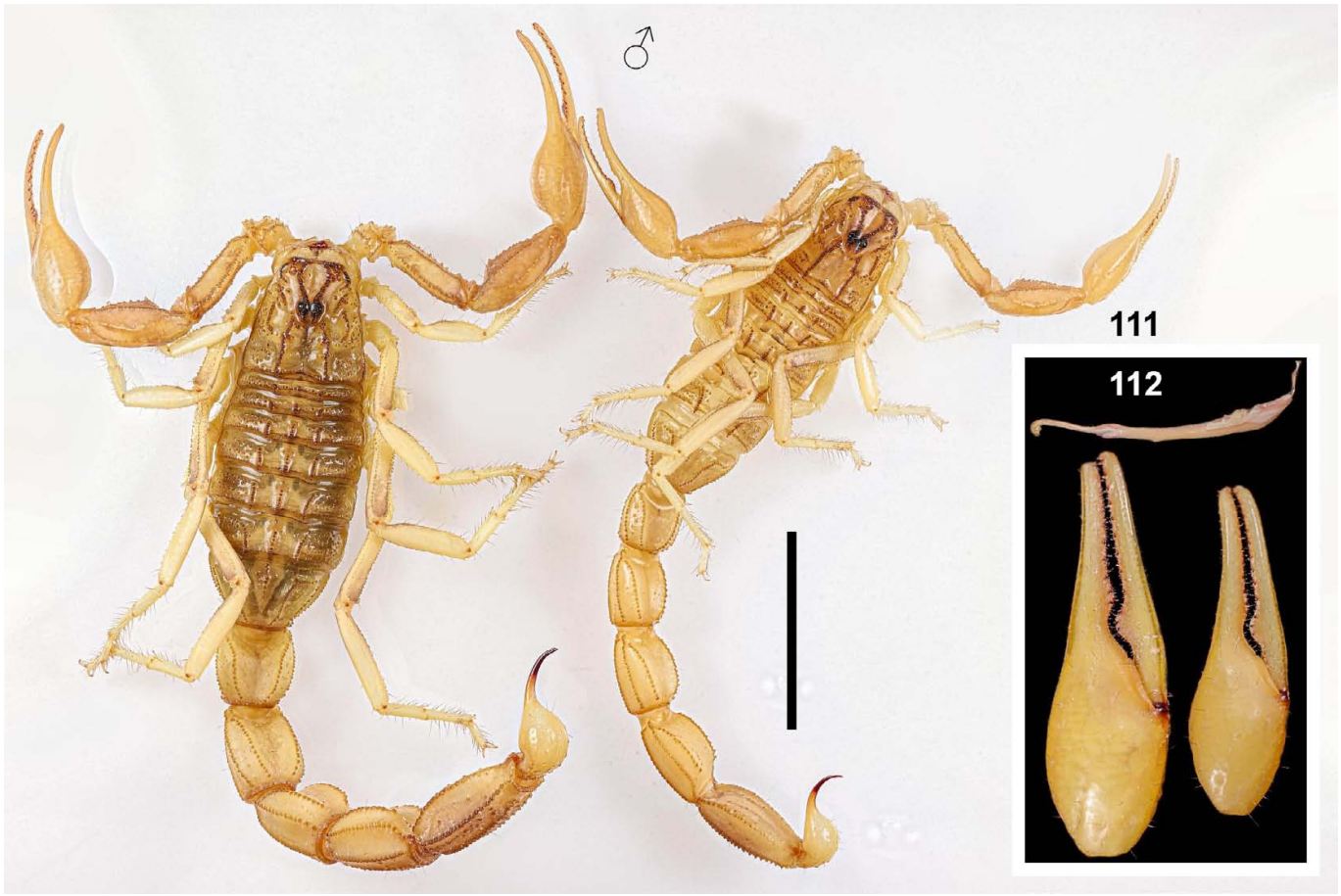

Figures 111–112. Size comparison between two adult males of *O. przewalskii* from Makit. The hemispermatophore was retrieved from the smaller male, verifying the pronounced lobe as a credible indicator for sexual maturity in males of this species. Scale bar = 10 mm (Fig. 111).

古亚种 (Li et al., 2016; ET-G&S); (5) M*esobuthus eupeus mongolicus*: 蒙古正钳蝎 (Zhu et al., 2004; ET-G, TM-S), 蒙条正钳蝎 (Sun, 2010; ET-G&S), 蒙古条纹正钳蝎 (VN), 条纹正钳蝎蒙古亚种 (Di et al., 2015; ET-G&S); (6) Mesob*uthus beijiangensis*: 北疆正钳蝎 (Zhang, 2009; ET-G).

Chinese appellations and conservation status

1. Chinese appellations

The commonly appeared Chinese name "钳蝎 (qián xiē)" ("pincer scorpion" in English) could be an auditory misinterpretation of "全蝎 (quán xiē)" ("integral scorpion" in English, denoting the integrity of the raw medical material), the traditional Chinese medicine based on *O. martensii*, both of which cannot be traced in any Chinese ancient books. Traditional Chinese names of scorpion appeared in books during the ancient dynasties include: "蚓" and "蚓尾虫" (from <*Festal Songs·Durenshi*>, <*Shuowen Jiezi*>, <*Guangya*>), "蜥祁" and "主薄" (from <*Shu Bencao*>, <*YawYang Essays·Chapter Insecta*>), and "蠍" and "杜伯" (from <*Kaibao Bencao*>, <*Bencao Tujing*>, <*Compendium of Materia Medica*>). Modern dictionaries of Chinese medicines initiated to use the terms like "全虫", "全蝎", "茯背虫", etc.

To the best of our knowledge, the name "钳蝎" did not officially appear in any literature until the latter part of the 20th century, after the establishment of The People's Republic of China, and thus cannot be reckoned as a traditional Chinese name that conveys any presumed historical sense of Chinese culture. In the 1963 edition of <*Pharmacopoeia of the People's Republic of China* (1st ed.)> (p. 110), the Chinese medicine "全蝎" was referred to as "问荆蝎" (for "*Buthus martensii*") subordinate to "钳蝎科" (for Buthidae). Subsequently, for the first time, the name "东亚钳蝎" was applied to *O. martensii* in the 1977 edition of the same publication (p. 234). It is likely that the term "钳蝎" was informally coined between 1936 and 1963, after Wu (1936) provided the first report on China's scorpiofauna within the framework of modern taxonomy and identified the materials of *O. martensii* deposited in Chinese Academy of Science. *Lychas mucronatus* (Fabricius, 1798) was the other buthid species identified by the author. Li et al. (2016) mentioned that Chengzhao Liu was the subsequent scholar who reported on the anatomical structures of *O. martensii* in 1940. However, despite efforts, the specific paper by Liu (1940) could not be located. Furthermore, the authors highlighted a notable gap in research on this species, with no additional studies recorded until 1982.

Ancient records of scorpions in China were limited to Hebei, Henan, Liaoning, Shaanxi and Shandong (Yang et al., 2018), which lied within the distribution range of *O. martensii* while being allopatric with *L. mucronatus*. Yang et al. (2018)

Figures 113–**114**: Females of *O. przewalskii* from Yarkant (Shache). **Figure 113**. Size comparison between large adult female, small adult female and juvenile female (left to right). **Figure 114**. Smaller female after one-day immersion in pure ethanol with tergites removed, showing ovarian follicle, confirming the maturity of this size class; explicit ovariuterus was not successfully revealed.

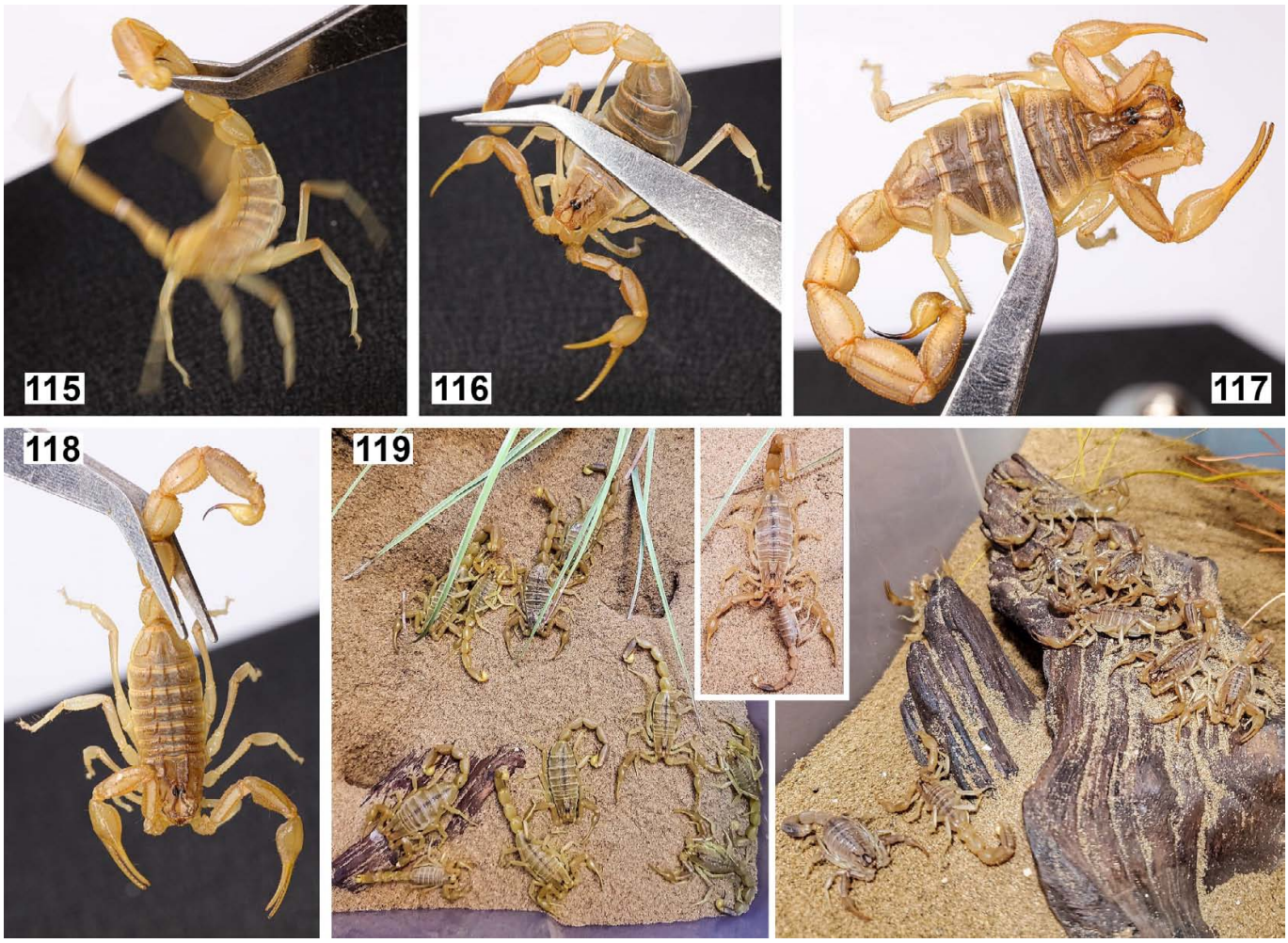

Figures 115–119: Observations under captive condition. **Figures 115–118**. Behavioral response tests conducted on live specimens: tweezer clamping on metasoma and dorsoventrally on mesosoma. **Figures 115–116**. Male (115) and female (116) *O. longichelus* showed resistance and aggression. **Figures 117–118**. Female (117) and male (118) *O. przewalskii* remained immobile. **Figure 119**. Spontaneously clustered *O. longichelus* (left; including one *M. thersites*) and *O. przewalskii* (right) observed under captive condition at night, and a case of cannibalism in *O. longichelus* (middle).

confirmed that all the Chinese appellations of scorpion occurred in ancient and modern medical books exclusively pertained to *O. martensii*. Put differently, the colloquial names "钳蝎" or "全蝎" were originally ascribed to a singular species with widespread distribution in China. As expostulated in Tang (2022a), these facts argue against the appropriateness of assigning the term "钳蝎" to either the genus *Buthus* Leach, 1815 that does not distribute in China (or any genus that contains the name "*buthus*") or the family Buthidae C. L. Koch, 1837 at large. The term "钳蝎" may had been simply extended to those supraspecific ranks (genus and family) subsequent to its designation for a particular species (*O. martensii*), which is a typical *modus operandi* in the "nomenclature" of Formal Chinese Names for animals. Crucially, the genus *Mesobuthus* was incorrectly translated as "正钳蝎" even if one were to accept the usage of "钳蝎". As clarified in Tang (2022a: 10), the prefix "*meso*-" implies "median", "middle" or "medium" ("中") rather than "straight", "upright" or "ortho" ("正"). A taxon described recently, *Qianxie solegladi* Tang, 2022, is not semantically equivalent to the vernacular name "钳蝎" for *O. martensii*. No endemic genera except for *Qianxie* Tang, 2022 and *Langxie* Tang et al., 2023 exist in China (except for the dubious genus *Tibetiomachus* Lourenço & Qi, 2006). Consequently, it is imperative to refrain from assigning any purported "traditional Chinese name" to any scorpion genus and instead reserve such appellation for a particular species exclusively.

2. Conservation status

The conservation of scorpions in China has, unfortunately, been a longstanding oversight (Tang, 2022b: 17). Wild Chinese scorpions are primarily harvested for medicinal, culinary, and liquor ingredient purposes. Around the year 2020, amid the COVID pandemic in China, *O. martensii* received a regional protection status in Yimeng. Stringent regulations were imposed, prohibiting individuals from excessively collecting wild scorpions (beyond 20 specimens); violators faced criminal prosecution. Notably, as mentioned earlier, *M. thersites* (as "条纹正钳蝎 *M. eupeus*") was officially designated as the sole protected scorpion species since June 2023. This legislative measure is commendable given the severe exploitation of wild populations of this species in the past years (Tang, 2022b: 17).

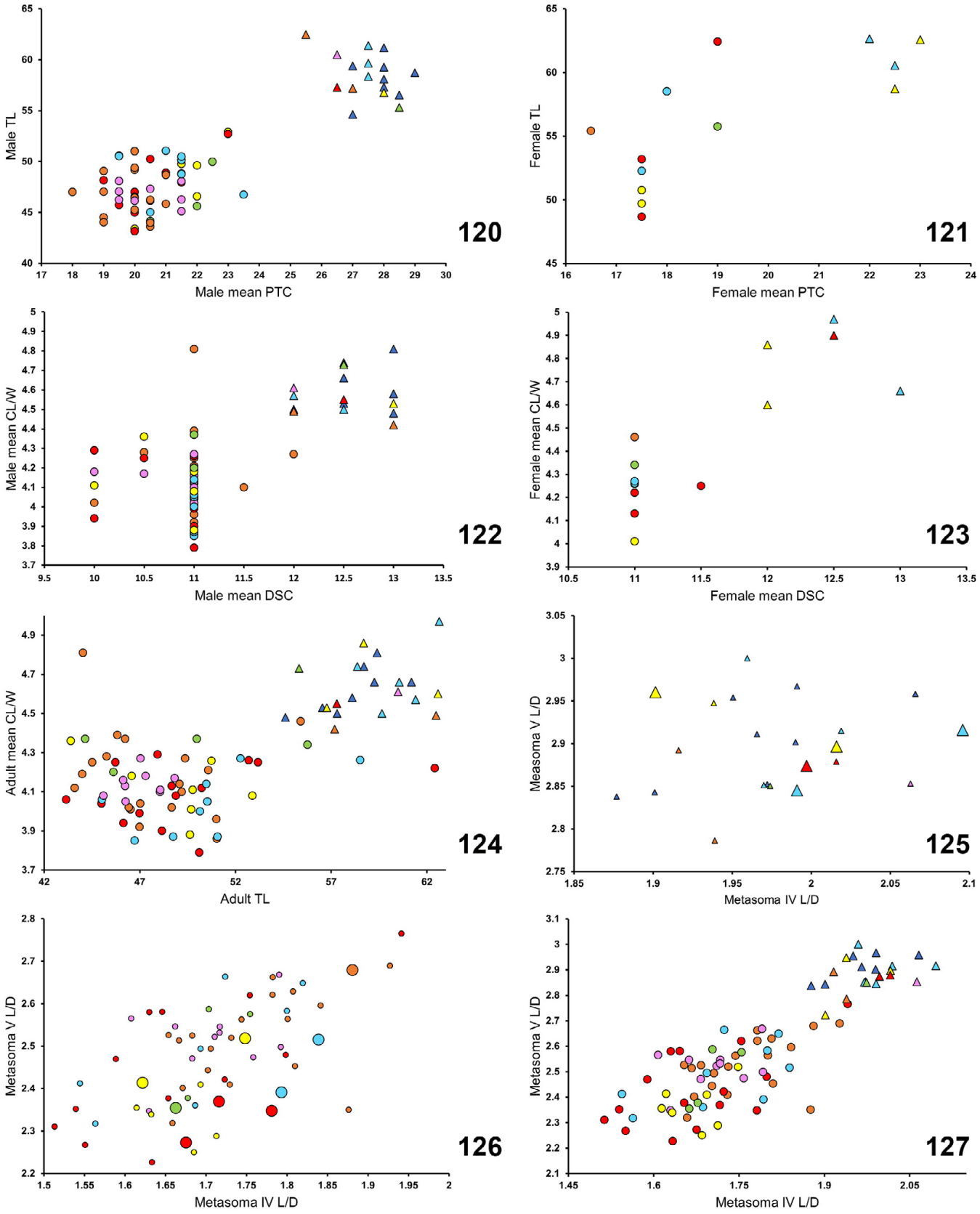

Figures 120–**127**: Bivariate scatterplot comparisons among studied populations of *O. longichelus* (triangle) and *O. przewalskii* (circle). Yellow, Bole; green, Ghulja; blue, Jinghe; orange, Makit; cyan, Qiemo; pink, Ruoqiang; red, Yarkant. **Figure 120**. Means of adult male PTC (abscissa) vs. TL (ordinate) between *O. longichelus* and *O. przewalskii*. **Figure 121**. Means of adult female PTC (abscissa) vs. TL (ordinate) between *O. longichelus* and *O. przewalskii*. **Figure 122**. Means of adult male DSC (abscissa) vs. CL/W (ordinate) between *O. longichelus* and *O. przewalskii*. **Figure 123**. Means of adult female DSC (abscissa) vs. CL/W (ordinate) between *O. longichelus* and *O. przewalskii*. **Figure 124**. Comparing adult TL (abscissa) and mean CL/W (ordinate) of *O. longichelus* and *O. przewalskii* with males and females pooled together. **Figure 125**. Metasoma IV L/D (abscissa) vs. V L/D (ordinate) between adult males (small triangle) and females (large triangle) of *O. longichelus*. **Figure 126**. Metasoma IV L/D (abscissa) vs. V L/D (ordinate) between adult males (small circle) and females (large circle) of *O. przewalskii*. **Figure 127**. Comparing L/D ratio of adult metasoma IV (abscissa) and V (ordinate) between *O. longichelus* and *O. przewalskii*; males and females are pooled together as they do not show significant difference (sexual dimorphism) in this aspect.

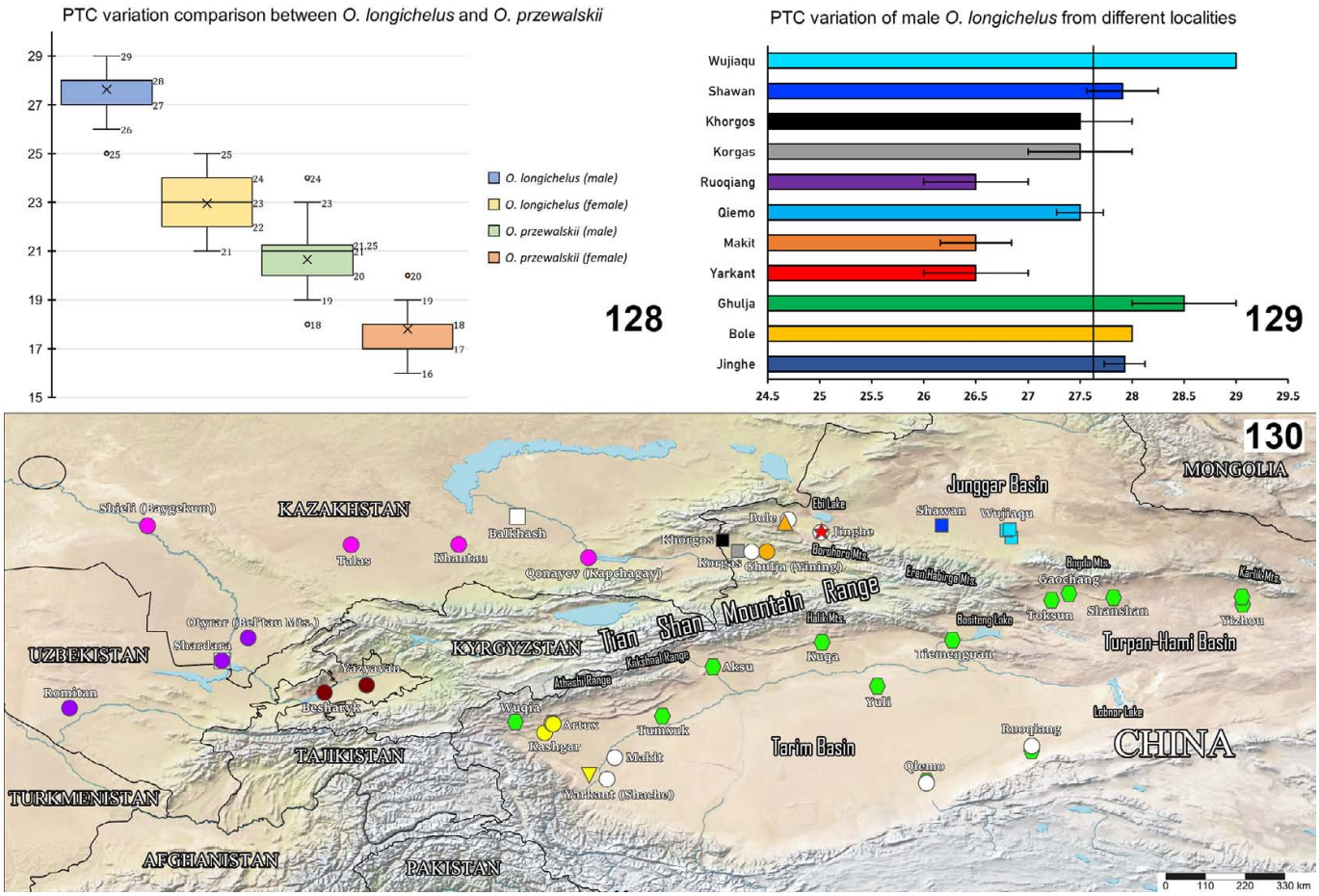

Figures 128–**130**: Morphometric visualization of PTC and distribution map. **Figure 128**. Box and whisker plot visualizing the discrepancy of PTC frequency between male and female *O. longichelus* (all localities) and *O. przewalskii* based on "exclusive" method (median of each quartile *Q* excluded), with values of maximum, Q_3, median, Q_1, minimum, and outliers labeled. Means (denoted as ×) for each box are as follows (left to right): 27.62, 22.95, 20.65, and 17.79. Medians for male *O. longichelus* and female *O. przewalskii* are 28 and 18, respectively. **Figure 129**. Horizontal bar plot visualizing the mean PTC of male *O. longichelus*. Error bars are standard errors. Vertical line represents the mean male PTC of all localities (27.62). Note that the sample sizes for different localities can be significantly different (see Table 4). **Figure 130**. Map showing the localities of *Olivierus* spp. in Xinjiang (China) and adjacent countries with exact coordinates: topotypes examined in this study; "*M. c. intermedius*" studied in previous Chinese papers; *O. longichelus* holotype locality (★); *O. bolensis* (**syn**. **n**. with *O. longichelus*) holotype (▲) and paratype (●) localities; *O. karshius* (**syn**. **n**. with *O. longichelus*) holotype (▼) and paratype (●) localities; *O. przewalskii* localities (⬢); *O.* sp. (now confirmed as *O. longichelus*) from Wujiaqu (■); *O.* sp. (now confirmed as *O. longichelus*) from Shawan (■); *O.* sp. (now confirmed as *O. longichelus*) from Korgas (■); *O.* sp. (now confirmed as *O. longichelus*) from Khorgos (■); *O. mikhailovi* localities (●); *O. tarabaevi* (**syn**. **n**. with *O. longichelus*) localities (●; the locality in Kapchagay, as above discussed, may be erroneous in terms of the specimen identity but reasonable in terms of the geography); *O. voldemari* localities (●). One locality of *O. karshius* in Artux is exactly the same as one locality of *O. przewalskii* (39°42'N 76°09'E (Sun & Sun, 2011: 60, 63)); locality of "*M. c. intermedius*" in Chardara is overlapped with one locality of *O. mikhailovi*.

Regrettably, a noteworthy challenge lies in a discernible gap in the accurate understanding of scorpion identification and taxonomy. During an interview, Mrs. Hongying Hu, a professor from the College of Life Science and Technology at Xinjiang University, asserted that "*M. eupeus*" is a narrowly distributed species in China, particularly the subspecies *M. e. thersites*. This statement indicates an outdated perspective, echoing views held 12 years ago by Sun & Sun (2011). In an online report associated with the protection of "*M. eupeus*" by a Xinjiang TV station, a photograph mistakenly depicted an adult male *O. longichelus* instead of *M. thersites*. Effective animal conservation entails not only governmental and public involvement but also a sound taxonomic foundation that aligns with contemporary understanding, enabling accurate species identification. In addition to *O. martensii* and *M. thersites*, it is imperative to draw attention to other Chinese scorpion species that show higher micro-endemism, substrate preferences, and vulnerability from environmental degradation stemming from land reclamation and urbanization, notably exemplified by the genus *Scorpiops*. It is essential to underscore that effective conservation mandates comprehensive recognition of species distribution, facilitating the implementation of targeted protective measures in specific regions. Concealing the whereabouts of scorpions proves inadequate in safeguarding

Species	*O. longichelus* ♀ Holotype	*O. longichelus* ♂ Paratype (immature)	*O. bolensis* ♂ Holotype	*O. bolensis* ♀ Paratype	*O. karshius* ♀ Holotype
Locality	Jinghe	Jinghe	Bole	Ghulja (Yining)	Yarkant (Shache)
TL (mm)	52.08	-	56.56	70.78	67.67
PTC	22–23	27–28	28–12	22–22	22–21
DSC	12	12	12	12	12
C-L/W	5.41836	-	4.07719	4.76712	3.83383
MIV-L/W	1.76774	-	1.5	1.65484	1.54603
MV-L/W	2.08135	-	1.88983	2.23724	2.10392
AL/TeL	0.54414	-	0.56497	0.49936	0.50975
MV-VL	With larger denticles posteriorly	-	With large denticles posteriorly	With large denticles posteriorly	Without large denticles posteriorly
MV-VM	Explicit granular	-	Explicit granular	-	Dispersive granular
MV-I	Infuscate	-	Non-infuscate	Non-infuscate	Non-infuscate
C-G	Small, sparser	-	Small, denser	Small, denser	Small, dense
C&P-C	Explicit granular	-	Dispersive granular	Dispersive granular	Explicit granular
F-ICG	Smooth	-	Granulated	-	Smooth
EAD	Smaller ↑; < IAD	-	?	?	Not smaller ↑; = IAD
TS	Long	-	Long	Long	-
Source	Sun & Zhu (2010) Sun et al. (2010)	Sun & Zhu (2010)	Sun et al. (2010)	Sun et al. (2010)	Sun & Sun (2011)
Species	*O. karshius* ♂ Paratype	*O. karshius* ♂	*O. karshius* ♀	*O. przewalskii* ♂	*O. przewalskii* ♀
Locality	Yarkant (Shache)	Artux, Kashgar, Yarkant	Artux, Kashgar, Yarkant	See source	See source
TL (mm)	61.11	46–62	56–72	50–68	68–78
PTC	25–25	23–28	19–23	19–23	15–19
DSC	-	12	12	11	11
C-L/W	3.95205	-	-	3.87795	4.13698
MIV-L/W	1.49019	-	-	1.46070	1.48192
MV-L/W	2.01977	-	-	2.07619	2.06779
AL/TeL	0.5	-	-	0.51452	0.50478
MV-VL	-	"Posteriorly marked, not uniform"	"Posteriorly marked, not uniform"	Without large denticles posteriorly	Without large denticles posteriorly
MV-VM	-	-	-	-	Dispersive granular
MV-I	-	Non-infuscate/infuscate	Non-infuscate/infuscate	Infuscate	Infuscate
C-G	-	-	-	Coarse	Coarse
C&P-C	-	-	-	Explicit granular	Explicit granular
F-ICG	-	Smooth	Smooth	-	Smooth
EAD	-	Not smaller ↑; = IAD	Not smaller ↑; = IAD	Smaller ↑; < IAD	Smaller ↑; < IAD
TS	-	Short	Short	Moderate to long	Moderate to long
Source	Sun & Sun (2011)	Sun & Sun (2011)	Sun & Sun (2011)	Sun & Zhu (2010) Sun & Sun (2011)	Sun & Zhu (2010) Sun & Sun (2011)

Table 1. Potentially useful characters retrieved from previous papers. Abbreviations: TL, total length; PTC, pectinal tooth count; DSC, denticle subrow count of movable finger; C-L/W, length to width ratio of pedipalp chela; MIV-L/W, length to width ratio of metasoma IV; MV-L/W, length to width ratio of metasoma V; AL/TelL, aculeus length to telson length ratio; MV-VL, ventrolateral carina of metasoma V; MV-VM, ventromedian carina of metasoma V; MV-I, infuscation of metasoma V; C-G, granulation of carapace; C&P-C, carinae of carapace and patella; F-ICG, intercarinal granulation of pedipalp femur; EAD, external accessory denticle(s); IAD, internal accessory denticle(s); ↑, to the tip of pedipalp movable finger; TS, tarsal setation. Several qualitative characters were referred to the original illustrations. Morphometrics of *O. przewalskii* were taken from table 1 in Sun & Sun (2011: 62). L/W of metasomal segments IV and V was not calculated in this study as the L/D thereof appeared to be more informative (indicator for dorsoventral dilation); previous papers for metasoma IV included only the length and width.

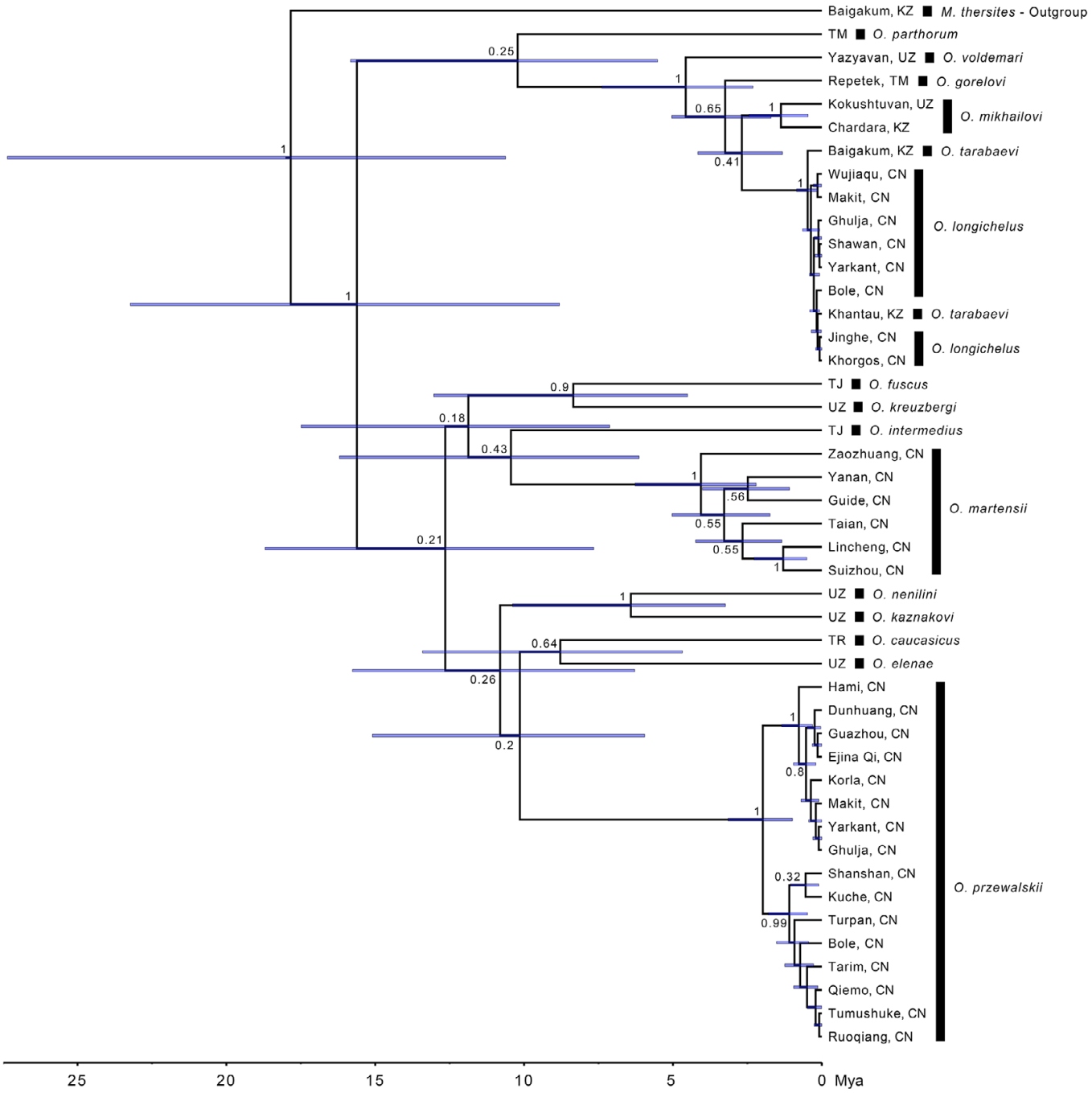

Figure 131. Time-calibrated phylogeny of *Olivierus* species inferred from analysis of an 840 base pair alignment of partial COI sequences in BEAST (version 1.8.0). Horizontal bars indicate 95% highest posterior density intervals for date estimates. Posterior probabilities are provided at nodes, with some removed from the youngest nodes for clarity. The phylogeny was calibrated using mutation rates estimated for related buthid scorpions (see text for details).

their wild populations, as awareness of their existence is a premise for successful conservation efforts. Such method is not a sustainable long-term solution, as stochastic collection activities by amateurs, natural enthusiasts, or hired collectors (those who harvest wild scorpions for purely consumptive purposes) may inadvertently encounter the habitats, including the type localities, of these scorpions. This situation poses a potential threat to the wild populations due to variations in individual ethical standards. A more preferable approach would be to advocate for species protection by informing authorities about their distributions with the efforts of scientific institutions. Although the implementation of such a strategy may require considerable time for legislative processes to take effect, it offers a more enduring solution to safeguarding these species.

Nevertheless, the enactment of such legislation could potentially impede future scientific investigations. Taxonomy, being an undervalued discipline in China due to its lack of immediate advantages or financial incentives, may face challenges. Commencing a taxonomic revision typically

PTC Frequency	*f*(16)	*f*(17)	*f*(18)	*f*(19)	*f*(20)	*f*(21)	*f*(22)	*f*(23)	*f*(24)	*f*(25)	*f*(26)	*f*(27)	*f*(28)	*f*(29)
O. longichelus (♂, n = 34)	0	0	0	0	0	0	0	0	0	0.0294	0.0882	**0.3824**	**0.3824**	**0.1176**
O. longichelus (♀, n = 12)	0	0	0	0	0	0	**0.5833**	**0.4167**	0	0	0	0	0	0
O. przewalskii (♂, n = 114)	0	0	0.0263	0.1228	**0.3421**	**0.2632**	0.1842	0.0439	0.0175	0	0	0	0	0
O. przewalskii (♀, n = 34)	0.0588	**0.3235**	**0.4118**	0.1765	0.0294	0	0	0	0	0	0	0	0	0

Table 2

DSC Frequency	*f*(9)	*f*(10)	*f*(11)	*f*(12)	*f*(13)
O. longichelus (n = 51)	0	0	0	**0.5098**	**0.4902**
O. przewalskii (n = 155)	0.0065	**0.1032**	**0.8581**	0.0323	0

Table 3

PTC Frequency	*f*(21)	*f*(22)	*f*(23)	*f*(24)	*f*(25)	*f*(26)	*f*(27)	*f*(28)	*f*(29)
O. longichelus (J♂, n = 14)	0	0	0	0	0	0	0.2857	0.5	0.2143
O. longichelus (B♂, n = 2)	0	0	0	0	0	0	0	1	0
O. longichelus (G♂, n = 2)	0	0	0	0	0	0	0	0.5	0.5
O. longichelus (Y♂, n = 2)	0	0	0	0	0	0,5	0.5	0	0
O. longichelus (M♂, n = 6)	0	0	0	0	0.1667	0.1667	0.6667	0	0
O. longichelus (Q♂, n = 6)	0	0	0	0	0	0	0.5	0.5	0
O. longichelus (R♂, n = 2)	0	0	0	0	0	0.5	0.5	0	0
O. longichelus (K♂, n = 2)	0	0	0	0	0	0	**0.5**	**0.5**	0
O. longichelus (k♂, n = 2)	0	0	0	0	0	0	**0.5**	**0.5**	0
O. longichelus (S♂, n = 11)	0	0	0	0	0	**0.1818**	0.0909	**0.3636**	**0.3636**
O. longichelus (S♀, n = 10)	0.1	0.1	0	**0.6**	**0.2**	0	0	0	0
O. longichelus (W♂, n = 2)	0	0	0	0	0	0	0	0	**1**
O. longichelus (W♀, n = 18)	0	**0.2778**	**0.5556**	0.1667	0	0	0	0	0
O. longichelus (P♂, n = 51)	0	0	0	0	0.0196	0.098	**0.3137**	**0.3725**	0.1961
O. longichelus (P♀, n = 40)	0.025	**0.325**	**0.375**	0.225	0.05	0	0	0	0

Table 4

Tables 2–4. Relative frequencies of discrete quantitative morphometrics; *n* refers to number of pectines/fingers. **Tables 2–3**. Relative frequencies of certain PTC and DSC values present in each sex of each species (DSC pooled together for both sexes), based on the examined materials from Bole (B), Ghulja (G), Jinghe (J), Makit (M), Qiemo (Q), Ruoqiang (R), and Yarkant (Y). Modal values are reddened and bolded, second frequent values are bolded. **Table 4**. Relative frequencies of PTC value in newly examined males and females of *O. longichelus* from Korgas (K), Khorgos (k), Shawan (S) and Wujiaqu (W), and pooled samples from all localities (P) (below), in comparison with isolated male PTC frequencies from localities in Table 2 (above). *Note*: male *O. longichelus* had been recorded with 30 teeth in the previously studied specimens from Wujiaqu (Tang, 2022b: table 1) and not included here.

necessitates a substantial sample size to mitigate statistical bias. Imposing restraint on the field collection of wild specimens can therefore significantly impact the attendant laboratory examination. Meanwhile, the differentiation between invasive and/or wild animals and non-invasive and/or wild (or captive) animals tends to be conveniently overlooked during the administration of animal control and protection in China. This oversight has led to a blanket classification of a majority of captive invertebrates that either do not carry zoonotic disease or have extreme requirements for their survival, as hazardous, wild animals that may give rise to ecological damage, without truly confirming such asserted properties. In the case of invertebrates like scorpions, there is no provision for obtaining a license to import foreign species, or to export specimens to other countries for scientific study even when certain regulations are followed (Tang et al., 2023: 31–32). Authorities typically do not address individual requests of this nature. If this trend extends to the scenario of collecting domestic wild scorpions, it is conceivable that only individuals affiliated with specific domestic institutions would likely have the opportunity to secure permission for the scientific study of scorpions.

Scorpiology remains in its infancy in China, with numerous overlooked issues coming to light only recently (Tang, 2022c, 2023). The acquisition of materials for the personal scientific research of the first author, such as those utilized in the present study, was made possible by the dedication of several genuine enthusiasts. Indeed, the first author is not a solitary instance of an amateur demonstrating interest in scientific study. The accessibility to material of wild Chinese animals has similarly enabled several other enthusiasts to establish a foundational understanding, paving the way for their inaugural

Olivierus spp.	TL (mm)	PTC	DSC	CL/W	Manus	MFL	Tt III VS	PSH	MV VL S	Met. infuscation	Distribution
O. brutus	♂ 50–61 ♀ 60–62	♂ 25–28 ♀ 20–22	13	♂ 3.13–3.15 ♀ 3.58–3.65	♂ M, L ♀ N, S	♂ strong ♀ weak[ex]	spiniform	sparse	5	Ant. 3/4 V All surfaces	IR
O. caucasicus	♂ 50–55 ♀ 58–75	♂ 28–32 ♀ 22–25	12–13	♂ 3.43–3.62 ♀ 3.39–3.94	♂ N, S ♀ N, S	♂ moderate ♀ weak	thin	sparse	0	Ant. 2/3 V All surfaces	AM, AZ, GE, IR, RU, TA AU
O. elenae	♂ - ♀ 74–80	♂ 25–27 ♀ 21–22	12	♂ - ♀ 3.54–4.11	♂ - ♀ N, S	♂ - ♀ weak	thin	dense	0	Non-infus. All surfaces	TJ, UZ
**O. extremus*	50	19–22	?14	4	-	-	-	-	-	V	?MY
O. fuscus	♂ 70 ♀ 74–80	♂ 26–29 ♀ 21–25	13–14	♂ 2.84 ♀ 3.13–3.40	♂ G, L ♀ G, S	♂ strong ♀ weak	spiniform	sparse	4	Ant. > 3/4 V All surfaces	TJ, UZ
O. gorelovi	♂ 49–52 ♀ 61–70	♂ 24–28 ♀ 17–23	12–13	♂ 3.72–4.60 ♀ 3.90–4.22	♂ N, S ♀ N, S	♂ weak ♀ weak[ex]	thin	dense	2	V moderately Mainly ventral	TM, UZ
**O. hainanensis*	-	♂ 22 ♀ 19	-	-	♂ M, L ♀ N, S	-	-	-	-	V All surfaces	CN
O. intermedius	♂ 55–70 ♀ 55–70	♂ 21–23 ♀ 17–19	13–14	♂ 3.72–4.60 ♀ 3.90–4.22	♂ N, S ♀ N, S	♂ strong ♀ -	spiniform	sparse	-	Non-infus. All surfaces	TJ
O. kaznakovi	♂ 68–70 ♀ 68–75	♂ 25–27 ♀ 19–23	13	♂ 3.50–3.65 ♀ 3.81–3.93	♂ M, L ♀ N, S	♂ moderate ♀ weak[ex]	spiniform	sparse	4	Ant. 2/3 V All surfaces	TJ, UZ
O. kreuzbergi	♂ 65–70 ♀ 74–85	♂ 26–30 ♀ 20–25	13	♂ 3.15–3.39 ♀ 3.35–3.66	♂ M, L ♀ N, S	♂ strong ♀ weak	thin	sparse	♂3 ♀4	IV & ant. 1/2 V All surfaces	TJ, UZ
O. longichelus	♂ 55–62 ♀ 58–67	♂ 25–30 ♀ 21–25	12–13	♂ 4.42–4.81 ♀ 4.6–4.97	♂ N, S ♀ N, S	♂ moderate ♀ weak	thin	sparse	4	V barely to moderately Mainly ventral & lateral	CN
O. martensii	♂ ~53 ♀ ~60	♂ 21–26 ♀ 17–22	12	♂ 3.48 ♀ 4.42	♂ M, L ♀ N, S	♂ moderate ♀ weak[ex]	thin	sparse	3	Ant. 2/3 V All surfaces	CN, KP, KR, MN
O. mikhailovi	♂ 50–52 ♀ 68–75	♂ 26–28 ♀ 21–23	13	♂ 3.5–3.7 ♀ 4.3–4.5	♂ N, S ♀ N, S	♂ moderate ♀ weak	thin	sparse	4	V moderately Mainly ventral & lateral	KZ, UZ
O. mischi	♂ 71 ♀ 64–71	♂ 25–26 ♀ 20–24	13–14	♂ 2.95 ♀ 3.11–3.62	♂ G, S ♀ M, S	♂ strong ♀ weak	spiniform	sparse	♂4 ♀1	Non-infus. All surfaces	AF
O. nenilini	♂ 51.5 ♀ 50–58	♂ 26–28 ♀ 21–24	13	♂ 4.31 ♀ 4.09–4.30	♂ N[ex], S ♀ N[ex], S	♂ weak[ex] ♀ weak[ex]	thin	sparse	♂2 ♀3	Pos. 2/3 V Mainly ventral	UZ
O. parthorum	♂ 55–64 ♀ 70–85	♂ 26–30 ♀ 20–24	12–14	♂ 3.62–4.03 ♀ 3.52–4.09	♂ N[ex], S ♀ M, S	♂ moderate ♀ weak	♂ thin ♀ spiniform	sparse	2	V barely to moderately Mainly ventral & lateral	AF, IR, TM
O. przewalskii	♂ 44–53 ♀ 49–63	♂ 18–24 ♀ 16–20	9–11	♂ 3.79–4.39 ♀ 4.01–4.46	♂ N, S ♀ N, S	♂ moderate ♀ weak	thin	sparse	1	V moderately Mainly ventral & lateral	CN, MN
O. tarabaevi	♂ 48 ♀ 64–66	♂ 24–27 ♀ 19–22	12–13	♂ 4.14 ♀ 4.1–4.2	♂ N, S ♀ N, S	♂ weak ♀ weak	thin	sparse	♂3 ♀4	V moderately Mainly ventral & lateral	KZ
O. voldemari	♂ - ♀ 64–66	♂ - ♀ 22–23	12–13	♂ - ♀ 4.1–4.2	♂ - ♀ N, S	♂ - ♀ weak[ex]	thin	sparse	2	Pos. 1/2 V Mainly ventral & lateral	UZ

Table 5. Comparative morphological matrix of currently recognized *Olivierus* species (*O. tarabaevi* is a synonym of *O. longichelus*); qualitative characters are susceptible to subjective biases. *: species with doubtful validity, likely synonymous with *O. martensii*. **Morphology abbreviations**: TL, total length; PTC, pectinal tooth count; DSC, denticle subrow count; CL/W, length/width ratio of chela (only referential, our data for *O. longichelus* and *O. przewalskii* might not be appropriate for direct comparison with those for their congeners); MFL, movable finger lobe; ex, extremely; Tt III VS, telotarsus III ventral setation; PSH, pedal spur hirsuteness; MV VL S, metasoma V ventrolateral carinae serration; met, metasoma; infus., infuscate; ant., anterior; pos., posterior. **Pedipalp chela manus profile with respect to finger**: G, globous; M, moderate (pertains to width); N, narrow; S, short; L, long. **Metasoma V ventrolateral carinae serration types**: 0, flattened and sparse; 1, small, blunt and dense; 2, small, sharp and dense; 3, moderate and sharp; 4, lobiform with narrow spacing; 5, lobiform with wide spacing. **Country abbreviations**: AF, Afghanistan; AM, Armenia; AZ, Azerbaijan; CN, China; GE, Georgia; IR, Iran; KZ, Kazakhstan; MY, Malaysia; MN, Mongolia; KP, North Korea; RU, Russia; KR, South Korea; TJ, Tajikistan; TR, Turkey; TM, Turkmenistan; UA, Ukraine; UZ, Uzbekistan. Data sourced from (except for *O. longichelus* and *O. przewalskii*): Fet et al. (2018), Fet et al. (2021), Kovařík (2019), Qi et al. (2004), Werner (1936); qualitative characters of *O. martensii* further based on the personal collection of the first author (cf. Figs. 157–158, 163–168). The overall coloration is neglected here since many species were only known from preserved specimens suffered from discoloration.

scientific research after years of knowledge accumulation. Given the competitive nature of this field and the existence of bureaucracy, from the perspective of an independent researcher, establishing a registration system for collectors to disclose personal information, date of collection, collection site, number of specimens, or subordinate groups of specimens may not be advisable. The concern lies in the accessibility of such data by institutional researchers, potentially leading to a shift in their research focus in an adversarial manner against independent researchers. However, this is nonetheless a feasible compromise for animal protection and independent research, given the premise that the stipulation includes robust measures for safeguarding and maintaining the confidentiality of such data.

Behavioral observation under captive condition

1. **Anti-predatory response**

The first thing deserving special attention pertains to the discrepancy in antagonism between the two *Olivierus* species (Figs. 115–118). All 37 living specimens were performed with a "tweezer clamp" test: the scorpion was lifted from the plane it rested upon by gently clamping its metasomal segment with a tweezer, followed by its return to the surface. The result showed a contrasting response to this tactile stimulus: 18/18 *O. longichelus* reacted aggressively by fiercely and rapidly pinching the tweezer with both pedipalps, accompanied by an upward arching motion directed towards the metasomal region held by the tweezer. Conversely, only 3/19 *O. przewalskii* reacted in a relatively pugnacious manner, mirroring the actions witnessed in *O. longichelus*. Among these three belligerent male *O. przewalskii*, one of them only mildly bended and touched the tweezer, shortly before desisting. All the remaining *O. przewalskii* were motionless and displayed a rigid posture resembling a cataleptic response. After the scorpion being repositioned onto the plane, *O. longichelus* immediately initiated a flight response, while most *O. przewalskii* remained static unless prompted by a vibration. Notably, those *O. przewalskii* exhibited a periodic locomotion pattern, marching over a limited distance each time. This behavioral discrepancy was age- and sex-independent. Another trial was also conducted: scorpions were clamped dorsoventrally on mesosoma with tweezer and placed onto the plane, with their agitation mitigated by the imposition of a plastic cover. After a while, the plastic cover was removed, and the scorpions were left undisturbed. *O. longichelus* may remain *in situ* for a while, but *O. przewalskii* exhibited an immediate proclivity to seek shelter. It is worth noting that the physiological state of the scorpions likely played a role in their responses, and factors such as light exposure and its attendant heat energy could influence their behavior.

The scorpions were allowed to acclimate in their respective enclosures for several days prior to the trials. However, prolonged exposure to intense illumination (along with the associated heat) could agitate the scorpions, even in the case of *O. przewalskii*, rendering them more prone to aggression.

According to the collector, the two species can be found on the same dune. The above behavioral discrepancy was also noticed during the collection: *O. przewalskii* remained immobile and a tendency towards thanatosis when detected, while *O. longichelus* instantly retreated into its burrow upon sensing the presence of the collector. An assumption could be made: the larger size of *O. longichelus* predisposes them to a higher possibility of encountering or being detected by predators, which in turn leads to an more sensitive temperament and aggressive behavior; on the other hand, *O. przewalskii* may instead adopt thanatosis to evade detection from the visual predators. This behavioral discrepancy, in combination with the distinct morphologies, may have contributed to the coexistence of the two species in the same region. *M. thersites* is another sympatric species mainly discovered in northern Xinjiang, but also found from southern region (Yarkant and Qiemo counties) in this study. All the three species appeared peaceful when placed together in a small, empty container (when the first author received them). However, *O. longichelus* may prey upon at least the *M. thersites* (observed under captive condition; also observed in *O. przewalskii*). *O. longichelus* appears to be the apex scorpion species in Xinjiang, with additional anecdotal observations on its predation upon the local solifugid (*Galeodes* sp.).

2. **Gregariousness**, **cannibalism and hostility**

Both species displayed a remarkable proclivity for gregariousness, typically maintaining harmonious coexistence within conspecific communities (Fig. 119, left and right). Scorpions usually remained unperturbed towards the tactile stimuli induced by approaching conspecifics, even when a wandering individual traversed over a resting one. This lack of aggression was also independent of sex and age, notwithstanding some young individuals were seemingly more vigilant and inclined toward self-defense behaviors. The tendency towards gregariousness also yielded a diminished motivation in performing courtship (nonetheless occurred), with adult males and females often cohabiting in peaceful concord. Intraspecific communication was primarily achieved through the conspicuous juddering behavior and metasoma swaying. Observations unveiled instances of cooperation among individuals in the construction of subterranean burrows in the sandy substrate. Cannibalism, while seldom occurred, occurred primarily in cases of insufficient food supply (e.g., Fig. 119, middle). In a rarer scenario, certain individuals nonetheless resorted to intraguild predation even in the presence of ample sustenance. Nevertheless, cannibalistic events remained infrequent, while random inspections upon the community often revealed a sign of overall harmony.

Hostility was only observed when an individual holding its captured prey was inadvertently touched by another passing individual. In such instances, the aggressor employed its metasoma to repel the encroaching individual, a kind of response, which can be aptly defined as "food guarding". Snatching behavior was also observed when an individual was apparently attempting to pilfer the prey held by another individual with its chelae. However, the "robber" might not

always be cognizant of the prey's possession by another individual, and the snatching behavior might result from a perceived opportunity for sustenance.

3. Common behavior

Burrowing was the predominantly displayed behavior observed in *O. longichelus*. When isolated in small, sand-filled containers, scorpions occasionally attempted to dig burrows in the corner of the container. Both pedipalps and the 4th pair of legs were consistently utilized as supports during the process, while the preceding three pairs of legs were responsible for excavating sand alternately. The foremost two pairs of legs were most frequently employed, especially when digging in the corner. On the other hand, when attempting to accelerate the process, the scorpion may engage the third pair as well. Another pattern was observed when the scorpion tilted to one side, employing the three leg pairs on the same side for excavation while leaving the remaining legs for support. In contrast, burrowing behavior was less frequently observed in *O. przewalskii*, where scorpions often opted to perch on a slope they established within the container (or at least after the surface was rendered uneven), without further adjustments.

In dim or dark environments when housed in small containers, both species typically adopted a state of immobility, with occasional instances of burrowing and patrolling behavior. Notably, in conditions of low humidity, both species manifested restlessness and an increased propensity for burrowing. Interestingly, after the substrate was moistened, the scorpion would extend its appendages and adopt a flattened posture on the surface, seemingly engaged in the collection of evaporated water molecules through their spiracle openings on the ventral side. However, in the case of communal housing for scorpions within a more expansive enclosure, upon the extinguishing of the lights at night, they consistently left their refuges and started running or meandering through the environment. On occasion, they attempted scaling higher elevations. Intriguingly, these behaviors did not appear linked to either courtship or predatory desire; instead, they seemed rather purposeless, which may be plausibly construed as "acquainting themselves with their surroundings" or "seeking better shelters under the cloak of darkness". More captivatingly, *O. longichelus* would occasionally assemble and rest upon a small patch of flat ground, remaining motionless. This behavior could be attributed to their need for fresh air or a means of unwinding after spending their daylight hours hiding in burrows. When exposed to direct illumination, even in undisturbed circumstances, scorpions displayed signs of agitation, constantly seeking out shaded crevices or corners, sporadically accompanied by burrowing behavior. Nevertheless, following acclimatization to the environment, scorpions were observed occasionally emerging from their burrows and wandering in areas exposed to direct light. Compared to LED white light, UV light tended to elicit an instant agitation more readily in scorpions (tested under 365 nm); on the contrary, IR light became undetectable, even when directly illuminated upon their median ocelli. Predatory behavior remained unaffected by the light intensity, and occurred whenever the scorpion was stimulated by the prey, provided that the scorpion was not fed. It is worth noting that the scorpion may not necessarily consume its prey immediately after capture, unless it was particularly hungry. In some cases, the scorpion might not even make an initial attempt to apprehend the prey, but the continual movement of the prey eventually provoked the scorpion into action.

Escaping behavior was observed with an occasional inclination of negative geotaxis for *O. longichelus*. When the scorpion was resting motionless on the substrate, after dripping water onto it and the surrounding substrate, it began to escape after several tail flicks as a display of resistance. During this period, it was continually discouraged by the ongoing dripping of water. If the scorpion was unable to locate accommodating crevices within its immediate vicinity, it would seek refuge at higher elevations in the environment, such as the driftwood and artificial tussock placed within its enclosure. However, while the *M. thersites* kept in the same enclosure has been observed to consume its prey on the top of the driftwood, *O. longichelus* merely sought shadows or crevices under driftwood or artificial tussock after predation. They appeared to be more negligent and may initiate consumption *in situ*. Interestingly, *O. przewalskii* were also observed to be frequently associated with the higher elevation on artificial tussock, resting near the tips of the plastic grass, even if they were the only species in the environment (i.e., devoid of predatory pressure). The grass-climbing tendency was also observed in the wild by the collector. It thus appears that the life strategy of *O. przewalskii* is characterized by an avoidance of aggression or active defiance.

Envenomation by adult *Olivierus longichelus*

Instances of scorpion stings within this genus have been exceedingly rare. Most documented cases were confined to the "umbrella" species, "*O. caucasicus*", primarily because the "*caucasicus*" complex has long been regarded as a single species comprised of several subspecies (Jalalia & Rahim et al., 2014; Sanaei-Zadeh et al., 2017; Fet et al., 2018; Firooziyan et al., 2020). Reports of envenomation by "*O. caucasicus*" in Iran involved populations from the provinces of Khuzestan and West Azerbaijan. Given the current knowledge regarding the distribution of this species, the record from Khuzestan may have been a misidentification (Fet et al., 2018: 9); additionally, no known *Olivierus* species have been recorded from there. Furthermore, the venom composition of *O. martensii* has been extensively studied. The LD_{50} value of this species via intraperitoneal injection varies across different populations (Zheng et al., 2014): 1.67 mg/kg for Jiangxi population, 2.4 mg/kg for Henan and Shandong population, and 10.3 mg/kg for Liaoning population. Gao et al. (1990) also reported the different LD50 values in mice induced by intravenous injection (1.72±0.16 mg/kg) and intraperitoneal injection (2.74±0.07 mg/kg), in comparison with subcutaneous injection (2.6 mg/kg). Zheng et al. (2014) summarized clinical reports for the envenomation by *O. martensii*, which we translated from

Figures 132–**135**: Selected *Olivierus longichelus* specimens in vivo habitus. **Figures 132**–**133**. Adult males from Jinghe County, showing different colorations. **Figures 134**–**135**. Adult female (134) and male (135) from Bole City.

Chinese and paraphrased herein: "*The clinical response of scorpion injured patients is mainly characterized by localized redness, swelling, and severe pain. Systemic symptoms can appear within 2 hours after injury as a symptom of neurotoxicity. In severe cases, this can lead to acute renal failure, respiratory muscle paralysis, myocardial paralysis, and even death. Occasionally, severe stings can result in fatal allergic shock or complications like high blood sugar, urine sugar, and pancreatitis. Timely treatment typically results in gradual improvement and symptom resolution within 24 hours for most patients. However, severe cases may result in neurological complications, and individuals with a high fever above 39 ℃ often succumb within 24 hours after the envenomation. Severe scorpion stings are common in infants and young children, and often cause symptoms such as shortness of breath, fluid accumulation in the lungs, difficulty breathing, blurred vision, difficulty swallowing, muscle twitching, walking disorders, and other muscle ataxia. Absence of treatment with antiserum predisposes them to a higher mortality rate.*" As supplementary information, brief description for the post-envenomation symptoms caused by the sting of an adult female *O. longichelus* is hereby provided, derived from the personal experience of the first author. This section aims to provide a referential understanding of the potential hazards associated with the sting of this species.

The dorsal surface of the left index finger was inadvertently pierced by an escaping adult female *O. longichelus* during the transfer of the scorpion. This triggered an immediate and intense pain, akin to a "hypodermal explosion", followed by a burning sensation at the sting site, rendering mild psychological unease. The discomfort extended along the left arm, presumably impacting the intercostal nerves. Disjunct, local soreness emerged along the ventral side of the left arm, resulting in irregular, localized petechiae beneath the skin. The soreness along the left arm was notably less severe than that experienced at the index finger but was spasmodic in nature. Shortly thereafter, vasodilation occurred, accompanied by a local rise in temperature. Redness extended to the triangular region between the index finger and thumb, visually shattered into irregular petechiae at the proximal boundary of the reddened area. Swelling stood as the predominant symptom, most pronounced at the index finger and gradually diminishing at the elbow joint, petrifying the left hand. Dire vasodilation also induced moderate sweating on the skin of the finger, as well as severely impeding the flexibility of both the index finger and the adjacent digits. The intense pain further resulted in numbness surrounding the affected hand. Approximately over two hours later, the flexibility of the fingers began to gradually return, along with a reduction in soreness (which completely disappeared in the arm and left chest region). Around 4 to 5

Figures 136–139: Selected *Olivierus longichelus* specimens in vivo habitus. **Figure 136**. Adult male from Ghulja (Yining) County. **Figure 137**. Adult male from Yarkant (Shache) County. **Figures 138–139**. Adult (138) and subadult (139) males from Makit County.

hours following the incident, redness alleviated with a gradual recovery to the normal skin color. However, swelling in the index finger persisted, albeit diminishing, accompanied by moderate numbness when pressure was applied, even after 6 hours. Despite this, the normal function of the left hand had been restored, enabling actions such as forming a tight fist. Swelling symptom became negligible after 48 hours.

No special treatment was administered for the envenomation, apart from cooling the affected area with cold water. The first author had quite a few previous experiences with the scorpion sting and was aware of the resistance. It is imperative to highlight that the manifestation of symptoms can vary greatly based on several variables, including the specific venom components of the scorpion, the venom dosage, and the individual's physiological constitution. Conversely, an inadvertent contact with a resting adult female *O. przewalskii* led to a much milder symptom caused by its envenomation. The sting introduced an instant sensation on the dorsal surface of the middle finger as if it was stimulated by cold ice. Followed by pruritus and regional redness, the earlier sensation did not convert into prolonged pain. After a while, a white, irregularly raised bump was formed surrounding the sting site. Subsequent symptoms were predominantly characterized by itching and occasional, mild tingling. All symptoms vanished after a couple of hours. This mild symptom aligns with the above hypothesized life strategy of this species.

Discussion

The maturity determination for females can prove challenging in that they usually lack distinct external characters that become pronounced after the final ecdysis (e.g., CL/W and proximal lobe on movable finger). With irrespective to the presence of eggs or embryos, or visible offspring-carrying behavior, ascertaining female maturity often relies on empirical approaches, focusing on certain indicators such as the total length, coloration, and development of granules and carinae. In addition, some species exhibit a greyish hue on their pleural membrane after reaching adulthood due to the thickening of those tissues, resulting in diminished translucence. On the other hand, in certain species that possess a pronounced subaculear tubercle on their telson, such structure might diminish when reaching adulthood. While large individuals can often be confidently identified as mature, the intraspecific variation in size caused either by genes alone or early maturation (typically a single instar less than the normal instar for mature females) obstruct the determination. Consequently, maturity determination for smaller females entails the dissection of internal organs that signifies the maturity, i.e., the presence of a developed ovariuterus or the ovarian follicles attached thereto containing oocytes (unfertilized eggs). This method, however, would inherently destroy the specimen. Therefore, it is only recommended provided that a sufficient sample size is available, or the data for that specimen have

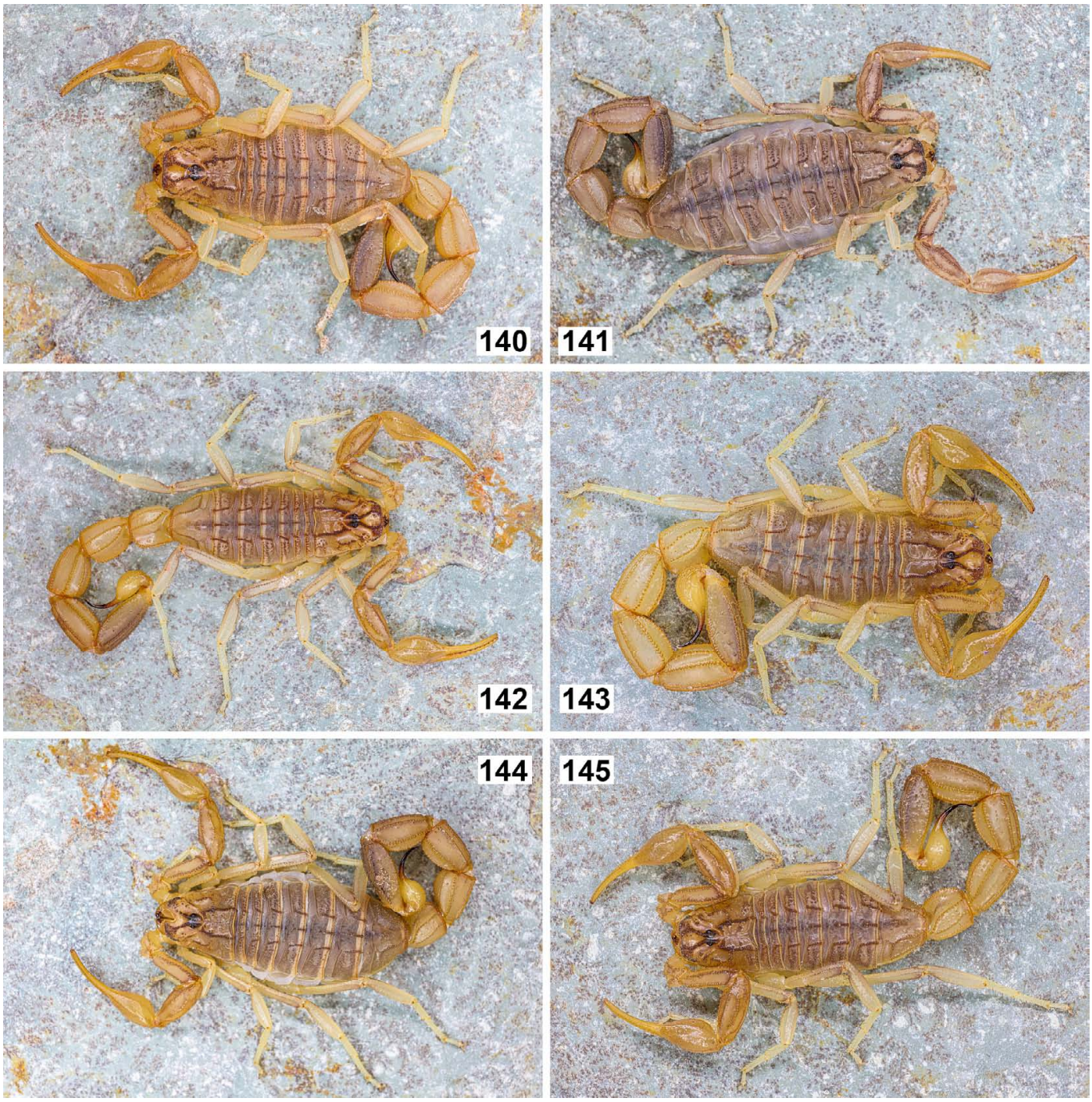

Figures 140–145: Selected *Olivierus przewalskii* specimens from northern Xinjiang in vivo habitus. **Figures 140–143**. Specimens from Bole City: adult female (140), juvenile female (141) and adult males (142–143) of different sizes. **Figures 144–145**. Specimens from Ghulja (Yining) County: adult female (144) and male (145).

been recorded. Sun & Zhu (2010) described *O. longichelus* based on only three specimens with two being immature. Their conclusion of another larger specimen representing a mature female likely relied on the discernible size disparity with respect to the two paratypes. The dearth of specimens can introduce bias into the maturity determination, particularly if the investigator lacks prior experience in such assessments with closely related taxa. In this study, a juvenile female from Bole was selected to compare with the original sketches of the holotype female *O. longichelus* from Jinghe County (Figs. 101–110). The congruent morphological traits indicate that the holotype *O. longichelus* was indeed immature, and most of the characters used by Sun et al. (2010) to discriminate *O. bolensis* from *O. longichelus* are therefore abolished.

The obscurity of the type specimen of *O. karshius* prevented us from drawing a confident conclusion about its real identity. Species descriptions based solely on hand-drawn illustrations are suboptimal. Doubts remain as to whether those

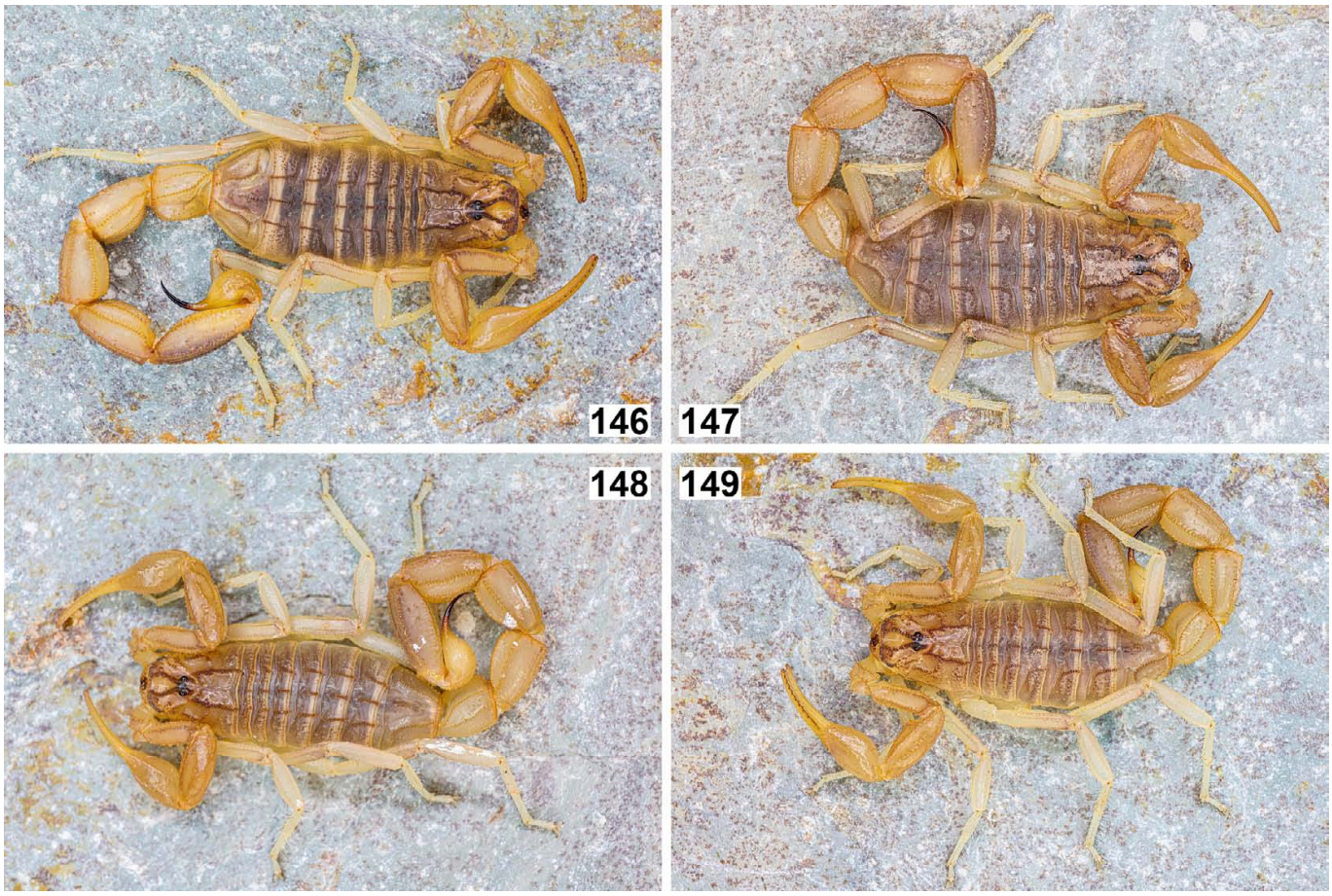

Figures 146–149: Selected *Olivierus przewalskii* specimens from southern Xinjiang in vivo habitus. **Figures 146–148**. Specimens from Yarkant (Shache) County: adult females (146–147) of different sizes and adult male (148). **Figure 149**. Specimen from Makit County: adult male.

artificial sketches properly match with the authentic specimen, given that portraying a specimen is based on the subjective understanding and interpretation of the illustrator towards those structures. However, those illustrations do have their unique merits, such as highlighting the characters of interest (e.g., trichobothria patterns, main geometric contours) while minimizing the "noise" from other features. Nevertheless, many illustrations remain logically questionable as they are not the direct representation of the species, hindering the subsequent readers from acknowledging the true morphology. A stunning example of high-quality illustration is the work conducted by Graeme Lowe in his review of picobuthoids in Oman (Lowe, 2010) which represents a highly reliable replication of the authentic morphology alongside additional photographs for the specimens. Considering the aforementioned impediments, it is imperative to underscore the significance of disseminating visual materials, such as photographs, through online platforms, particularly for taxa that lack photographic documentation. An exemplary instance in this regard is the official website of the National Museum of Natural History (Muséum national d'Histoire naturelle) in Paris, France. This institution has set a noteworthy precedent by providing a repository of habitus photographs for various scorpion taxa that can be accessed (science.mnhn.fr/institution/mnhn/collection/rs/item/search). Providing accessible, high-quality images of type specimens can greatly assist researchers in their taxonomic work and help maintain transparency in scientific research, enhancing the reproducibility and verification of taxonomic research and ultimately contributing to the accuracy of scientific knowledge. Efforts to digitize and make such materials available online should be encouraged and supported whenever possible.

While Zhang et al. (2020: 83) considered *O. bolensis*, *O. karshius* and *O. longichelus* narrowly distributed, they did not investigate their true identities or distributional ranges. In contrary to what Sun & Zhu (2010: 2) speculated, the scorpiofauna of Xinjiang have been largely overestimated. The current investigation in combination with previous literature confirmed only 5 species for Xinjiang: *M. thersites*, *O. longichelus*, *O. przewalskii*, *R. xinjianganus* and *S. taxkorgan*. The morphological characters, combined with molecular evidence in this study demonstrated the overlapping and extensive distribution of *O. longichelus* and *O. przewalskii* in Xinjiang. Further studies are required to disclose the scorpiofauna in the southwest end of Tarim Basin where both species have not been reported. In addition, we predict that, with imbalanced densities, *O. longichelus* may also be sympatric with *O. przewalskii* from other localities that were not investigated in this study.

Figures 150–**151**: Additional *Olivierus longichelus* populations used for DNA sequencing. **Figure 150**. Juvenile male from Korgas County (left) and adult male from Khorgos City (right). **Figure 151**. Adult male from Shawan City (left) and adult female from Wujiaqu City (right).

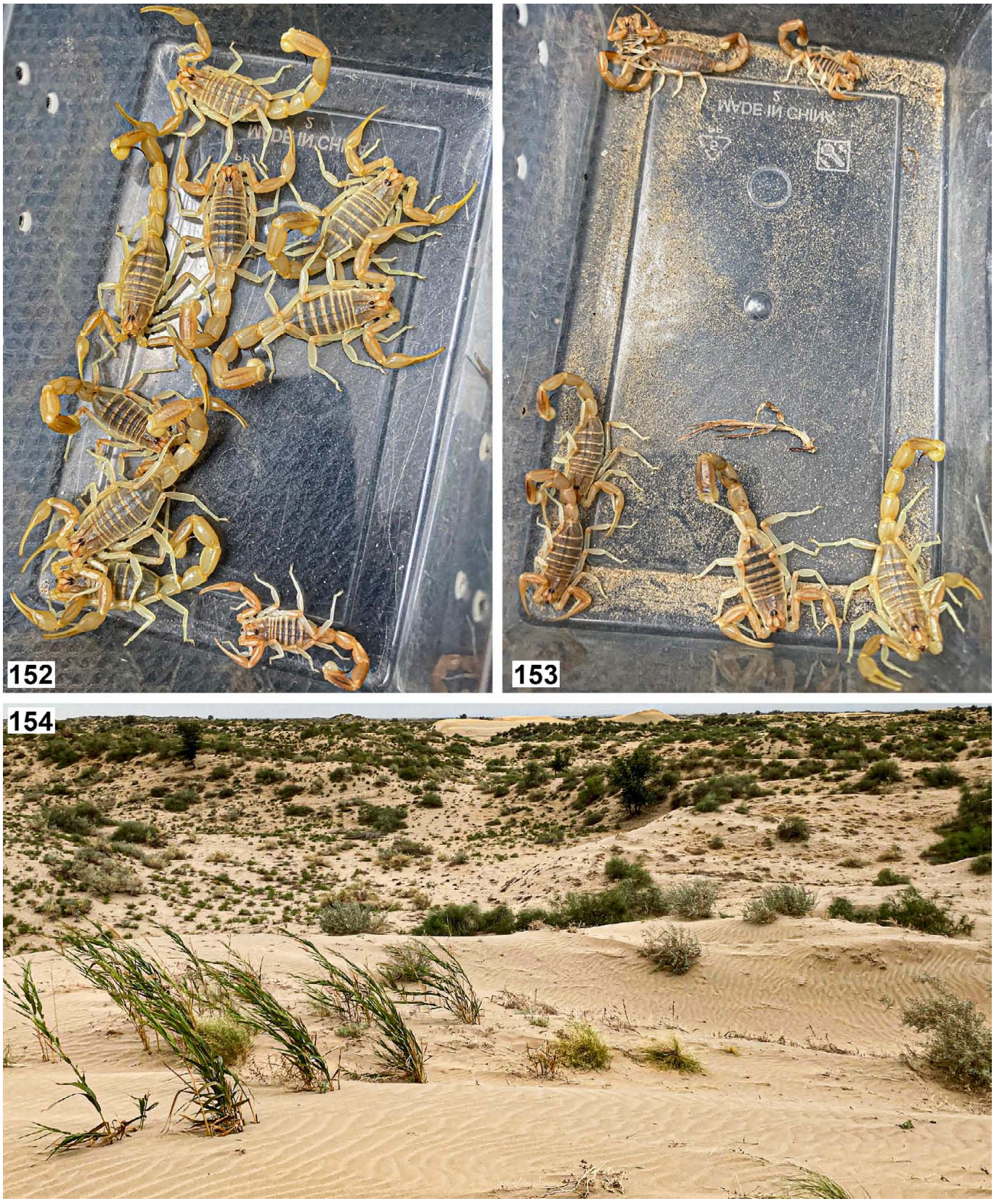

Figures 152–154. *Olivierus longichelus* from Korgas County (152–153) and its natural habitat (154). Photo: Yizun Wang.

Figures 155–**156**: Comparison between *Olivierus longichelus*, *O. przewalskii* and *Mesobuthus thersites* (left to right). **Figure 155**. Adult females. **Figure 156**. Adult males.

Recently, Shi et al. (2023) undertook a phylogeographic investigation to evaluate the "out-of-Central Asia" hypothesis for populations of "*Mesobuthus mongolicus*" spanning from Central Asia to the Gobi region. In their phylogenetic tree (Shi et al., 2023: fig. 2), the "*M. mongolicus*" lineage was separated from that of *M. thersites*. However, the authors did not explain the single DNA sequence material they used for *M. thersites*, thus prompting the reference to "*M. mongolicus*"

Figures 157–**162**: Exemplar specimens of *Olivierus martensii* (Karsch, 1879) in vivo habitus. **Figures 157**–**158**. Adult male (157) and female (158) of typical phenotype from Luoyang City, Henan Province, China. **Figures 159**–**160**. Hypomelanistic (159; adult male) and piebaldistic (160; immature males) phenotypes. **Figures 161**–**162**. Leucistic (161; immature male) and albino (162; adult female) phenotypes.

as "*M. thersites*" below since it is out of the scope of this study to authenticate whether their "*M. mongolicus*" was indeed genetically distinct from *M. thersites*. The authors continued to follow the taxonomic decision proposed by Gantenbein et al. (2003) and placed *O. przewalskii* and *O. martensii* within *Mesobuthus*, although their phylogenetic result again confirmed the monophyly of the clade comprising those two species. While their conclusion aligned with the "out-of-Central-Asia" hypothesis regarding the dispersal of *M. thersites* into China, the recent instances of new geographical records, as established in this study, underscore a significantly wider distribution range for this species which extends to the western and southern regions of Xinjiang.

As deduced by the authors, the most recent common ancestors of *M. thersites* embarked on an eastward migration from the boundary between Tajikistan and Kazakhstan, venturing into the Junggar Basin. This population dispersed further east to the southern part of the Gobi Desert,

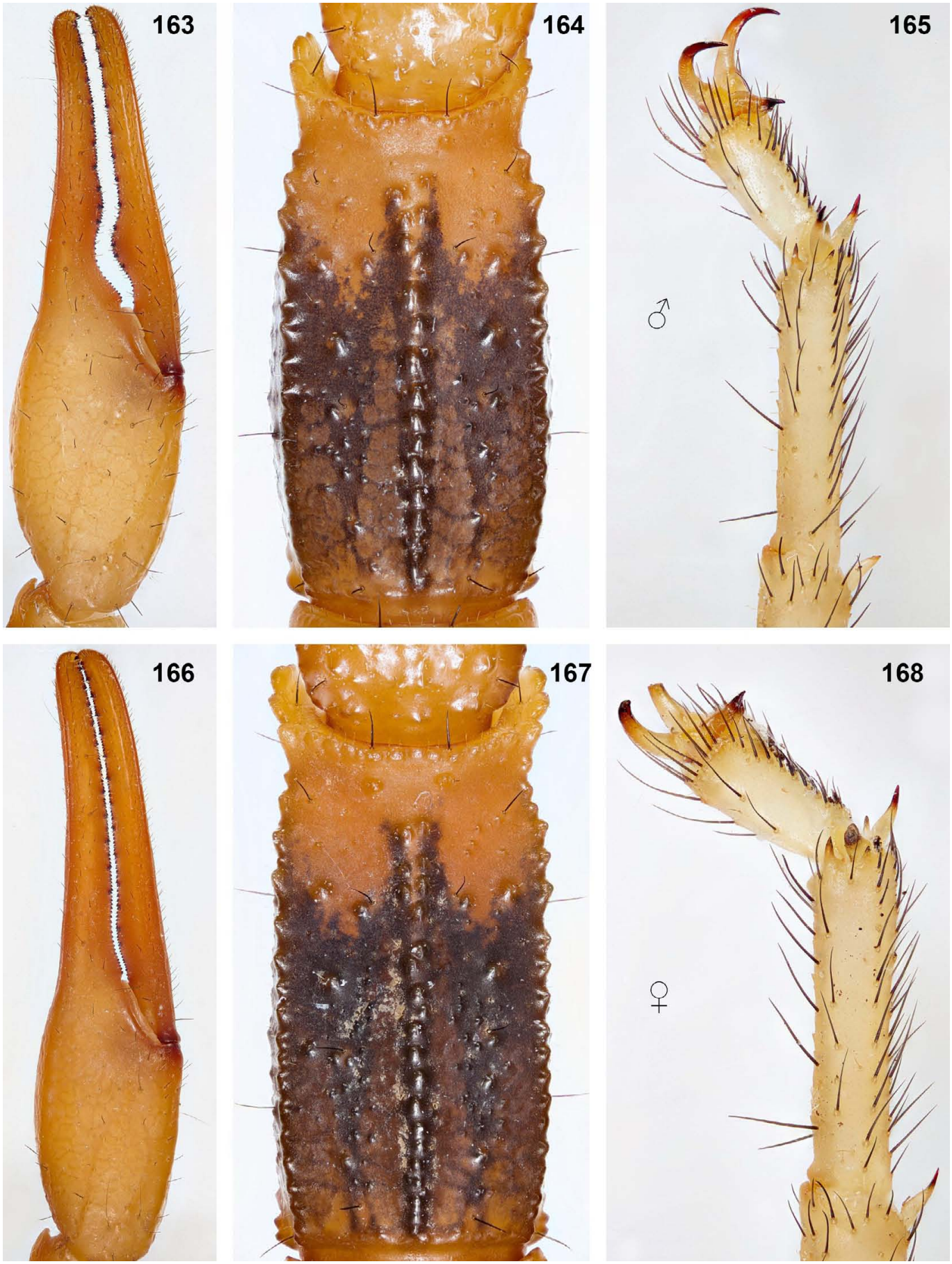

Figures 163–**168**: Raw stacked photos (unmatted) of typical adult male and female *O. martensii* from Luoyang City, Henan Province, China, under white light: chelae in external view (163, 166), metasoma V in ventral view (164, 167), and telo- and basitarsi of right 3rd leg in retrolateral view (165, 168). **Figures 163**–**165**. Male. **Figures 166**–**168**. Female.

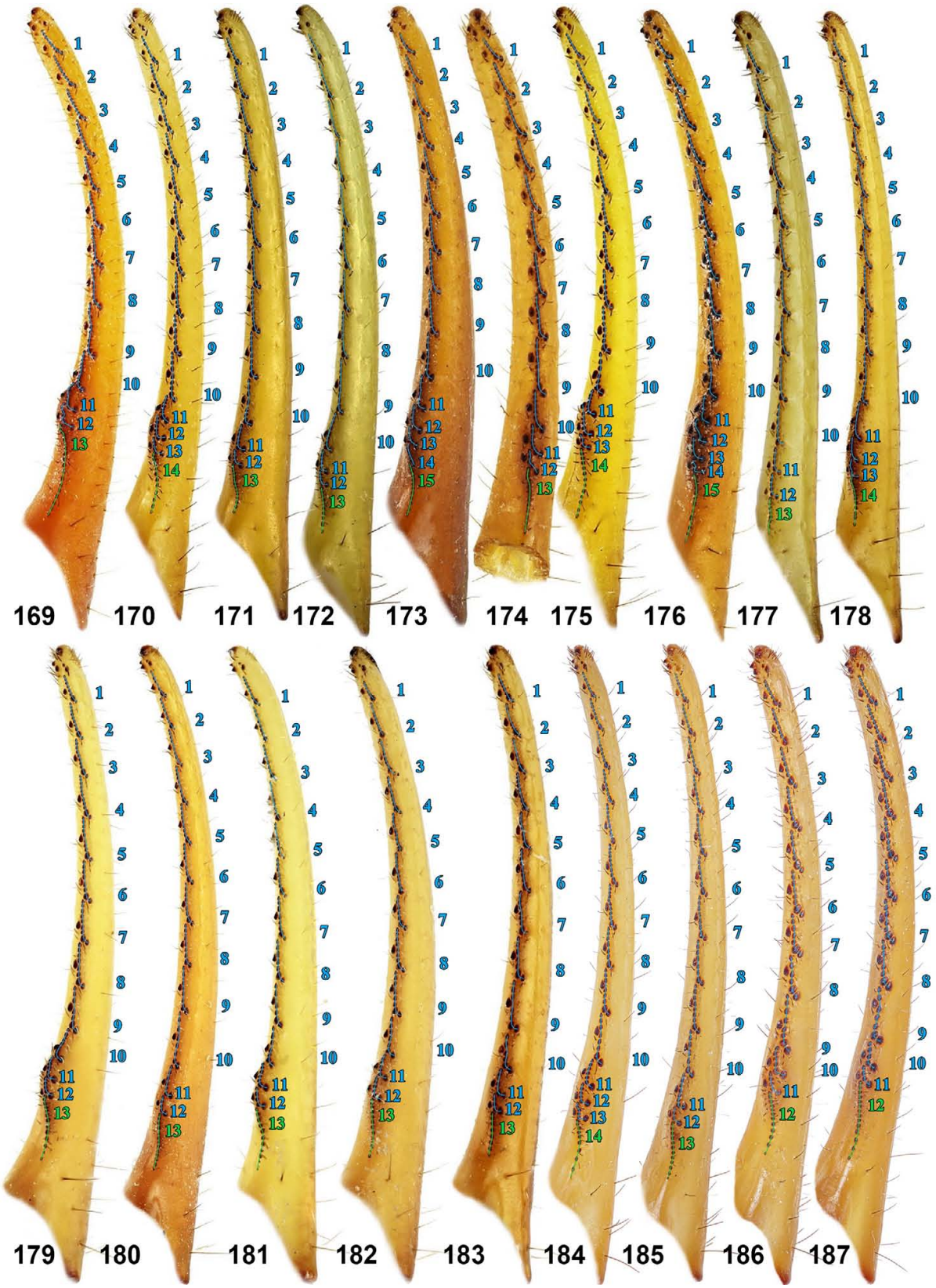

Figures 169–187: Dentate margin of movable finger in *Olivierus*, showing complex (blue) and simple (green) subrows defined here; note: for clarity of explanation, the EAD is included within each complex subrow, but by definition it should be excluded. Figs. 169–183 are modified from Fet et al. (2018: figs. 304–313) and Fet et al. (2021: figs. 32, 43, 73, 84, 107). **Figure 169**. *O. brutus*, male paratype from Alamut, Qazvin Province, Iran. **Figure 170**. *O. caucasicus*, male from Melekli, Iğdir Province, Turkey. **Figure 171**. *O. elenae*, female holotype from Angor, Surxondaryo Province, Uzbekistan. **Figure 172**. *O. gorelovi*, male holotype from Tejen, Akhal Province, Turkmenistan. **Figure 173**. *O. fuscus*, female from Khuroson, Khatlon Province, Tajikistan. **Figure 174**. *O. kaznakovi*, male from Romit State Nature Reserve, Khatlon Province, Tajikistan. **Figure 175**. *O. kreuzbergi*, male holotype from Uzun, Surxondaryo Province, Uzbekistan. **Figure 176**. *O. mischi*, male holotype from Hazara Toghai, Balkh Province, Afghanistan. **Figure 177**. *O. nenilini*, male holotype from Mingbulak, Namangan Province, Uzbekistan. **Figure 178**. *O. parthorum*, male from Afghanistan. **Figures 179–180**. *O. mikhailovi*, paratype male (179) and female (180) from Bel'tau Mts., Turkistan Province, Kazakhstan. **Figures 181–182**. *O. tarabaevi* (**syn**. **n**. with *O. longichelus*), paratype male from Kapchagai, Almaty Region and holotype female from Shieli, Kyzylorda Province, Kazakhstan. **Figure 183**. *O. voldemari*, female holotype from Yazyavan, Fergana Province, Uzbekistan. **Figures 184–185**. *O. longichelus*, male (184) and female (185), same as before. **Figures 186–187**. *O. przewalskii*, male (186) and female (187), same as before.

subsequently followed by a northward colonization along the Altai mountains and Gobi-Altai Province. Employing ecological niche modeling based on their collection records of *M. thersites*, the authors discovered two major parts of its present suitable distributional area, linked by a belt extending southeastwardly (Hexi Corridor): the entire Junggar Basin in the west, and two main deserts (Gobi and Tengger) in the east. As suggested by the authors, the Tian Shan-Pamir range acts as an insurmountable physical barrier that demarcates the distributional range of *O. przewalskii* (to the south) and *M. thersites* (to the north). Nevertheless, the lineages of *M. thersites* took a detour via the Junggar Basin after the uplift of Tian Shan mountains. Coupled with the current findings, the specimens collected from Yarkant and Qiemo counties within the Tarim Basin indicate that another lineage must have also dispersed towards the southwestern regions. Several explanatory hypotheses require further phylogeographic verifications in the future: **(1)** the southwestern lineage dispersed southward from the Junggar Basin prior to the uplift of Tian Shan mountains (before 10–11 mya), or when the elevations were not yet extremely high; **(2)** the southwestern lineage dispersed through a narrow corridor (north of Gaochang) that connects the Junggar and Turpan-Hami basins, between the Eren Habirga Mts. and Bodga Mts. of the Tian Shan mountain range; **(3)** the southwestern lineage moved westward into the Taklamakan Desert in the Tarim Basin after its ancestors colonized the Gobi region in the east.

The same statements could potentially be extrapolated to the trans-barrier distribution of *O. longichelus* and *O. przewalskii* (Fig. 130). However, our preliminary phylogenetic results suggest that the diversification of *O. longichelus* in Xinjiang is a relatively recent event (ca. 0.5 mya), implying a diminished likelihood for the first hypothesis to explicate the phenomenon. If the "⌒" shape mountain configuration formed by the middle Tian Shan range (where Halik Mountains situate) and the north Tian Shan range (i.e., the Boro-Eren Range) has confined the *O. longichelus* population in the Ili River Valley (where Khorgos, Korgas and Ghulja are located), then their progenitors would have needed to disperse northeastward, traversing the western end of Borohoro Mountains where elevations are lower, beyond which the Bole and Jinghe populations were formed. The presence of *O. longichelus* in the south of Junggar Basin (Wujiaqu) lends credence to the second hypothesis. The ancestral population might have migrated through the Eren-Bodga corridor, at which juncture two potential dispersal routes became available. The ancestors could have dispersed along the Tian Shan range (i.e., northern boundary of Tarim Basin) to the west, culminating in the Yarkant population. Conversely, they ventured further southeast, circumventing the Lobnor Lake, entering the Tarim Basin and establishing the Qiemo and Ruoqiang populations near the Qinghai-Tibetan Plateau (i.e., southern boundary of Tarim Basin). If intermediate populations are discovered between Yarkant and Qiemo in the southwest of Tarim Basin, then it is conceivable that those progenitors ultimately reached Yarkant. Captive observations suggest a certain degree of water demand in those scorpions. It is unlikely that they would transverse the dry, vast Taklamakan Desert in the heart of the Tarim Basin. Current records reveal that the majority of populations are located in proximity to the nearby mountain range or waterbodies, although such superficial pattern could be biased by the sampling procedure where field investigations are typically restricted to regions with available roadways. The geographic history of those landscapes could proffer insights into the ancestral dispersal of those scorpions. If future investigation confirms their presence along any, if not all, of those routes, then the "out-of-Junggar" hypothesis becomes plausible.

Acknowledgements

We are most grateful to Qiu Du (杜丘) who has been collecting specimens of Xinjiang buthids on the first author's behalf for multiple times and collected the topotypes examined in this study. We also thank a friend of the first author's, Yizun Wang (汪义尊), for providing two specimens from Korgas County and Khorgos City freely. Special recognition goes to Maxwell Wang (Zi Wang, 王子) from University College London, as well as Jan Beccaloni and Danniella Sherwood from Natural History Museum, London, UK, for their assistance in the delivery of DNA samples. We thank two anonymous reviewers for their comments.

References

BIRULA, A. A. 1897. Miscellanea Scorpiologica. II. Zur Synonymie der russischen Scorpione. *Annuaire du Musée Zoologique de l'Académie Impériale des Sciences de St.-Pétersbourg*, 2: 377–391.

BIRULA, A. A. 1904. Miscellanea Scorpiologica. VI. Ueber die *Buthus*-Arten des Centralasiens. A*nnuaire du Musée Zoologique de l'Académie Impériale des Sciences de St. Pétersbourg*, 9: 20–27.

BIRULA, A. A. 1911. Arachnologische Beiträge. I. Zur Scorpionen- und Solifugen-Fauna des Chinesischen Reichs. *Revue Russe d'Entomologie*, 11: 195–201.

BIRULA, A.A. [BYALYNITSKII-BIRULYA, A.A.]. 1917. *Chlenistobryukhie paukoobraznye Kavkazskogo Kraya. Chast' 1. Scorpiones* [Arthrogastric Arachnids of Caucasia. Part I. Scorpiones.] Tiflis: Mémoires du Musée du Caucase, Sér. A 5: 1–253 (in Russian). [English translation: Jerusalem: Israel Program for Scientific Translation, 1964].

BIRULA, A. A. 1927. Zoologische Ergebnisse der von P.K. Kozlov in den Jahren 1925–1926 ausgeführten Expedition nach der Mongolei. I. Skorpione und Solifugen. *Annuaire du Musée Zoologique de l'Academie des Sciences de l'URSS*, 28: 201–218.

BRYSON, R. W., L. PRENDINI, W. E. SAVARY & P. B. PEARMAN. 2014. Caves as microrefugia: Pleistocene phylogeography of the troglophilic North American scorpion *Pseudouroctonus reddelli*. *BMC evolutionary biology*, 14(1): 1–17.

DI, Z.-Y., Z.-Z. YANG, S.-J. YIN, Z-J. CAO & W.-X. LI. 2014. History of study, updated checklist, distribution and key of scorpions (Arachnida: Scorpiones) from China. *Zoological Research*, 35(1): 3−19.

DI, Z.-Y., Z.-Z. YANG, Z.-J. CAO, Y.-L. WU & W.-X. LI. 2015. The scorpion fauna of China (Chelicerata: Arachnida). *Acta Arachnologica Sinica*, 24: 109–115. [in Chinese].

DRUMMOND, A. J., M. A. SUCHARD, D. XIE & A. RAMBAUT. 2012. Bayesian phylogenetics with BEAUti and the BEAST 1.7. *Molecular biology and evolution*, 29(8): 1969–1973.

FARZANPAY, R. 1987. *Knowing Scorpoins. No. 312, Biology 4*. Teheran: Central Univeristy Publication, 231 pp.

FET, V. 1989. A catalogue of scorpions (Chelicerata: Scorpiones) of the USSR. *Rivista del Museo Civico di Scienze Naturali "Enrico Caffi"*, 13 (1988): 73–171.

FET, V. 1994. Fauna and zoogeography of scorpions (Arachnida: Scorpiones) in Turkmenistan. *In*: Fet, V. & K.I. Atamuradov (eds.). *Biogeography and Ecology of Turkmenistan*. Dordrecht: Kluwer Academic Publishers, pp. 525–534. https://doi.org/10.1007/978-94-011-1116-4_31

FET, V., F. KOVAŘÍK, B. GANTENBEIN & M. R. GRAHAM. 2021. Three new species of *Olivierus* (Scorpiones: Buthidae) from Kazakhstan and Uzbekistan. *Zootaxa*, 5006(1): 054–072.

FET, V., F. KOVAŘÍK, B. GANTENBEIN, R. C. KAISER, A. K. STEWART & M. R. GRAHAM. 2018. Revision of the *Mesobuthus caucasicus* complex from Central Asia, with descriptions of six new species (Scorpiones: Buthidae). *Euscorpius*, 255: 1–77.

FET, V. & G. LOWE. 2000. Family Buthidae. Pp. 54–286 *in*: Fet, V., W.D. Sissom, G. Lowe & M.E. Braunwalder (eds.). *Catalog of the Scorpions of the World (1758–1998)*. New York: New York Entomological Society, 690 pp.

FIROOZIYAN, F., A. SADAGHIANIFAR, J. RAFINEJAD, H. VATANDOOST, & M. M. BAVANI. 2020. Epidemiological characteristics of scorpionism in West Azerbaijan Province, Northwest of Iran. *Journal of Arthropod-Borne Diseases*, 14(2): 193–201.

GANTENBEIN, B., V. FET, I. A. GANTENBEIN-RITTER & F. BALLOUX. 2005. Evidence for recombination in scorpion mitochondrial DNA (Scorpiones: Buthidae). *Proceedings of the Royal Society B: Biological Sciences*, 272(1564): 697–704.

GANTENBEIN, B., V. FET & A. V. GROMOV. 2003. The first DNA phylogeny of four species of *Mesobuthus* (Scorpiones, Buthidae) from Eurasia. *The Journal of Arachnology*, 31: 412–420.

GAO, E., H.-Z. LI & X.-R. LV. 1990. Acute toxic action of the venom of *Buthus martensii* Karsch. *Wei Fang Yi Xue Yuan Xue Bao*, 12(3): 31–32. [in Chinese].

GRAHAM, M. R., E. A. MYERS, R.C. KAISER & V. FET. 2019. Cryptic species and co-diversification in sand scorpions from the Karakum and Kyzylkum deserts of Central Asia. *Zoologica Scripta*, 48(6): 801–812.

GRAHAM, M. R., D. A. WOOD, J. A. HENAULT, Z. J. VALOIS & P. E. CUSHING. 2017. Ancient lakes, Pleistocene climates and river avulsions structure the phylogeography of a large but little-known rock scorpion from the Mojave and Sonoran deserts. *Biological Journal of the Linnean Society*, 122(1): 133–146.

GROMOV, A. V. & YE. YE. KOPDYKBAEV. 1994. The fauna of the scorpions and solpugids (Arachnida: Scorpiones, Solifugae) in Kazakhstan. *Selevinia*, 2(2): 19–23. [in Russian].

HEDDERGOTT, M., M. STUBBE, W. STUBBE, P. STEINBACH & A. STUBBE. 2016. Geographical distribution of the genus *Mesobuthus* (Scorpiones: Buthidae) in Mongolia. *Erförschung biologischer Ressourcen der Mongolei / Exploration into the Biological Resources of Mongolia*, 13: 147–164.

JALALIA, A. & F. RAHIM. 2014. Epidemiological review of scorpion envenomation in Iran. *Iranian Journal of Pharmaceutical Research*, 13(3): 743–756.

KARSCH, F. 1879. Scorpionologische Beiträge. Part II. *Mitteilungen des Münchener Entomologischen Vereins*, 3: 97–136.

KISHIDA, K. 1939. Arachnida of Jehol. Order Scorpiones. *Report of the First Scientific Expedition to Manchoukuo Under the Leadership of Shigeyasu Tokunaga, June-October 1933*, Sect. 5, 1(4): 49–67.

KOCH, C. L. 1839. *Die Arachniden*. Nürnberg: C. H. Zeh'sche Buchhandlung, 6(3): 51–53, figs. 466–467.

KOVAŘÍK, F. 2019. Taxonomic reassessment of the genera *Lychas*, *Mesobuthus*, and *Olivierus*, with descriptions of four new genera (Scorpiones: Buthidae). *Euscorpius*, 288: 1–27.

KOVAŘÍK, F., V. FET, B. GANTENBEIN, M. R. GRAHAM, E. A. YAĞMUR, F. ŠŤÁHLAVSKÝ, N. M. POVERENNYI & N. E. NOVRUZOV. 2022. A revision of the genus *Mesobuthus* Vachon, 1950, with a description of 14 new species (Scorpiones: Buthidae). *Euscorpius*, 348: 1–189.

KRAEPELIN, K. 1899. Scorpiones und Pedipalpi. *In*: Dahl, F. (ed.), *Das Tierreich. Herausgegeben von der Deutscehen Zoologischen Gesellschaft, 8 (Arachnoidea)*. Berlin: R. Friedländer und Sohn Verlag, 265 pp.

KUMAR, S., G. STECHER, M. LI, C. KNYAZ & K. TAMURA. 2018. MEGA X: molecular evolutionary genetics analysis across computing platforms. *Molecular biology and evolution*, 35(6): 1547–1549.

LARSSON, A. 2014. AliView: a fast and lightweight alignment viewer and editor for large datasets. *Bioinformatics*, 30(22): 3276–3278.

LI, W.-X., Y.-L. WU, Z.-J. CAO & Z.-Y. DI. 2016. *Scorpion biology and toxins*. Beijing: Science Press, 555 pp. [in Chinese]

LOURENÇO, W. R., D. SUN & M.-S. ZHU. 2010. *Razianus xinjianganus* sp. nov.: a new record genus and new species of (Scorpiones, Buthidae) from China. *Journal of Hebei University (Natural Science Edition)*, 30: 307–318.

LOURENÇO, W. R. 2018. Scorpions at high altitudes: A new species of *Scorpiops* Peters, 1861 (Scorpiones: Scorpiopidae) from the Taxkorgan Reserve, Xinjiang, China. *Comptes Rendus Biologies*, 341: 362–369.

LOWE, G. 2010. New picobuthoid scorpions (Scorpiones: Buthidae) from Oman. *Euscorpius*, 93: 1–53.

LOWE, G. & V. FET. 2024. A survey of proximal sensilla associated with denticle subrows on scorpion pedipalp fingers (Arachnida: Scorpiones), with observations on scorpion fluorescence. *Euscorpius*, 382: 1–107.

LOWE, G. & F. KOVAŘÍK. 2022. Reanalysis of *Teruelius* and *Grosphus* (Scorpiones: Buthidae) with descriptions of two new species. *Euscorpius*, 356: 1–105.

MONOD, L., L. CAUWET, E. GONZÁLEZ-SANTILLÁN & S. HUBER. 2017. The male sexual apparatus in the order Scorpiones (Arachnida): a comparative study of functional morphology as a tool to define hypotheses of homology. *Frontiers in Zoology*, 14: 51: 1–48.

[National Forestry and Grassland Administration] 国家林业和草原局. 2023. 有重要生态、科学、社会价值的陆生野生动物名录. 2023年第17号. ('List of terrestrial wildlife with significant ecological, scientific, and social value (2023, No. 17)'). [in Chinese]. http://www.zs.gov.cn/attachment/0/471/471942/2298648.pdf

PÉREZ, S. M. 1974. Un inventario preliminar de los escorpiones de la región Paleártica y claves para la identificación de los géneros de la región Paleártica Occidental. *Universidad Complutense de Madrid, Facultad de Ciencias, Departamento de Zoología, Cátedra de Artrópodos*, 7: 1–45.

PRENDINI, L., V. L. EHRENTHAL & S. F. LORIA. 2021. Systematics of the relictual Asian scorpion family Pseudochactidae Gromov, 1998, with a review of cavernicolous, troglobitic, and troglomorphic scorpions. *Bulletin of the American Museum of Natural History*, 453: 1–149.

PRENDINI, L. & S. F. LORIA. 2020. Systematic revision of the Asian forest scorpions (Heterometrinae Simon, 1879), revised suprageneric classification of Scorpionidae Latreille, 1802, and revalidation of Rugodentidae Bastawade et al., 2005. *Bulletin of the American Museum of Natural History*, 442: 1–480.

PUILLANDRE, N., S. BROUILLET & G. ACHAZ. 2021. ASAP: assemble species by automatic partitioning. *Molecular Ecology Resources*, 21(2): 609–620.

QI, J.-X., M.-S. ZHU & W. R. LOURENÇO. 2004. Redescription of *Mesobuthus martensii martensii* (Karsch, 1879) (Scorpiones: Buthidae) from China. *Revista Ibérica de Aracnología*, 10: 137–144.

RAMBAUT, A., A. J. DRUMMOND, D. XIE, G. BAELE & M. A. SUCHARD. 2018. Posterior summarization in Bayesian phylogenetics using Tracer 1.7. *Systematic Biology*, 67(5): 901–904.

SANAEI-ZADEH, H., S. M. MARASHI, & R. DEHGHANI. 2017. Epidemiological and clinical characteristics of scorpionism in Shiraz (2012-2016); development of a clinical severity grading for Iranian scorpion envenomation. *Medical Journal of The Islamic Republic of Iran*, 31: 27.

SHI, C.-M., Y.-J. JI, L. LIU, L. WANG & D.-X. ZHANG. 2013. Impact of climate changes from Middle Miocene onwards on evolutionary diversification in Eurasia: Insights from the mesobuthid scorpions. *Molecular Ecology*, 22: 1700–1716.

SHI, C.-M. & D.-X. ZHANG. 2005. A review of the systematic research on buthid scorpions (Scorpiones, Buthidae). *Acta Zootaxonomica Sinica*, 30: 470–477.

SHI, C.-M., X.-S. ZHANG, L. LIU, Y.-J. JI & D.-X. ZHANG. 2023. Phylogeography of the desert scorpion illuminates a route out of Central Asia. *Current Zoology*, 69: 442–455.

SOLEGLAD, M. E. & V. FET. 2003a. The scorpion sternum: structure and phylogeny (Scorpiones: Orthosterni). *Euscorpius*, 5: 1–34.

SOLEGLAD, M. E. & V. FET. 2003b. High-level systematics and phylogeny of the extant scorpions (Scorpiones: Orthosterni). *Euscorpius*, 11: 1–175.

STAHNKE, H. L. 1971. Scorpion nomenclature and mensuration. *Entomological News*, 81(12): 297–316.

ŠTUNDLOVÁ, J., F. ŠŤÁHLAVSKÝ, V. OPATOVÁ, J. ŠTUNDL, F. KOVAŘÍK, P. DOLEJŠ & J. ŠMÍD. 2022. Molecular data do not support the traditional morphology-based groupings in the scorpion family Buthidae (Arachnida: Scorpiones). *Molecular Phylogenetics and Evolution*, May 14; 173(2022) 107511: 1–5 and Supplementary Information. https://www.sciencedirect.com/science/article/pii/S1055790322001245

SULAKHE, S., S. DESHPANDE, G. GOWANDE , N. DANDEKAR & M. KETKAR. 2022. Arboreal gems: resurrection of *Isometrus sankeriensis* Tikader & Bastwade, 1983 and descriptions of two new species of *Isometrus* Ehrenberg, 1828 (Scorpiones: Buthidae) from the Western Ghats, India. *European Journal of Taxonomy*, 811: 1–50.

SUN, D. 2010. *Taxonomy and Status of Resources of the Scorpiones from China (Chelicerata: Arachnida)*. M.S. thesis, 274 pp. Hebei University. Hebei Province, China. [unpublished, in Chinese].

SUN, D. & Z.-N. SUN. 2011. Notes on the genus *Mesobuthus* (Scorpiones: Buthidae) in China, with description of a new species. *The Journal of Arachnology*, 39: 59–75.

SUN, D. & M.-S. ZHU. 2010. A new species of the genus *Mesobuthus* Vachon, 1950 (Scorpiones: Buthidae) from Xinjiang, China. *ZooKeys*, 37: 1–12.

SUN, D., M.-S. ZHU & W. R. LOURENÇO. 2010. A new species of *Mesobuthus* (Scorpiones: Buthidae) from Xinjiang, China with notes on *Mesobuthus songi*. *The Journal of Arachnology*, 38: 35–43.

TAKASHIMA, H. 1945. Scorpions of Eastern Asia. *Acta Arachnologica*, 9 (3–4): 68–106. [in Japanese].

TANG, V. 2022a. A standardized list of scorpion names in Chinese, with an etymological approach. *Euscorpius*, 350: 1–91.

TANG, V. 2022b. A new scorpion genus and species from China, *Qianxie solegladi* gen. et sp. n. (Scorpiones: Pseudochactidae). *Euscorpius*, 351: 1–19.

TANG, V. 2022c. Scorpions of China: an updated checklist with comments on some taxonomic issues (Arachnida: Scorpiones). *Euscorpius*, 355: 1–18.

TANG, V. 2023. Description of the adult male *Scorpiops tongtongi* Tang, 2022, with further comments on the genus *Scorpiops* Peters, 1861 in China (Scorpiones: Scorpiopidae). *Euscorpius*, 377: 1–52.

TANG, V., Q.-Q. JIA, & L. LIU. 2023. A new monotypic genus and species from China, *Langxie feti* gen. et sp. n. (Scorpiones: Buthidae). *Euscorpius*, 370: 1–101.

VACHON, M. 1950. Études sur les Scorpions. Chapitre III (suite). Déscription des Scorpions du Nord de l'Afrique. *Archives de l'Institut Pasteur d'Algérie*, 28(2): 71–365.

VACHON, M. 1958. Scorpionidea (Chelicerata) de l'Afghanistan. (The 3d Danish Expedition to Central Asia Zoological Results 23). *Videnskabelige Meddelelser fra Dansk Naturhistorisk Forening i Købehavn*, 120: 121–187.

VACHON, M. 1974. Etude des caractères utilisés pour classer les familles et les genres de Scorpions (Arachnides). 1. La trichobothriotaxie en Arachnologie. Sigles trichobothriaux et types de trichobothriotaxie chez les scorpions. *Bulletin du Muséum National d'Histoire Naturelle, Paris*, (3), 140 (Zool. 104), mai-juin 1973: 857–958.

WEIDNER, H. 1959. Die Entomologischen Sammlungen des Zoologischen Staatsinstituts und Zoologischen Museums Hamburg, I, Teil, Parathropoda und Chelicerata I. *Mitteilungen aus dem Hamburgischen Zoologischen Museum und Institut*, 54(49): 89–142.

WERNER, F. 1936. Neue-Eingänge von Skorpionen im Zoologischen Museum in Hamburg. Teil II. *Festschrift zum 60. Geburtstage von Professor Dr. Embrik Strand*, 2: 171–193.

WU, X.-W. 1936. A review of the scorpions and whip-scorpions of China. *Sinensia*, 7: 113–127.

YANG, X.-F. 2008. *Scorpion Fauna and Taxonomy in China (Chelicerata: Arachnida)*. M.S. thesis, 108 pp. Hebei University. Hebei Province, China. [unpublished, in Chinese].

YANG, X.-F., Y. NORMA-RASHID, W. R. LOURENÇO & M.-S. ZHU. 2013. True lateral eye numbers for extant buthids: a new discovery on an old character. *PLoS ONE*, 8(1): e55125. doi:10.1371/journal.pone.0055125.

YANG, Y.-C., C.-D. MA, E.-H. WANG, H. CHANG, LI A., Y.-N. DANG & T.-T. LIU. 2018. Herbalogical study and modern research progress of traditional Chinese medicine scorpio [*sic*]. *Anhui Agricultural Science Bulletin*, 8: 105–106. [in Chinese]

ZHANG, L. 2009. *Scorpion Fauna and Morphological Variation of Some Species in Northern China (Chelicerata: Arachnida)*. M.S. thesis, 145 pp. Hebei University. Hebei Province, China. [unpublished, in Chinese].

ZHANG, X.-S., G.-M. LIU, Y. FENG, D.-X. ZHANG & C.-M. SHI. 2020. Genetic analysis and ecological niche modeling delimit species boundary of the Przewalski's scorpion (Scorpiones: Buthidae) in arid Asian inland. Zoological Systematics, 45(2): 81–96.

ZHENG, Y., Q.-S. FAN, Q. WEI, & F.-Q. ZHANG. 2014. Toxicity of *Buthus martensii* Karsch venom and preparation of its F(ab')_2 antibody. *Chinese Journal of Biologicals*, 27(5): 647–651. [in Chinese].

ZHU, M.-S., J.-X. QI & D.-X. SONG. 2004. A checklist of scorpions from China (Arachnida: Scorpines). *Acata Arachnologica Sinica*, 13: 111–118.

ZHU, M.-S. & X.-F. YANG. 2007. Two species of the genus *Heterometrus* Ehrenberg, 1828 (Scorpionidae) from south Vietnam sold in pet shops in China. *Acta Arachnologica Sinica*, 16: 92–103.